The role of the Pygopus chromatin modulator in cell growth and division

by

© Phillip G. P. Andrews

A Thesis submitted to the

School of Graduate Studies in Partial Fulfillment

of the Requirements for the Degree of

Doctor of Philosophy

Division of Biomedical Sciences

Faculty of Medicine

Memorial University of Newfoundland

St. John's, Newfoundland

October 2017

Abstract

In adults, precisely regulated gene expression results in strict control of cell proliferation required for healthy tissues. Abnormal gene expression, on the other hand, can result in uncontrolled cell proliferation and tumor formation. Gene expression largely depends on changes to chromatin structure; it is remodeled in response to epigenetic stimuli to accommodate transcriptional activation and/or repression. Chromatin remodeling, therefore, is very broadly fundamental to normal and aberrant cellular function. Here, my research has focused on a key epigenetic effector that facilitates gene activation, called Pygopus 2 (Pygo2). Pygo2 functions primarily to link histone acetylation to active gene expression, by bridging transcription factors and modified histone proteins at gene promoters to histone acetyltransferases.

In this thesis, I first examined the role of Pygo2 in the canonical Wnt signaling pathway and found that Pygo2 is transiently and specifically acetylated when bound to the activated β-catenin complex. Acetylation of Pygo2 correlated with a displacement of nuclear Pygo2 to the cytoplasm, suggesting that acetylation of Pygo2 may control the recycling of β-catenin complexes, following target gene activation. Upon examination of the broader role of Pygo2 beyond Wnt signalling, I found that it promotes ribosomal (r)RNA transcription within the nucleolus. In this context, Pygo2 was required for histone H4 acetylation at the rDNA promoter, suggesting a novel involvement of Pygo2 in rRNA transcription. Finally, using a whole genome approach, I discovered that Pygo2 acts as a pleiotropic chromatin effector, revealing a function for Pygo2 in gene expression required for segregation and bi-orientation of chromosomes during mitosis. Further analysis identified an interaction between Pygo2 and c-myc oncoprotein, suggesting that the

chromatin effector Pygo2 may cooperate with c-myc, directing the expression of growth and division genes.

Taken together, my findings suggest that in association with other important regulators of growth in cancer, Pygo2 facilitates gene expression by interpreting and relaying positive epigenetic marks on histones, which is essential to promote the expression of proliferation-related transcriptional programs.

Acknowledgements

I wanted to make this as short and sweet as possible. First, I am very grateful to Dr. Ken Kao for giving me this opportunity to study in his lab. I also want to thank him for his encouragement, guidance and support throughout my research career.

Next, I would like to express my deepest gratitude to my wife, Christine, for her support and her initial encouragement to pursue my Ph.D. I am also thankful to my daughter Eva, who right now, probably doesn't realize how seeing her every day helped me through the ups and the downs.

Finally, I would like to thank committee members Gary Paterno and Jackie Vanderluit for all their helpful suggestions. I would also like to acknowledge past and present lab members: Mark, Zhijian, Youlian, Paola, Tahrim, Satoko, Corinne, Roya, Leena and Shannon, for providing thoughtful advice and expertise and for listening when I was rambling on about science or anything else for that matter.

Table of Contents

List of Tables

List of Figures

List of Symbols, Nomenclature or Abbreviations

47S	pre-ribosomal RNA
Ab	antibody
Ac-K	acetylated Lysine
AMD	actinomycin D
ANOVA	analysis of variance
APC	Adenomatous Polyposis Coli
ARF	Alternate Reading Frame
ARPP-P0	Acidic Ribosomal Phosphoprotein-P0
ATCC	American Type Culture Company
ATP	adenosine triphosphate
AurK	Aurora Kinase
BAF	Brg/Brahma Associated Factor
Bcl9	B-cell Lymphoma 9
BET	bromodomain and extraterminal domain
BOD1	Biorientation of Chromosomes in Division 1
BRD4	Bromodomain Containing Protein 4
BrdU	bromodeoxyuridine
Bro-Q	region of CBP: encompassing the bromodomain to glutamine rich domain
BrUTP	bromouridine triphosphate
C	carboxy
CBP	Cyclic AMP Binding Protein Binding Protein
CDC2	Cell Division Control 2
cDNA	copy deoxyribonucleic acid
CENP-A	Centromere Protein A
CEP290	Centrosomal Protein 290
CH1	region of CBP: cysteine histidine rich 1
CH3	region of CBP: cysteine histidine rich 3
ChIP	chromatin immunoprecipitation
CK1	Casein Kinase 1
CO_2	carbon dioxide
CoA	coenzyme A
CPC	chromosomal passenger complex
CpG	cytosine-guanosine dinucleotide
CREST	anti-centromere antisera
DAPI	4,6-diamidino-2-phenylindole
DAVID	Database for Annotation, Visualization and Integrated Discovery
DFC	dense fibrillar component
DIC	differential interference contrast
DMEM	Dulbecco's Modified Eagle's Medium
DMSO	dimethyl sulfoxide
DNA	deoxyribonucleic acid
DNMTs	DNA Methyltransferases
DTT	dithiothreitol

DOT1	Disruptor of Telomeric Silencing 1
Dvl	Disheveled
EDTA	ethylenediaminetetraacetic acid
Elf-1	E-74 like factor 1
ENCODE	Encyclopedia of DNA Elements
EtBr	ethidium bromide
EtOH	ethanol
EV	empty vector
FACS	fluorescence activated cell sorting
FC	fibrillar center
FITC	fluorescein isothiocyanate
FOXP1	Forkhead Box P1
Fz	Frizzled
G1	growth 1 phase of cell cycle
G2/M	growth 2/mitotic phase of cell cycle
GC	granular component
GCN5	General control non-derepressible 5
GFP	green fluorescent protein
GNATs	GCN5 related N-acetyltransferases
GO	gene ontology
GSK3β	Glycogen Synthase Kinase 3β
GST	glutathione S-transferase
H3K18Ac	histone H3 acetylated at lysine 18
H3K27Ac	histone H3 acetylated at lysine 27
H3K27me3	histone H3 methylated at lysine 27
H3K4me3	histone H3 methylated at lysine 4
HAT	histone acetyltransferase
HD1	homology domain 1
HDAC	histone deacetylase
HDM2	Human Double Minute 2
HP1	Heterochromain Protein 1
HPB	Harvard primer bank
IB	immunoblot
IgG	immunoglobulin
INCENP	Inner Centromere Protein
ING1/2	Inhibitor of Growth proteins 1 and 2
IP	immunoprecipitation
IRES	internal ribosome entry site
ITS-1	internal transcribed sequence 1
JHDM1	Jumonji C domain containing histone demethylase 1
JmjC	Jumonji C
kDa	kilodalton
KMT	lysine methyltransferase
LiCl	lithium chloride
LRP	Leukemia Related Protein
LSD1	Lysine Specific Demethylase 1

LUC	luciferase
MACS	model based analysis for ChIP-seq
MBT	Malignant Brain Tumor
mdm2	Murine Double Minute 2
MED	Mediator
MG132	carbobenzoxy-Leu-Leu-leucinal
MLL2	Mixed-Lineage Leukemia 2
MMLV	Moloney Murine Leukemia Virus
MMTV	mouse mammary tumor virus
MOPS	3-morpholinopropane-1-sulfonic acid
mRNA	messenger ribonucleic acid
MT	myc-tagged
mut	mutant
MYST	MOZ/Ybf2/Sas2/3/Tip60
N	amino
NaCl	sodium chloride
NAH+	nicotinamide adenine dinucleotide
NaHCO3	sodium bicarbonate
NHD	N-terminal homology domain
NLS	nuclear localization sequence
Nop56	Nucleolar protein 5A (56 kDa)
NOR	nucleolar organizing region
NPF	asparagine-proline-phenylalanine
PAS	polyadenylation sites
PCAF	p300/CBP Associated Factor
PCR	polymerase chain reaction
PHD	plant homeodomain
p-HH3	phospho-histone H3
PIC	preinitiation complex
Plk	Polo-like Kinase
PMSF	phenylmethanesulfonyl fluoride
Pol	polymerase
PRMT	Protein Arginine N-methyltransferase
pro	promoter
P-TEFb	Positive Transcription Elongation Factor b
PWWP	proline-tryptophan-tryptophan-proline
Pygo2	Pygopus homolog 2
qPCR	quantitative polymerase chain reaction
RanGTP	Ras-related nuclear protein bound to guanosine triphosphate
Rb	Retinoblastoma
RCC1	Regulator of Chromosome Condensation 1
rDNA	ribosomal gene encoding DNA
RIPA	radioimmunoprecipitation assay buffer
RNA	ribonucleic acid
RNAi	ribonucleic acid interference
RNA-seq	ribonucleic acid sequencing

RP	ribosomal protein
RPA194	the large 194 kDa subunit of RNA polymerase I
RPL11	Ribosomal Protein L11
rRNA	ribosomal ribonucleic acid
RT-qPCR	reverse transcription quantitative polymerase chain reaction
S	Svedburg unit
SAC	spindle assembly checkpoint
SD	standard deviation
SDS-PAGE	sodium dodecyl sulfate polyacrylamide gel electrophoresis
SEM	standard error of the mean
seq	sequencing
SET	Suv, Enhancer of Zeste, Trithorax
sh	short hairpin
si	short interfering
siNTC	short interfering non-targeting control
SIRT	Sirtuin
SL-1	Selectivity Factor 1
SWI/SNF	Switch/Sucrose non-fermentable
TBP	TATA Binding Protein
TCF/LEF	T Cell Factor/Lymphoid Enhancing Factor
Tcfcp2l1	Transcription factor cp2 like 1
TCOF-1	Treacher Collins-Franceschetti Syndrome 1
TLE	Transducin-like Enhancer
TPX2	Targeting Protein for Xklp2
TSS	transcriptional start site
UBF1	Upstream Binding Factor 1
WD40	tryptophan- aspartate motif of approximately 40 amino acids
Wg	Wingless
Wnt	Wingless/INT1
WRE	Wnt responsive element
XENA	*Xenopus* neural related
Δ	delta
β-TrCP	β-transducin repeat containing protein
μm	micrometer

Co-authorship statements

Chapter 2:

Kenneth Kao contributed with overall experimental design, data analysis and manuscript preparation.

Chapter 3:

Nuclear/nucleolar fractionation experiment (Figure 3.2) was performed with the assistance of Zhijian He. Rescue of cell cycle markers (Figure 3.11A) and Pygo2 depletion in SKOV3 cells (Figure 3.16) was performed by Youlian Tzenov. Catherine Popadiuk provided intellectual input and co-supervised the project. Kenneth Kao contributed overall experimental design, data analysis and manuscript preparation.

Chapter 1: Introduction

1.1 Foreword: The abnormal growth of cancer cells

The idea of the "hallmarks of cancer" was first introduced in 2000 by Douglas Hanahan and Robert Weinberg, in which they described six defining characteristics of a cancer: Activation of growth signalling, inactivation of growth suppression, inactivation of cell death mechanisms, acquisition of immortality, activation of angiogenesis, acquisition of invasion and metastasis (Hanahan & Weinburg, 2000). In 2011, two new defining characteristics were added: reprogramming of energy metabolism and evasion of the immune system (Hanahan & Weinberg, 2011).

Cancer is a multistep process that occurs over many years arising from three to six driver mutations affecting gene function (Vogelstein & Kinzler, 1993), with additional mutation(s) leading to an increased detrimental or aggressive phenotype. Whole genome sequencing has revealed that cancers can exhibit thousands of mutations, consisting mostly of "passenger" mutations that do not directly confer a growth advantage, while a subset of mutations occurring in more than 120 genes were likely responsible for driving cancer development (Greenman *et al*, 2007). More recently, the number of identified driver mutations has increased to over 140 genes and as few as two to eight of these "driver" mutations are sufficient to initiate and promote tumorigenesis, consistent with Vogelstein and Kinzler's original theory in 1993 (reviewed in: Vogelstein et al., 2013).

Somatic mutations occur either from environmental agents or from errors associated with DNA replication, while hereditary germline mutations result in the predisposition of an individual to cancer and likely result in a more rapid accumulation of mutations (reviewed in Brücher and Jamall, 2016). With the accumulation of mutations

there is an increased likelihood that driver mutations will occur in genes whose functions are involved in one or more of the "hallmarks" described above. Driver mutations likely directly affect the function of master regulator proteins (Califano & Alvarez, 2016), which play many roles controlling the expression of regulatory circuits necessary and required for transformation. For example, the proto-oncogene c-myc functions as a master regulator protein by controlling a growth promoting transcriptional program.

Tumor cell growth is complex and driven by the acquisition of mutations that confer selective growth advantages; the more driving mutations acquired, the more aggressive the tumor becomes. Cancer cells "evolve" into more aggressive groups of cells that make up tumors. Tumors start with one cell; the cell grows and divides to form a clonal population. The more cells existing in the tumor the higher chance there is that a second cell that acquires an additional mutation giving selective advantages over the first clonal population. It is here where it is possible for a cell from the first population to evolve to produce a new subset of the previous tumor, hence with each new driving mutation, a tumor will eventually become a heterogeneous collection of smaller tumors, thereby posing a big challenge for therapy (reviewed in: McGranahan and Swanton, 2015).

Cancer cell growth is therefore dynamic and is largely dependent on driver mutations affecting gene expression. With gene expression partly depending on transcription, it is not surprising that transcription is often aberrantly regulated in cancer. In the following section, I will take a closer look at transcription, how it is regulated and how its' deregulation is associated with cancer.

1.2 Transcriptional regulation and chromatin remodeling

The central dogma of genes being transcribed into RNA, which is translated into protein, is a powerful but simplistic model of gene expression. Gene expression is a far more complex process that can be viewed as a cellular response to a variety of intrinsic and extrinsic stimuli required for every cell to adapt to its local environment. If the transcription of genes involved in cell growth is not tightly controlled or regulated the result might be a constant growth or cancer phenotype.

Transcription is regulated primarily by protein factors that are responsible for controlling two broad processes. First, different sets of DNA binding proteins and transcription-associated factors direct the core transcriptional components to specific DNA sequences that reside within close proximity to the sequence to be transcribed. Second, due to the compact packaging of DNA into chromatin, chromatin associated factors are required to influence an amenable DNA structure to allow transcriptional components access to the DNA sequences. While this is a very simplistic view, the complexity of transcription depends on a several sequential protein-protein, protein-DNA and RNA interactions with proteins and DNA. I will begin by taking a closer look at transcriptional regulation and then later look at gene structure and chromatin organization, which is fundamental to transcriptional regulation.

1.2.1 Transcription

To simplify, I will give a brief overview regarding the regulation of transcription apart from the surrounding chromatin, which I will discuss in a later section. Thousands

of RNA and protein-coding genes in the human genome are controlled by transcription associated protein complexes that associate with DNA sequences as well as the machinery responsible for transcription. Transcription itself can be broken down into three distinct phases, including initiation, elongation and termination (Figure 1.1; for description see below).

Transcription factors are typically regulated by upstream cell signalling cascades that promote or inhibit various protein-protein interactions and post-translational modifications, switching them to a favorable conformation that is amenable for their association with DNA. Initially, pioneer transcription factors bind directly to DNA and are required to recruit larger protein complexes to modify and physically bend the DNA, required to activate transcription (Zaret & Carroll, 2011).

Activated transcription factors bind to specific DNA sequences at genetic control elements known as enhancers and promoters, which lie upstream of each gene. Enhancer sequences are gene regulatory elements that are positioned hundreds to thousands of bases upstream, whereas promoter sequences reside in close proximity to the transcriptional start site (TSS) for each particular gene. Enhancer-promoter looping and interaction is mediated by intricate protein-protein, protein-DNA and protein-RNA interactions among transcription factors, transcription associated proteins and RNAs, as well as the surrounding chromatin. Enhancer-promoter looping is required for the targeted recruitment of the basal transcription machinery and RNA polymerase to promoter sequences adjacent to TSS to initiate gene transcription (Reviewed in: Krivega and Dean, 2012; Vernimmen and Bickmore, 2015).

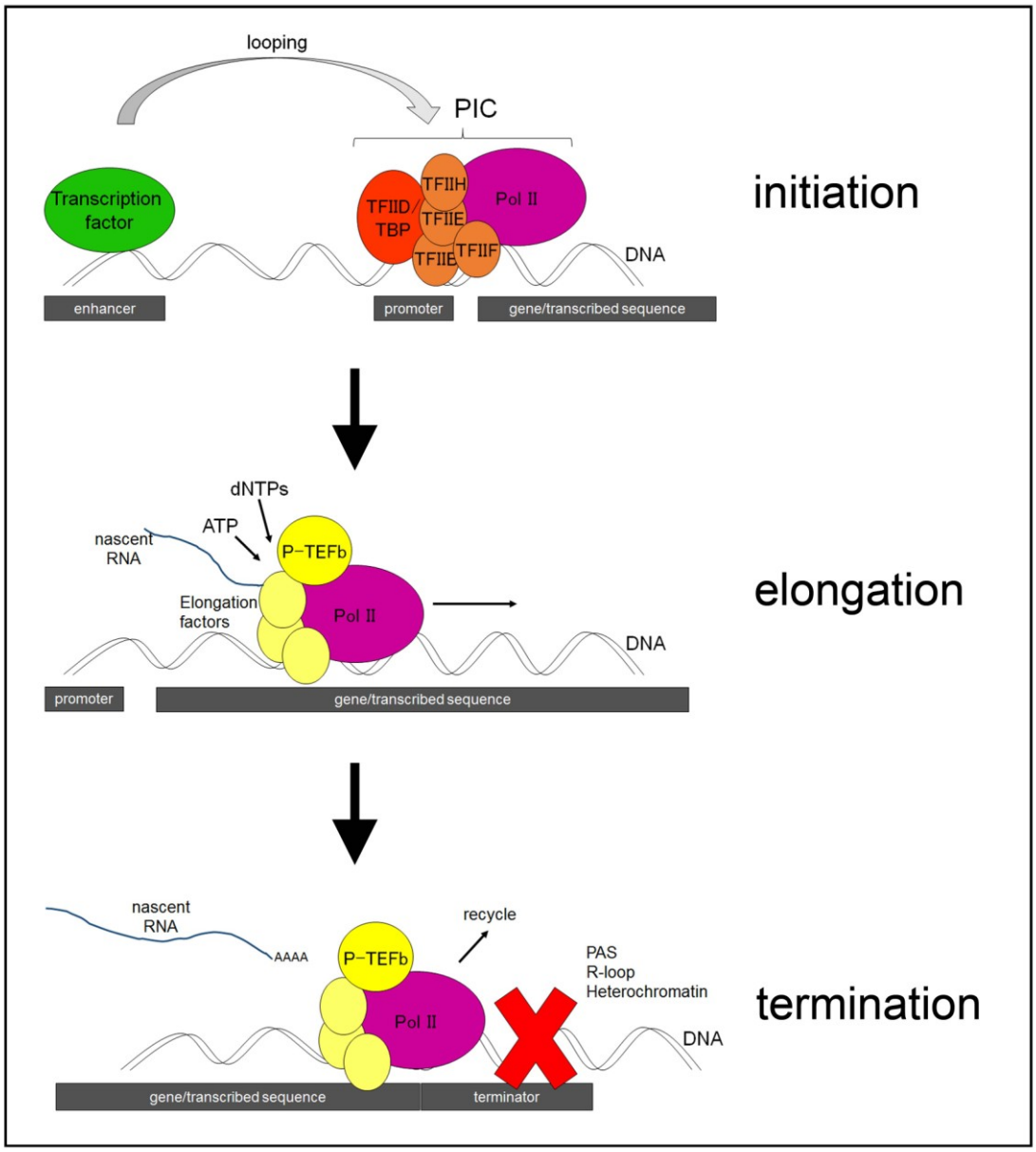

Figure 1.1. Transcription in eukaryotes. Transcription can be broken down into three distinct phases, initiation, elongation and termination. Initiation of transcription requires the sequence specific binding of transcription factors to both enhancer and promoter elements required for the recruitment of RNA polymerase II (Pol II). Transcriptional elongation resulting in the formation of a nascent mRNA requires the association of elongation factors, such as P-TEFb with Pol II. Several types of mechanisms can mediate transcriptional termination resulting in release of Pol II and the newly synthesized mRNA, including: PAS, R-loop structures and heterochromatin.

The basal transcription machinery consisting of TFIIB, TFIID, TFIIE, TFIIF and TFIIH complexes, along with RNA polymerase, make up a larger complex known as the preinitiation complex (PIC) that is associated with activated gene promoters. The TFIID complex contains the classical TATA binding protein (TBP) and TBP associated proteins that associate with specific TATA binding sequences approximately 30 bases upstream from the TSS and is required for transcription (Dynlacht *et al*, 1991). The basal transcription machinery binds to active promoters through association with the transcription associated proteins and is required to recruit RNA polymerases to initiate transcription. In eukaryotes, there are three RNA polymerase (Pol) enzymes capable of transcribing DNA sequence to produce RNA. RNA Pol I is required for transcription and production of ribosomal RNAs, RNA Pol III is required for transcription of transfer (t) RNAs, whereas, RNA Pol II is required for transcription of all other RNA species, including mRNAs and non-coding RNAs. Transcriptional initiation is achieved after assembly and activation of the PIC, whereby RNA polymerase is activated in the presence of ATP and then proceeds to melt or separate the double stranded DNA at the core through its DNA helicase activity, thereby forming a transcription "bubble". It is here where the surrounding DNA is unwound and decoded by RNA polymerase as RNA synthesis proceeds (reviewed in: Sainsbury et al., 2015; Sikorski and Buratowski, 2009)

During transcriptional elongation, RNA polymerase association with the Positive Transcription Elongation Factor b (P-TEFb) is required for the formation of nascent RNA (Zhou *et al*, 2012). RNA polymerase slows as it reaches specific DNA sequences known as transcriptional past the polyadenylation sites (PAS), which act a signals for transcriptional termination. PAS sites along with other termination mechanisms, such as

the R-loop structures formed by the RNA transcript and the DNA, the RNA polymerase association with termination factors and the chromatin dependent mechanisms, are required for termination of transcription, release of the nascent RNA and dissociation of the complex from the DNA (reviewed in: Proudfoot, 2016).

Transcription is, therefore, a coordinated process executed by many factors required for the recruitment and activation of the RNA polymerase. The tight packaging of DNA into chromosomes adds further complexity to this process, which must be overcome to facilitate RNA production. In the following section, I will focus on the organization of DNA into chromatin and how it is modified to facilitate transcription.

1.2.2 Chromatin structure

Due to physical space limitations within a eukaryotic cell, DNA is very efficiently packaged into chromatin, which consists of linear double stranded DNA molecules that are wrapped tightly around groups of histone proteins, making up the basic units known as nucleosomes. Complexes of histone octamers containing the core histone proteins H2A, H2B, H3 and H4 make up the foundation of the nucleosome and are arranged in such a way that the positively charged amino (N) -terminal tails of the histone proteins are free to interact with the negatively charged DNA. Each nucleosome consists of 146 base pairs of DNA that are wrapped around a histone octamer complex 1.65 times in a left-handed superhelix, resembling beads on a string (Luger *et al*, 1997). Histone H1 proteins interact with each nucleosome and are required to package the nuclesosomes into

higher order structures that make up the 30nm chromatin fibers of each chromosome (Reviewed in: Felsenfeld and Groudine, 2003; Grigoryev and Woodcock, 2012).

This highly ordered, tightly packaged structure represents a major hurdle, which must be overcome to facilitate transcriptional initiation and gene expression. Therefore, highly condensed chromatin or heterochromatin is modified in such a way that makes it accessible to transcription-associated proteins. This was first described based on the sensitivity of chromosomal DNA to nuclease digestion, whereby a DNA cutting enzyme could gain access to the chromosomal DNA and cut it to produce smaller fragments (Weisbrod, 1982). It was therefore hypothesized that the resulting open chromatin or euchromatin was a product of modified DNA or histone proteins and was likely required for transcription to take place. We now know that the interactions of DNA and histone proteins are highly dynamic and depend on chemical modifications to histones required to open or close chromatin structure. In the following section, I will take a closer look at the types of chromatin remodeling and focus on the chemical post-translational modifications that take place on histone proteins required to facilitate gene expression.

1.2.2.1 Chromatin remodeling

The structure of chromatin is highly dynamic to facilitate events required for major cellular functions, such as replication, transcription, DNA repair and cell division. For example, cell division requires DNA to be highly condensed and tightly associated with histones, on the other hand, transcription requires the DNA to be “relaxed” or less tightly associated with nucleosomes. Therefore, chromatin structure is malleable, and constantly being “remodeled” or changed.

As mentioned above, one major feature of chromatin remodeling is to facilitate access of transcription-associated protein complexes. Chromatin remodeling occurs primarily through the actions of enzymatic chromatin remodeling proteins that can either add or take away covalent chemical modifications to both DNA and histone proteins, resulting in either open (euchromatin) or closed (heterochromatin) chromatin structure. It is well known that chromatin remodeling is not limited to transcription and is required for many cellular processes, such as DNA damage repair (Price & D'Andrea, 2013) and DNA replication (Alabert & Groth, 2012). In the following sections, I will explore chromatin remodeling by first briefly touching on DNA methylation. Next, I will focus on two major classes of proteins: the ATP dependent chromatin remodelers and the post-translational chromatin remodelers.

1.2.2.2 DNA methylation

The first group of chromatin remodelers that I will briefly discuss are the DNA methyltransferases (DNMTs), which catalyze the covalent attachment of a single methyl group directly to the DNA, thereby generating 5-methylcytosine residues at cytosine-guanosine dinucleotide (CpG) sequences (Goll & Bestor, 2005). Following methylation of CpG dinucleotides by DNMTs, complexes of methyl-CpG binding proteins mediate the repression of gene expression by recruiting other chromatin modifiers, resulting in repressive histone modifications. DNA methylation is typically associated with long term repression of chromatin and plays important roles in both normal development and cancer, such as in X chromosome inactivation and the repression of tumor suppressor expression, respectively (reviewed in: Cedar & Bergman, 2009; Klose & Bird, 2006).

1.2.2.3 ATP-dependent chromatin remodeling

The group of chromatin remodelers that utilize energy generated from the hydrolysis of ATP, are therefore dubbed the ATP-dependent chromatin remodelers. The yeast Switch/Sucrose non-fermentable (SWI/SNF) proteins were the first ATP-dependent chromatin remodelers identified (Côté *et al*, 1994). SWI/SNF homologues in humans are called Brg/Brahma associated factors (BAF), however, ATP-dependent chromatin remodeling is often referred to as SWI/SNF chromatin remodeling. ATP-dependent chromatin remodeling involves the displacement or mobilization of nucleosomes with respect to the DNA, resulting in rapid large scale changes to chromatin structure (Hargreaves & Crabtree, 2011; Narlikar *et al*, 2013; Clapier & Cairns, 2009) . The mechanism of ATP-dependent chromatin remodeling relies on the DNA translocase activity possessed by ATP-dependent chromatin remodelers. These remodelers disrupt the DNA-histone interactions and move the DNA with respect to the histones, thereby resulting in nucleosome displacement or sliding (Saha *et al*, 2002) required for transcription, DNA replication and DNA damage repair. In the following section, I will look at chromatin remodeling that occurs by the direct chemical modification of histone proteins that result in changes to chromatin structure.

1.2.2.4 Chromatin remodeling by the post-translational modification of histones

The second group of chromatin remodelers that modify chromatin generally do not require ATP for energy and contain catalytic regions within their sequences, which promote covalent post-translational modification of the N-terminal histone tails protruding from nucleosomes. This type of chromatin remodeling exists in an

equilibrium, whereby covalent modifications are added or "written" and taken away or "erased" from the histones tails. The families of enzymes that "write" or "erase" histone modifications, are classified primarily on the chemical modification they add and remove, for example: acetylation, methylation, phosphorylation, ubiquitination and sumoylation. In this thesis, I will focus primarily on two modifications relevant to my work, which are histone acetylation and histone methylation.

1.2.2.5 Histone acetylation

Acetylation involves the enzymatic transfer of acetyl groups from the donor molecule acetyl-CoA to the positively charged lysine residues of target proteins. Lysine acetylation is not limited to histone proteins and is very important in the broad regulation of protein function (Close *et al*, 2010). Nonetheless, histone acetylation is probably one of the most well studied examples of histone modifications and in general is strongly correlated with the formation of an open chromatin structure required for transcriptional activation. The mechanism by which histone acetylation affects chromatin structure is relatively simple: Acetylation reversibly modifies the positive charge of the amino (N) terminal histone tails existing on the outer surface of the nucleosome into a neutral charge. This charge switch is sufficient to repel the negatively charged phosphodiester DNA backbone away from the histones resulting in an open chromatin structure (Grunstein, 1997).

Like all acetyltransferases, families of histone Acetyl Transferase (HAT) proteins possess enzymatic domains responsible for the catalytic transfer of acetyl groups to target proteins, in particular, histones, as their name implies. Nuclear HATs all play major roles

in transcription and can be divided into several different subfamilies including the Cyclic AMP Binding Protein Binding Protein (CBP)/p300, the General Control non-derepressible (GCN5)-related N-acetyltransferase and the MOZ/Ybf2/Sas2/3/Tip60 (MYST) subfamilies (reviewed in: Kouzarides, 2007; Tessarz and Kouzarides, 2014).

With respect to chromatin remodelling, each HAT subfamily targets unique lysine residues on N-terminal histone tails for acetylation. For example, in mouse embryonic fibroblast cells CBP/p300 targets histone H3 Lysine 18 (H3K18) and Lysine 27 (H3K27) acetylation, while GCN5 and its related subfamily member, p300/CBP Associated Factor (PCAF) target histone H3 lysine 9 for acetylation (Jin *et al*, 2011). It is also likely that multiple HAT complexes are recruited to transcriptional start sites of active genes given that acetylation of histones at different lysine residues tend to co-localize at specific sites in the genome and correlate with transcriptional activation (Wang *et al*, 2008).

Histone deacetylase (HDAC) proteins on the other hand, shift chromatin structure from an open state to a closed state. The enzymatic activity of HDACs results in the hydrolysis of acetylated lysine residues, thereby releasing the acetyl group as a single molecule of acetate (Lombardi *et al*, 2011). Protein deacetylases exist as two broad families; the first classical family comprising the Zn2+ dependent HDACs share homology to the yeast protein Rpd3, while the second family comprising the NAH+ dependent Sirtuins (SIRT) share homology to the yeast protein Sir2 (reviewed in: Haberland et al., 2009; Roth and Chen, 2014). While both families of deacetylases display a broad range of substrates, both play roles in chromatin remodelling and largely function as transcriptional co-repressors.

1.2.2.6 Histone methylation

Similar to acetylation, methylation requires specialized enzymes required for the post-translational addition of methyl groups from the donor molecule S-adenosylmethionine to positively charged lysine and arginine residues of target proteins. In contrast to acetylation by which only one acetyl group is added to one amino acid, methylation occurs at different levels through the addition of one, two or three methyl groups per amino acid and does not change the overall charge of the residue. It is therefore not likely that histone methylation significantly changes chromatin structure in the same way acetylation does, and likely serves to promote or take away docking sites for transcriptional regulatory proteins (Tessarz & Kouzarides, 2014; Greer & Shi, 2012).

Three families of methyltransferases have been identified and are classified based on their ability to methylate lysine and arginine residues. The lysine methyltransferases (KMTs): Suv, Enhancer of Zeste, Trithorax (SET) group, which share a conserved SET domain, and the Disruptor of Telomeric silencing (DOT1) group both target Lysine residues for methylation, whereas the Protein arginine N-methyltransferase (PRMT) group targets arginine residues for methylation (reviewed in: Bannister and Kouzarides, 2011; Greer and Shi, 2012).

Even though methylation is an important post-translational modification regulating non-histone protein function (Hamamoto *et al*, 2015), the context dependent methylation of histones can be associated with either activation or repression of transcription. For example, trimethylation of histone H3 at lysine 4 (H3K4me3) is associated with transcriptional activation (Santos-Rosa *et al*, 2002) and trimethylation of

histone H3 at lysine 27 (H3K27me3) is associated with the recruitment of Polycomb-group transcriptional repressors (Cao *et al*, 2002).

Early studies examining histone methylation suggested that it was an irreversible process (Byvoet *et al*, 1972), however we now know protein methylation is indeed a reversible process and is carried out by specific families of histone methylases and demethylases. The revisited concept that histone methylation is a reversible process (Bannister *et al*, 2002) prompted the search for enzymes capable of demethylating histones, which led to the functional identification of one of the first histone demethylases, Lysine Specific Demethylase 1 (LSD1; Shi *et al*, 2004). However, LSD1 was only capable of demethylating monomethylated and dimethylated H3K4, therefore suggesting the existence of further demethylases capable of demethylating trimethylated lysines. It was later found that the Jumonji C (JmjC) domain containing histone demethylase 1 (JHDM1) was capable of demethylating H3K36 and hence represented a second class of histone demethylases (Tsukada *et al*, 2006). Finally, through a candidate approach, a larger family of more than thirty JmjC domain containing proteins were identified and shown to have broad histone demethylase activity, including the demethylation of trimethylated Lysines (Dimitrova *et al*, 2015).

1.2.3 Interpreting the histone code

Thus far, I have discussed mechanisms that cells have evolved to open and close chromatin to allow or deny access to DNA. From a global perspective, at any point in time, chromatin is a complex and dynamic mix of open and closed chromatin, which reflects the ongoing state of histone modifier activity. histone modifiers that add chemical

components have been called “writers” and those that remove components, “erasers”. The different combinations of modifications make up the “histone code”, thereby providing detailed instructions that can be interpreted by the histone “readers”, functioning as effector molecules involved in the positive or negative regulation of transcription (Figure 1.2).

As briefly mentioned above, histone methylation in contrast to histone acetylation, is not directly involved in promoting open chromatin structure. On the other hand, histone methylation together with acetylation can directly affect the interaction of numerous protein families involved in transcriptional regulation. Given the basic nature of the histone tails that protrude from each nucleosome, various combinations of histone modifications provided by the histone writers and erasers that make up the code are possible.

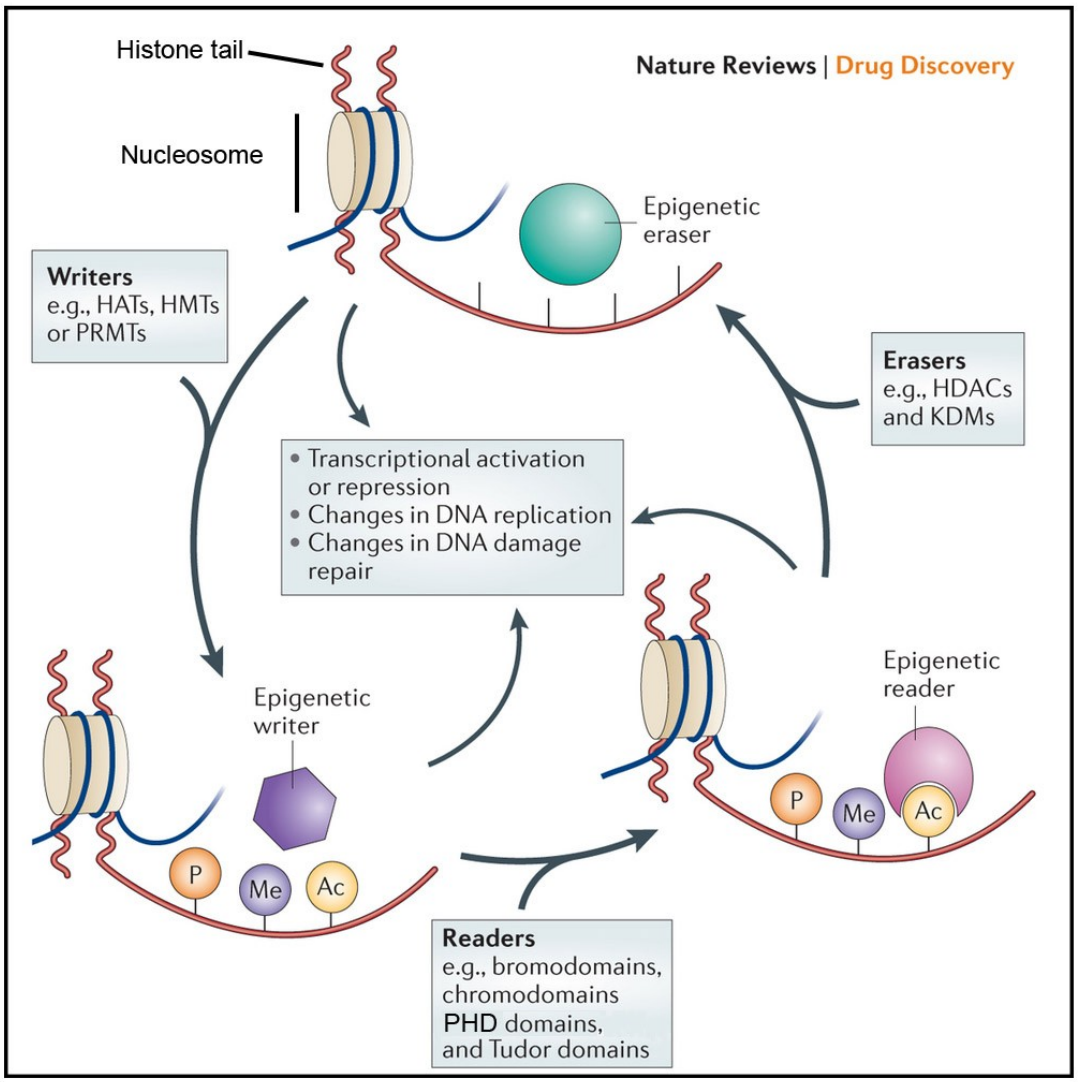

Figure 1.2. Histone code readers, writers and erasers. Reversible modifications made to histone proteins by epigenetic "writers" and "erasers" result in changes to nucleosomal structure resulting in the recruitment of factors or "readers", which directly associate with modified histones. Histone "readers" are involved in promoting several processes, such as DNA replication and repair, as well as transcription. Adapted by permission from Macmillan Publishers Ltd: [Nature Reviews Drug Discovery] (Falkenberg & Johnstone, 2014), copyright (2014).

1.2.3.1 Histone code readers

Post-translational modification of histones through the work of histone writers and erasers provide specific instructions at discrete sites of chromatin in the genome. However, these instructions must be interpreted by unique sets of proteins to elicit a cellular response. Instructions provided by the histone code induce the recruitment of a variety of protein families of code readers, capable of binding to specific histone modifications. The function of histone code readers is to provide effector functions that either open or close chromatin, as well as promote or inhibit recruitment of transcriptional activators and repressors.

To date, several protein families with highly conserved interaction domains have been identified, possessing the ability to interact directly with post-translationally modified residues of histone proteins. In this section, I will take a closer look at the different domains of chromatin reading proteins that interact directly with post-translationally modified histones, such as acetylated and methylated residues.

1.2.3.2 Readers of acetylated histones

The existence of histone code readers was unknown until the end of the millennium, when it was shown that the bromodomain of the acetyltransferase co-activator, PCAF, could specifically interact with acetylated lysine residues (Dhalluin *et al*, 1999). At this point in time, the importance of the bromodomain was unknown and had already been described as a conserved domain in a number of proteins, most of which had function in transcriptional activation (Haynes *et al*, 1992). Therefore, the landmark paper published by the Zhou lab in 1999 (Dhalluin *et al*, 1999) represented a huge leap

forward with respect to studies describing chromatin remodelling. To date, only a few protein domains have been identified to interact with acetylated Lysine residues including the bromodomain, the double plant homeodomain and the double pleckstrin homology domain, with the bromodomain being the most well described (Musselman *et al*, 2012).

The bromodomain containing proteins, comprising the largest group of acetyl-lysine readers, have been loosely classified into eight subfamilies (reviewed in: Filippakopoulos and Knapp, 2012). Class I and III subfamilies function as nuclear HATs and include the proteins: PCAF, GCN5, CBP and p300. Class II subfamilies represent the Bromodomain and Extraterminal (BET) domain proteins and often contain two adjacent bromodomains, such as BRD4. Class IV, V and VII families function as transcriptional regulators such as BRD1 and TATA binding proteins. Finally, Class VI and VIII bromodomain containing proteins include methyltansferases as well as SWI/SNF ATP-dependent chromatin remodellers. Therefore, bromodomain containing proteins encompass a diverse family of acetylated Lysine readers, most of which have some ascribed role in transcriptional activation, which is not surprising given the strong correlation between histone acetylation and transcriptional activation.

1.2.3.3 Readers of methylated lysines

Since both lysine and arginine can be modified with multiple methyl groups, histone methylation represents a multifaceted post-translational modification, that can be related to both transcriptional activation or repression. In brief, much less is known about arginine methylation. The most well known methyl arginine readers are the Tudor domain containing proteins, which represent a relatively poorly characterised group of

approximately thirty proteins that show some promiscuity towards methylated lysine residues. Tudor domain containing proteins have functions in protein-protein interaction as well as RNA-protein interactions and may play roles in both transcription and RNA splicing (reviewed in: Gayatri and Bedford, 2014).

Methylation readers are broadly categorized into three families based on the structure of the functional binding domain. The chromodomain, tudor domain, PWWP and the Malignant Brain Tumor (MBT) families with a barrel-like domain, WD40 proteins with a propeller-like domain and the plant homeodomain (PHD) proteins contain a zinc finger-like domain (reviewed in: Gayatri and Bedford, 2014). Similarly, all contain a methylated lysine binding pocket, which is dependent on the presence of 2-4 aromatic amino acids that form an aromatic cage-like structure.

There are many families of proteins that bind directly to methylated lysines, some of which recruit transcriptional repressors and some of which recruit transcriptional co-activators. For example, H3K9 and H3K27 acetylation is generally associated with transcriptional activation, H3K9me3 and H3K27me3 represent repressive histone marks that recruit the chromodomain proteins Heterochromatin Protein 1 (HP1) and the polycomb repressor complex which function as transcriptional co-repressors that silence gene expression (Cao *et al*, 2002; Bannister *et al*, 2001). Some PHD-containing proteins bind to H3K9me3 and also function as transcriptional co-repressors, such as the tumor suppressors Inhibitor of Growth proteins 1 and 2 (ING1/2), that function in transcriptional repression and are required for numerous processes related to cell growth (Guérillon *et al*, 2013).

Perhaps the most well known group of proteins that bind methylated lysines are the zinc-binding PHD containing proteins. While some PHD proteins function as transcriptional co-repressors as discussed above, many others function as transcriptional co-activators through their popular association with H3K4me3, a well known chromatin mark at gene promoters that is associated with active transcription (Santos-Rosa *et al*, 2002; Bernstein *et al*, 2002). PHD-containing proteins that bind to H3K4me3 are often associated with acetyltransferases, methyltransferases, as well as transcription factors required for transcriptional activation (Musselman & Kutateladze, 2011). Such is the case for the PHD containing chromatin effector protein Pygopus, whose hypothesized role is to couple active H3K4me3 marks promote further chromatin remodelling events to facilitate transcription of genes involved in cell growth and division, as I will discuss in subsequent sections.

1.3 The Pygopus family of transcriptional regulators

The focus of the following sections is on a gene called Pygopus (Pygo) and its potential role(s) in cancer. I will describe the initial identification of Pygo and its function in the active Wingless/INT1 (Wnt) signalling transcription complex. Finally, I will discuss Wnt independent functions of Pygopus and what is known about Pygopus with respect to cancer.

1.3.1 Wnt/β-catenin signalling

Wnt signalling is a conserved cell signalling pathway that is important to direct key aspects of embryonic development and adult stem cell/tissue maintenance. It is

involved in both cell proliferation and differentiation, therefore not surprisingly, the deregulation and the aberrant activation of Wnt signalling is important in a number of human cancers (reviewed in: Clevers and Nusse, 2012). Some of the most well-known Wnt target genes are directly involved in promoting cell growth and division, such as *cyclinD1* (Tetsu & McCormick, 1999; Shtutman *et al*, 1999) and *c-myc* (He *et al*, 1998).

In the canonical model, β-catenin, the key mediator of Wnt signalling, is normally bound to E-cadherin and associated with the cytoskeleton, while unbound β-catenin is kept at low levels due to a cytoplasmic destruction complex. This complex, which is composed of Axin, Adenomatous Polyposis Coli (APC), Casein Kinase 1 (CK1) and Glycogen Synthase Kinase 3β (GSK3β), is responsible for the binding and phosphorylation of β-catenin at specific amino (N)-terminal residues, which targets it for ubiquitination by β-Transducin Repeat Containing Protein (β-TrCP) and subsequent proteasome mediated degradation (Figure 1.4).

In the absence of a signal, Wnt target genes in the nucleus are bound by complexes of T Cell Factor/Lymphoid Enhancing Factor (TCF/LEF) and Groucho/Transducin-like Enhancer (Gro/TLE) family members, which are required to recruit HDAC activity to repress the expression Wnt target genes. Wnt signalling is initiated by the extracellular binding of a Wnt glycoprotein ligand to the Frizzled/Leukemia Related Protein (Fz/LRP) co-receptor. This triggers

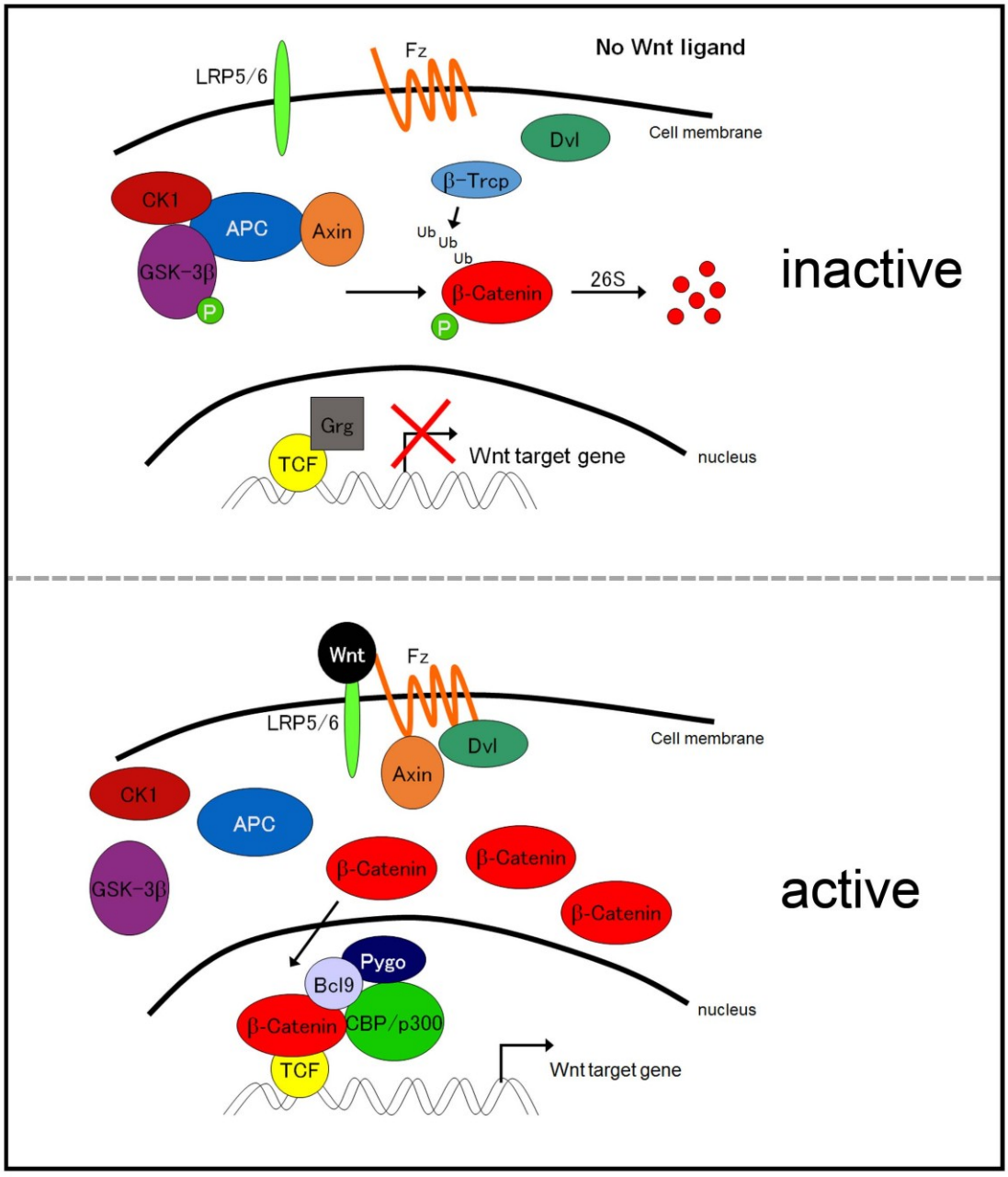

Figure 1.3. The Wnt signal transduction pathway. For description, see section 1.3.1.

the recruitment of Disheveled (Dvl) to the frizzled receptor, which then binds Axin and results in the inactivation the β-catenin destruction complex. Escaping phosphorylation and degradation, β-catenin protein accumulates in the cytoplasm and is translocated to the nucleus where it displaces Groucho/TLE co-repressor complexes at Wnt target genes. β-catenin recruits a number of co-activators involved in chromatin modification and transcriptional activation, namely Pygopus, which is indirectly bound to β-catenin though the adaptor protein Legless/B-cell lymphoma 9 (Bcl9) and is required for transcriptional activation (reviewed in: Cadigan and Peifer, 2015; Clevers and Nusse, 2012; Mosimann et al., 2009; Valenta et al., 2012).

1.3.2 Pygopus and Wnt signalling

Almost two decades ago, a study by Prieve and Waterman (Prieve & Waterman, 1999) showed that a complex between β-catenin and TCF was not sufficient to activate Wnt target gene expression and at least one other unknown factor, downstream of β-catenin, was required for Wnt target gene expression. This prompted an investigation by at least four groups to identify the unknown factor(s) by performing genetic screens in *Drosophila* to identify factors required for Wingless/Wnt signalling. Early in 2002, there were back-to-back publications identifying Pygopus (Thompson *et al*, 2002; Kramps *et al*, 2002; Belenkaya *et al*, 2002; Parker *et al*, 2002) as one of the "unknown factors" originally described by Prieve and Waterman. Additionally, in the landmark study by Kramps *et al*. (2002), the authors identified a second protein (legless/Bcl9) was required to link Pygopus indirectly to β-catenin (Kramps *et al*, 2002). The mutant phenotypes observed in *Drosophila* lacked legs and antennae and were therefore named legless and

Pygopus (the genus of a snake-like legless lizard found in Australia). Concurrently, Lake and Kao had isolated a novel cDNA encoding a PHD containing protein from *Xenopus* embryos that was required for embryonic brain development they originally named XENA (*Xenopus* Neural Related), which they later found was the Xenopus homolog of Pygopus 2 (Lake & Kao, 2003).

The structure of Pygopus proteins is very peculiar, showing little sequence similarity to any other proteins, except the carboxy (C)-terminal PHD domain, which is common to many proteins that function in H3K4me3 binding and chromatin remodeling, as discussed above. At the N-terminus, Pygopus proteins share a conserved region, termed the N-terminal homology domain (NHD), which contains a nuclear localization sequence (NLS) and a short amino acid sequence (asparagine-proline-phenylalanine; NPF) that may be important for the transcriptional activity of Pygopus (Städeli & Basler, 2005). The PHD and NHD domains of Pygopus are connected by an intervening amino acid sequence that is rich in proline and glycine residues (Figure 1.4).

The function of Pygopus in Wnt signalling depends primarily on its PHD domain, which binds directly to legless/Bcl9. Pygopus/BCl9 complexes target β-catenin to the nucleus required for transcriptional activation of Wnt target genes (Townsley *et al*, 2004). The interface of the PHD domain and Bcl9 binds directly to H3K4me3, which may be involved in linking the β-catenin complex to active promoters (Fiedler *et al*, 2008).

The functional role of the Pygo PHD domain is controversial, since it has been shown to be largely dispensable for normal mouse development, except in testes where

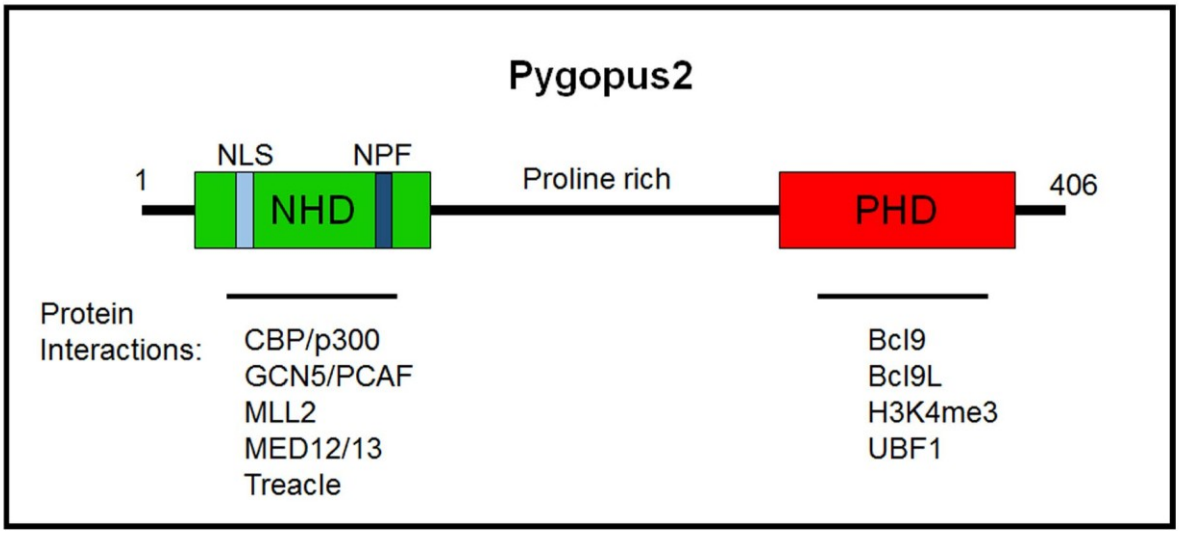

Figure 1.4. The functional domains of the chromatin effector Pygo2. A cartoon illustrating the two functional domains (NHD and PHD) common to Pygo2. Other regions of interest include the NLS, required for its nuclear localization and the NPF, required at least in part for transcription. Pygo2 interacting proteins are shown in lower section.

the interaction of Pygo with chromatin depends on its PHD domain (Cantù *et al*, 2013). While the exact role of the NHD in Wnt signalling is not completely understood, several studies indicate that it recruits factors that positively affect transcription, including the histone acetyltransferases CBP, p300, PCAF and GCN5, histone methyltransferases such as the SET domain containing protein Mixed-Lineage Leukemia 2 (MLL2) and factors linking it to RNA polymerase II, including the general transcription factor TFIID and the mediator complex proteins MED12 and MED13 (Andrews *et al*, 2009; Chen *et al*, 2010; Carrera *et al*, 2008; Wright & Tjian, 2009). Many factors that bind the NHD of Pygopus also bind directly to β-catenin. It therefore has been hypothesized that both β-catenin and Pygopus may be involved in the cooperative recruitment and binding to factors linking the active β-catenin transcriptional complex to euchromatin formation and recruitment of RNA polymerase (Andrews *et al*, 2009; Chen *et al*, 2010).

Only one Pygopus family member was identified in *Drosophila*, while in mammals, two Pygopus family members (Pygo1 and Pygo2) were identified (Kramps *et al*, 2002). However, of the two family members, Pygo2 appeared to play essential roles in development and hence is the more well studied family member. Developmental investigations in transgenic mice harboring null alleles for Pygo1 and Pygo2 revealed that Pygo1 null mice developed normally with no defects, while Pygo2 null mice die neonatally, were smaller in size and displayed defects in lens, kidney, pancreas and hair follicle development with occasional exencephaly (Song *et al*, 2007; Schwab *et al*, 2007; Jonckheere *et al*, 2008; Li *et al*, 2007a). Also, Pygo2 was expressed to some degree in all adult tissues, whereas the expression of Pygo1 was constrained to heart tissue (Li *et al*, 2004).

In *Drosophila*, Pygo was declared to play a dedicated role in Wg signalling (Kramps, 2002). Subsequent studies in Pygo2 null mice revealed, however, that while some of the observed developmental phenotypes could be attributable to a role for Pygo2 in Wnt signalling, others could not (Song *et al*, 2007). These studies, along with several others that we will discuss in the following section, revealed that the role of Pygo2 in vertebrates can be expanded to include Wnt independent functions.

1.3.3 Wnt independent functions of Pygo2

One could reason that since PHD domains bind to H3K4me3 marks and that all active genes display H3K4me3 at their promoters, Pygopus could possibly associate with any active gene promoter independently of β-catenin and the Wnt signalling complex. While this is not likely the case, there is accumulating experimental evidence suggesting that Pygo2 also functions outside of the active β-catenin transcriptional complex. The first experimental evidence suggesting a Wnt independent role for Pygo2 was in *Xenopus* development, where depletion of XPygo2 protein was achieved using morpholinos to inhibit translation of XPygo2 mRNA (Lake & Kao, 2003). Pygo2 was required in the developing brain for the expression of the well-known Wnt target gene *engrailed*, but it was also required for expression of the non-Wnt target genes *Pax6*, *brain factor 1* and *retinal homeobox gene 1*. This evidence therefore suggested that Pygo2 functions outside of the canonical Wnt signalling pathway. Subsequently, several studies have provided evidence that Pygo2 also functions outside of Wnt signalling, which I will briefly discuss below.

One of the first compelling lines of evidence to suggest a Wnt-independent role for Pygo2 was in TOV-21G ovarian cancer cells that do not express β-catenin, rendering them insensitive to β-catenin depletion. In contrast, depletion of Pygo2 had a strong growth suppressive phenotype (Popadiuk *et al*, 2006). Soon after, others reported that in the developing mouse lens where Wnt/β-catenin signalling is absent, Pygo2 played an essential Wnt-independent role in normal development (Song *et al*, 2007). Furthermore, Pygo2 plays a β-catenin independent role in the chromatin regulation and transcription of both histone genes (Gu *et al*, 2012) as well as the gene(s) encoding the precursor ribosomal RNA (Andrews *et al*, 2013), as will be discussed in detail in a following chapter. Importantly, these results suggested a strong Wnt/β-catenin independent requirement for Pygo2 in both normal development, as well as in cell growth regulation.

1.3.2 Pygo2 and cancer

The identification of Pygopus and its involvement in Wnt signalling immediately associated it *a priori* with colorectal carcinoma, where β-catenin is aberrantly activated with high frequency (Kramps *et al*, 2002; Thompson *et al*, 2002). However, any direct experimental evidence for an involvement of Pygo2 in colorectal cancer was many years later (Brembeck *et al*, 2011), after the expression and requirement of Pygo2 had already been established in cancer. We now know that Pygo2 is highly expressed in a number of different tumors and cells originating from a variety of tissues compared to their normal counterparts. Accordingly, in the following sections, I will review past and present literature to summarize what is known about the expression and requirement of Pygo2 in cancer.

1.3.2.1 Expression of Pygo2 in cancer

The first experimental evidence to report the elevated expression of Pygo2 in cancer originated from two back-to-back studies in the Kao laboratory. The first study was described in epithelial ovarian cancer where Pygo2 mRNA and protein were expressed in ovarian cancer cell lines and tumors at levels higher than normal ovarian epithelial cells (Popadiuk *et al*, 2006). The second study showed a similar elevated expression of Pygo2 in breast cancer cell lines and tumors (Andrews *et al*, 2007). Since these initial studies, elevated Pygo2 levels were demonstrated in cancers originating from the cervix (Tzenov *et al*, 2013; Andrews *et al*, 2008), breast (Tzenov *et al*, 2015), brain (Wang *et al*, 2010; Chen *et al*, 2011; Wang *et al*, 2016), intestine (Brembeck *et al*, 2011), lung (Zhou *et al*, 2014), prostate (Yang et al., 2013; Kao et al., unpublished) and liver (Zhang *et al*, 2015b, 2015a).

The high level of Pygo2 mRNA in the initial studies in breast and ovarian cancer suggested that the expression of Pygo2 was likely upregulated at the transcriptional level. Therefore, an investigation of factors that could bind directly to the Pygo2 promoter and upregulate its expression in cancer revealed that E-74 like factor 1 (Elf-1) was at least one factor that was both required and sufficient to modulate the mRNA expression of Pygo2 (Andrews *et al*, 2008). Significantly, the transcriptional activity of Elf-1 is regulated by the tumor suppressor protein Retinoblastoma (Rb) in human T-cells (Wang *et al*, 1993). Furthermore, Elf-1 mediated expression of Pygo2 appeared to be through an Rb-regulated mechanism in an immortalized cervical cell progression model (Tzenov *et al*, 2013). The correlation in expression between Elf-1 and Pygo2 in different cancer

types (Andrews *et al*, 2008) suggested that Pygo2 expression can be regulated by Rb in a number of different cancers.

The link between cell cycle progression and Rb has been well described. For example, in quiescent non-dividing cells, Rb exerts its tumor suppressor activity through the binding and sequestration of key regulators that drive cell growth and division, such as E2F and Elf-1. The function of Rb is inhibited by sequential phosphorylation events that eventually lead to the activation of genes that drive cell growth and division (reviewed in: Dick and Rubin, 2013; Dyson, 2016). It is not surprising that in a broad range of cancers the tumor suppressor activity of Rb is largely compromised through mutation and/or its inactivation. These observations suggest that Pygo2 expression may be carefully controlled in normal cells and the loss of Rb function in immortal and tumorigenic cells results in a consequential upregulation of Pygo2 gene expression.

1.3.2.2 Requirement of Pygo2 in cell growth

Since Pygo2 was highly expressed in cancer cells, the main strategy for determining its role and requirement in cancer has been by loss-of-function studies. Here, Pygo2 mRNA is reduced or degraded either by RNase H dependent mechanisms using antisense oligonucleotides, or by RNA interference (RNAi) dependent mechanisms using short interfering (si) or short hairpin (sh) RNAs. Again, the first two studies to show that Pygo2 was involved in the malignant growth of cancer cells were published by the Kao laboratory (Popadiuk *et al*, 2006; Andrews *et al*, 2007). Both studies utilized short antisense oligonucleotides that were complementary to the Pygo2 mRNA sequence to knock-down expression of the Pygo2 mRNA and hence the protein. Notably, in several

ovarian and breast cancer cell lines examined, it was demonstrated that the high expression of Pygo2 was required for cell growth.

Since these initial studies, many examples utilizing RNAi or genetic knock-outs demonstrated a role for Pygo2 in cell growth. Intriguingly, Pygo2 has been shown to be essential for maintaining the malignant growth characteristics in almost every cancer cell type examined. What makes the apparent role of Pygo2 so important for cell growth? To answer this question, the literature offers at least two important explanations related to its function as a transcriptional regulator.

Undoubtedly, the first explanation is the imperative role of Pygo2 in Wnt signalling, which is important to promote cell growth and division. In normal tissues, Wnt signalling is carefully regulated at many levels that occur post-activation and function to turn off the pathway. There are many examples of the aberrant activation of β-catenin in cancer, resulting in the overexpression of proto-oncogenes and proteins that drive cell cycle progression, thereby resulting in the activation of a cell growth promoting program (reviewed in: Clevers and Nusse, 2012).

The second explanation comes from the apparent role of Pygo2 as a promiscuous chromatin modulator in which it functions aside from its role in the Wnt signalling pathway. While the exact mechanism remains elusive, the direct involvement of Pygo2 in the chromatin regulation and transcription of histone mRNAs (Gu *et al*, 2012) and rRNAs (Andrews *et al*, 2013) offers a reasonable explanation for the role of Pygo2 in cell growth. Before a cell divides, there is a massive commitment of cellular resources to accumulate the adequate biomass required to replicate its DNA and prepare for division. Here, biomass accumulation largely depends on the *de novo* production of DNA and

histones, required for chromatin assembly. This process also requires a supplemental coordinated increase of ribosome production needed for translation of proteins involved in cell growth and division. Therefore, Pygo2 may act as a cell growth effector, required to help drive cell cycle progression and cell growth through its involvement in Wnt signalling and its concurrent or resultant role in histone and ribosome production.

1.3.2.3 Pygo2 plays a role in tumor initiation and stem cell expansion.

Stem cells possess the quality of self-renewal achieved through both symmetric and asymmetric cell division. It is imperative for maintaining a population of the founding stem cells, while promoting the clonal expansion of daughter cells. While required for normal tissue growth and development, deregulation of stem cell proliferation can most certainly result in tumor formation (reviewed in: Kreso and Dick, 2014). The environment or niche where stem cells reside is vitally important to supply the signals necessary to induce stem cell division. For example, Wnt signals that originate from the niche cells are important drivers of stem cell division required for adult tissue renewal and regeneration (reviewed in: Clevers et al., 2014). Concurrent with these functions, there have been several genetic studies in mice implicating a role for Pygo2 in stem cell-like expansion, as I will elaborate on below.

Pygo2 is expressed in mammary epithelial progenitor cells and while not required for their differentiation, it was required for progenitor cell proliferation and expansion (Gu *et al*, 2009). Furthermore, a similar requirement for Pygo2 in the expansion of breast cancer stem-like cells was demonstrated (Chen *et al*, 2010). In both instances, Pygo2 appeared to play both Wnt and chromatin dependent roles that were required to promote

cell proliferation. Importantly, Pygo2 was found to be highly expressed and required for tumor initiation and formation in a mouse mammary tumor virus (MMTV)-Wnt1 transgenic mouse model (Watanabe *et al*, 2013) as well as for hair follicle progenitor cell expansion and skin hyperplasia in a constitutively active β-catenin mouse model (Sun *et al*, 2014). Together, these data clearly implicate Pygo2 in stem cell and cancer stem-like cell proliferation.

1.4 Thesis rationale and objectives

One of the hallmarks of cancer is uncontrolled cell proliferation, encompassing both cell growth and cell division. Therefore, targeting cell proliferation mechanisms represents a rational avenue for cancer therapy. Cell proliferation is ultimately controlled at the transcriptional level, whereby chromatin remodeling and gene expression are essential to produce the proteins required to support both cell growth and division. The purpose of this thesis is to determine how the Pygo2 chromatin effector affects gene expression driving cell proliferation in cancer. To address this question, I examined the function of Pygo2 from two different perspectives. The first deals with the chromatin remodeling function of Pygo2 within the active Wnt/β-catenin signalling complex, while the second deals with Pygo2 chromatin remodeling complexes that function outside of Wnt signalling. The specific thesis objectives are outlined below.

1.4.1 Objective 1: The role of the chromatin effector Pygo2 in Wnt/β-catenin signalling

The Wnt signalling pathway supports cell proliferation and expansion during normal development and combined with the loss of tumor suppressor function can be aberrantly activated to drive cancer growth. Thus, I hypothesized that Pygo2 plays an essential role in histone acetylation through the recruitment of HATs, which coordinate chromatin remodeling necessary to promote transcriptional activation. In chapter 2, I provide evidence that Pygo2 itself is post-translationally modified by acetylation specifically by the HAT family members CBP and p300, while in a complex with activated β-catenin. I therefore hypothesized that acetylation of Pygo2 may regulate its chromatin effector function in the active β-catenin complex. My results suggest that acetylation of Pygo2 likely occurs concurrently with transcriptional activation of the Wnt target gene Axin2 and that it may be required subsequently for the transcriptional recycling of Pygo2 containing complexes to the cytoplasm.

1.4.2 Objective 2: Examination of the role of Pygo2 in ribosomal gene expression and cell growth

The hypothesized function of Pygo2 as an integral component of one or more chromatin remodelling complexes suggests that its chromatin modulator activity may be important for both the Wnt-dependent and Wnt independent expression of genes required for cell growth. Previous results in the lab indicated that Pygo2 interacted with Treacle, a protein involved in ribosome biogenesis. I therefore hypothesized that the recruitment of Pygo2 by Treacle may be necessary for chromatin remodeling and expression of the

ribosomal RNA genes. My results suggest that Pygo2 interacts with the transcriptional complex within nucleoli and promotes histone H4 acetylation, required for expression of the rRNAs.

1.4.3 Objective 3: Analysis of a Pygo2 gene expression program reveals an involvement in cell division

Continuing forward from objective 2, I found that depletion of Pygo2 triggered the nucleolar stress response, which resulted in the activation of the tumor suppressor p53 and subsequent G1 cell cycle arrest. On the other hand, in tumor cells that do not express functional p53, I found that depletion of Pygo2 resulted in reduced rRNA gene expression and subsequent G2/M cell cycle arrest.

Further analysis revealed that Pygo2 depletion resulted in aberrant mitotic spindle attachment to kinetochores and a subsequent accumulation of cells in metaphase. Here, I hypothesized that Pygo2 may be required for chromatin remodeling and transcription of key genes required for cell division. Therefore, to search for direct functional Pygo2 target genes, I employed a whole genome approach to identify Pygo2 binding sites across the genome and coupled this with a whole transcriptome analysis to identify Pygo2 responsive genes. I found that Pygo2 was required for H3K27 acetylation and the expression of a set of genes required to promote cell division.

Strikingly, some of the key Pygo2 target genes were also targets of the proto-oncogene c-myc. I therefore hypothesized that Pygo2 may interact with c-myc to promote the transcription of genes involved in cell division. I found that Pygo2 interacted with c-

myc and analysis of Pygo2/c-myc genes revealed that approximately one half of the Pygo2 target genes were also co-occupied by c-myc. Furthermore, Pygo2 co-localized with c-myc in both nuclei as well as presumptive nucleoli. These results suggest that Pygo2 may promote chromatin remodeling of a transcriptional program with c-myc that is required for both cell growth and cell division.

Chapter 2: Wnt/β-catenin dependent acetylation of Pygo2 by CBP/p300 histone acetyltransferase family members[1]

[1] A version of this Chapter has been published in: Andrews, P.G. and Kao K.R. Wnt/β-catenin-dependent acetylation of Pygo2 by CBP/p300 histone acetyltransferase family members. Biochemical Journal 473(22), pp. 4193-4203, 2016.

2.1 Introduction

The canonical wingless (Wg)/Wnt signal transduction cascade plays important roles during normal embryonic and adult tissue development and maintenance. Its deregulation at several levels can lead to multiple cancer phenotypes (Clevers & Nusse, 2012). Wnt target gene transcription relies on the activation of β-catenin, which is normally associated with the E-cadherin cytoskeleton or kept at low levels in the cytoplasm through the action of a destruction complex. Interaction of the Wnt ligand with the Frizzled/LRP co-receptor complex inhibits the destruction complex, releasing β-catenin from ubiquitin dependent proteosomal degradation. By an incompletely understood mechanism, cytoplasmic β-catenin translocates to the nucleus where it associates with Wnt target genes via TCF/LEF DNA binding proteins. Its interaction with a number of chromatin remodeling factors including Bcl9/Pygopus (Pygo) promote enhancer/promoter interactions and euchromatin formation required for transcription, reviewed in (Clevers & Nusse, 2012; Mosimann *et al*, 2009; Valenta *et al*, 2012; Clevers *et al*, 2014).

Classically, histone acetytransferases (HATs) promote nucleosomal relaxation and the formation of transcriptionally active euchromatin through the catalytic transfer of acetyl groups from acetyl-coenzyme A to ε-amino groups of positively charged lysine residues within the N-terminal tails of histones. Conversely, several families of histone deacetylases (HDACs) promote transcriptionally silent heterochromatin through the removal of the acetyl groups from histones, thereby restoring the positively charged lysine residues required for the strong interaction with the negatively charged DNA.

Furthermore, lysine residues of non-histone proteins are targets of acetylation resulting in consequent positive and negative effects on a plethora of cellular processes (reviewed in: (Choudhary *et al*, 2014; Close *et al*, 2010; Verdin & Ott, 2014)).

Nuclear histone acetyltransferases can be divided into CBP/p300, GCN5 related N-acetyltransferases (GNATs) and MOZ, Ybf2, Sas3, Sas2, Tip60 (MYST) subfamilies. Many transcription factors require the HAT catalytic activity of CBP/p300 to promote an open chromatin structure at the vicinity of active target genes, likely by targeting residues such as lysine 27 on histone H3 (H3K27), which associate with active gene enhancers and prevent polycomb-repressor complex mediated silencing (Tie *et al*, 2009). GNATs also affect histone acetylation on a global scale by targeting the histone residues such as H3K9 and H3K14 (Nagy & Tora, 2007). Therefore, it is not surprising that HATs are recognized as important targets for the development of anti-cancer therapies (Dawson & Kouzarides, 2012).

It is well established that HATs are integral to Wnt-signalling mediated gene expression. For instance, CBP is an essential player in promoting widespread chromatin remodeling at the vicinity of Wg target genes (Parker *et al*, 2008). However, the exact role of CBP/p300 in Wnt signalling is complicated and in certain instances, CBP and p300 can either activate or repress Wnt target gene transcription (Li *et al*, 2007b), not surprising given their classical roles as tumor suppressors. The context-dependent Wnt activation of target genes likely occurs through the usage of CBP or p300 by β-catenin, which can have distinct phenotypic outputs, such as proliferation versus differentiation (Ma *et al*, 2005). These variable activities may in part result from the direct acetylation of

β-catenin by different HATs, including CBP and p300. For example, acetylation of β-catenin by CBP inhibits c-myc transcription (Wolf *et al*, 2002), while acetylation of β-catenin by p300 increases its association with TCF4 and correlates with Wnt target gene activation (Lévy *et al*, 2004). Acetylation and stabilization of β-catenin by the p300 CBP associated factor (PCAF) is also important for β-catenin stabilization and Wnt target gene transcription (Ge *et al*, 2009).

Pygopus (Pygo) was described as a dedicated component of the Wnt/β-catenin transcription complex in *Drosophila*, tethered to β-catenin through Legless/Bcl-9 (Kramps *et al*, 2002; Thompson *et al*, 2002). In vertebrates two Pygo orthologs exist, with Pygo2 being the more well characterized protein, having both Wnt-dependent and Wnt-independent roles (Song *et al*, 2007). Currently, Pygo is postulated to act as a chromatin "effector", in which it binds active H3K4me3 marks through its plant homeodomain (PHD; Fiedler *et al*, 2008), resulting in an induction of open chromatin structure by the recruitment of HATs by its N-terminal homology domain (NHD; Andrews *et al*, 2009; Chen *et al*, 2010).

The role of Pygo2 in the active TCF/LEF complex may be to recruit HATs, such as CBP/p300 and GCN5 and position them so they can co-operatively bind to β-catenin, required for histone acetylation and Wnt target gene transcription. How Pygo2 is prompted to affect the euchromatic conformation is not completely known. I therefore examined the interactions of Pygo2 with HATs and found that Pygo2 itself was a substrate for CBP/p300-mediated acetylation at specific N-terminal homology domain

(NHD) lysine residues when indirectly bound to β-catenin, thereby suggesting that Pygo acetylation may be important for its role in Wnt target gene activation.

2.2 Materials and methods

2.2.1 Cells and antibodies

Hela S3 and HEK-293 cells were obtained from the American Type Tissue Collection and cultured in Dulbecco's Modified Eagle Medium supplemented with 10% fetal bovine serum. Antibodies used included: Pygo2 (Tzenov *et al*, 2015), Bcl9 (Kennedy *et al*, 2010), Pygo2 (Abe109) and H3K4me3 were from Millipore, Myc (9E10), p300 (N-15) and CBP (C-20) and were from Santa Cruz Biotechnology, Flag M2 and β-actin were from Sigma Aldrich, acetylated lysine antibodies (9441) were from Cell Signalling Technology.

2.2.2 Plasmids and transfections

Plasmids used included: pCMV, pCMV-CBP, pCMV-CBP Bro-q and pCS2+-β-catenin (Andrews *et al*, 2009). pcDNA p300 and pcDNA p300-HAT were gifts from Warner Greene (Addgene plasmids 23252 and 23254, respectively; Chen *et al*, 2002), pCI flag-PCAF was a gift from Yoshihiro Nakatani (Addgene plasmid 8941; Yang *et al*, 1996) and pCMV-flagGCN5 was a gift from Sharon Dent (Addgene plasmid 23098; Martínez-Balbás *et al*, 2000). Full length Myc-tagged Pygo2 and myc-tagged Pygo2 deletions were PCR amplified from pCS2+-Pygo2 (Popadiuk *et al*, 2006) and subcloned into pCS4+myc. Pygo2 ΔPHD (AA. 1-312) and Pygo2 ΔNHD (AA. 74-406) were PCR amplified from pCS2+-Pygo2 using F-5'- GTCCCCCACTCCATGGCCGCCTCG, R-5'- TCAGCCAGGGGGTGCCAAGCTGTTG and F-5'- GCATCCAACCCTTTTGAAGATGAC, R-5'- TCACCCATCGTTAGCAGCC,

respectively and inserted into pCS4+myc. All Pygo2 K-R and K-Q mutants were constructed using the Quickchange Site Directed Mutagenesis Kit (Stratagene). Bcl9 HD1 domain was PCR amplified from a human testis cDNA library (Stratagene) and inserted into pGEX4T1 using the primer sequences: F-5'-CACTCGATGACCCCATCAAATGCTACAGCC and R-5'-CCGAAGGGCAGATATCTGTGTGTTCAGAGG. All Plasmids were verified by sequencing.

Plasmids were transfected using Lipofectamine and Plus Reagent (Invitrogen), as per the manufacturers' instructions. TCF-dependent (OT/OF) reporter assays were performed exactly as described (Andrews *et al*, 2009), using pGL3-OT (wild type TCF binding sites) and pGL3-OF (mutant TCF binding sites; Shih *et al*, 2000). Briefly, cells were co-transfected with either OT or OF reporters along with equal amounts of pRSV-βgal, pCS2-βcatenin and pCS2-Pygo2 constructs. Luciferase assays were performed with the Luciferase Assay System (Promega) and values were normalized to β-galactosidase activity and expressed as ratios of OT/OF. All experiments were repeated three times. P-values were calculated using one-way analysis of variance (ANOVA), using Tukey's multiple comparison test.

2.2.3 RNA extraction and RT-qPCR

Approximately 2μg of RNA was extracted using the RNeasy kit (Qiagen) and was used to make cDNA with the Moloney Murine Leukemia Virus (MMLV) Reverse

Transcriptase kit (Invitrogen) using random hexamer primers, as per the manufacturers' protocols. For RT-qPCR analysis reactions used RT2 SYBR Green master mix (Qiagen). Relative values were calculated using the $2^{-\Delta\Delta Ct}$ method normalized to β-actin expression. Axin2 (Li & Wang, 2008) primers and β-actin (Andrews *et al*, 2013) primers were previously described. P-values were calculated using one-way ANOVA, using Tukey's multiple comparison test.

2.2.4 Immunoprecipitation, GST-pulldown assays and immunoblotting

Proteins were extracted in radioimmunoprecipitation assay (RIPA) buffer (1.1% triton X-100, 0.01% SDS, 1.2mM EDTA, 16.7mM Tris pH8.1 and 167mM NaCl) supplemented with 1X protease inhibitors, 1mM phenylmethylsufonyl fluoride and 10mM sodium butyrate. Immunoprecipitations and immunoblots were performed exactly as described (Andrews *et al*, 2013). Briefly, immunoprecipitates or approximately 50μg of protein was denatured in Laemmli sample buffer and separated by sodium dodecyl sulfate poly acrylamide gel electrophoresis (SDS-PAGE) and transferred to polyvinylidene fluoride membranes. Membranes were then probed with primary and secondary antibodies in tris buffered saline with 0.1% tween 20 and 5% skim milk powder. Bands were detected by chemilumenescence using Clarity western blot substrate (Biorad) and exposed to autoradiography film.

For immunoprecipitations, protein complexes were captured from approximately 500μg of cell extract and 1-2μg of antibody using either protein A or protein G agarose

beads. Bound proteins were washed three times with RIPA buffer and two times with 150mM sodium chloride and eluted using Laemmli sample buffer.

GST-pulldown assays were performed as described (Andrews *et al*, 2009). Approximately 1μg of purified GST proteins grown in Rosetta (Novagen) competent cells were purified using glutathione sepharose 4B beads (GE Biosciences). Purified proteins were incubated with HEK-293 cell extracts that were transfected with either myc-Pygo2 or myc-Pygo2 and CBP, beads were washed three times with RIPA and twice with sodium chloride and eluted with Laemmli sample buffer, resolved by SDS-PAGE and immunoblots were performed using anti-myc antibodies. After immunoblotting, membranes were stained with Ponceau S (Sigma Aldrich). All experiments were repeated at least three times.

2.2.5 Immunofluorescence and quantification of Pygo2 localization

Immunofluorescence was performed exactly as described (Andrews *et al*, 2013). Briefly, cells were grown on chamber slides and fixed with 4% paraformaldehyde. Fixed cells were permeabilized with 0.02% trition X-100 in phosphate buffered saline (PBS). Cells were blocked in 10% normal goat and/or donkey serum. Primary and secondary (Dylight 488 or Dylight 594 conjugated; Jackson Immunoresearch) antibodies were diluted in 1.5% normal serum. Finally, cells were incubated with 4',6-diamidino-2-phenylindol (DAPI) and mounted in PBS containing 10% glycerol. Images were taken using a FluoView FV1000 confocal microscope (Olympus).

For quantification of nuclear and nuclear/cytoplasmic Pygo2, HEK-293 cells were co-transfected with either CBP or p300 along with empty vector (myc) or myc-tagged Pygo2. Cells that were co-stained with myc and CBP or p300 were scored from three random fields per experiment with a total number (N) of 573 for EV, 187 for CBP and 205 for p300. Results shown are means and standard deviations from three separate experiments, p-values were calculated using one-way ANOVA, using Tukey's multiple comparison test.

2.3 Results

2.3.1 Pygo2 acetylation is synchronous with β-catenin binding and transcriptional activation

Current evidence suggests that Pygo2 functions in the TCF/β-catenin transcriptional complex to aid in the recruitment of HATs required for target gene transcription (Andrews *et al*, 2009; Chen *et al*, 2010). In this context, HATs promote acetylation of both histone N-terminal tails, as well as other Wnt transcriptional components to facilitate transcription. For example, acetylation of β-catenin by CBP/p300 correlates with an increased affinity for TCF4 and is associated with transcriptional activation (Lévy *et al*, 2004). I therefore hypothesized that Pygo2 may also be acetylated when present in a complex with β-catenin. HeLa S3 cells were treated with LiCl over a time course of six hours to activate TCF/β-catenin dependent transcription of the Wnt-activated gene *Axin2* (Figure 2.1A). Maximum expression of *Axin2* mRNA in response to LiCl occurred four hours after treatment ($p<0.01$), correlating with an increase in β-catenin protein, while Pygo2 and Bcl9 expression showed no change in expression (Figure 2.1B; upper panel). Interestingly, there was a repression of Axin2 expression at the one hour timepoint. Since Axin2 acts as a feedback repressor of activated β-catenin (Leung *et al*, 2002), this may reflect a compensatory mechanism to prevent feedback of the pathway at early timepoints following stimulation.

Endogenous Pygo2 protein was immunoprecipitated at each time point and immunoblots were performed to analyze potential Pygo2 acetylation, as well as its

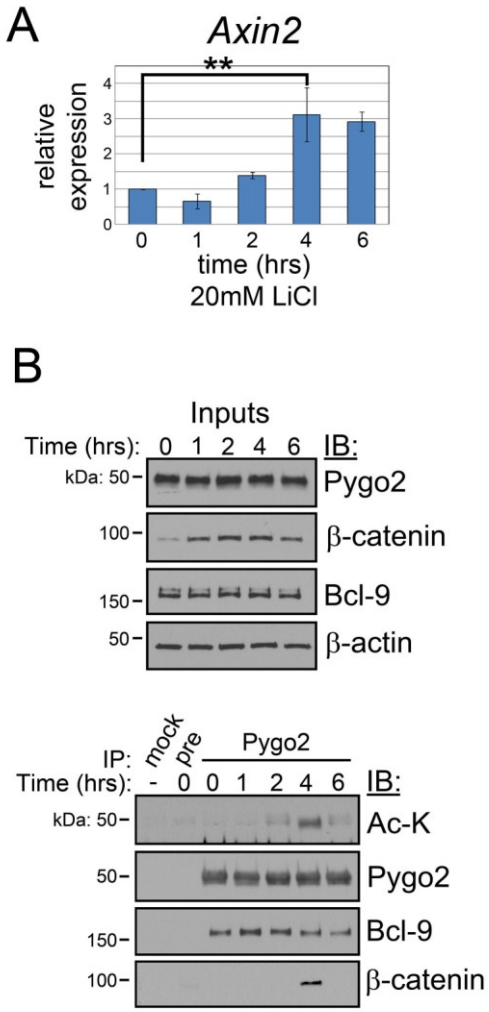

Figure 2.1. Pygo2 acetylation correlates with β-catenin dependent transcription. (A) Temporal analysis of Wnt target gene *Axin2* by RT-qPCR in response to 20mM LiCl in HeLa S3 cells. Bar graphs indicate means +/- SD. (**p<0.01; **B)** Pygo2 acetylation correlates with its interaction with β-catenin. Relative inputs are shown in the upper panel. Immunoprecipitation (IP) of endogenous Pygo2 protein from HeLa S3 cells that were treated with 20mM LiCl for various timepoints, followed by immunoblotting (IB) with antibodies recognizing acetylated Lysine (Ac-K), Bcl9, Pygo2 and β-catenin (lower panel). β-actin was used as a loading control.

interactions with Bcl9 and β-catenin (Figure 2.1B; lower panel). Pygo2 binding to Bcl9 did not change significantly in response to LiCl treatment, indicating that their interaction is largely independent of active TCF signalling. Interestingly, Pygo2 was acetylated four hours after LiCl treatment, coinciding with its association with β-catenin binding and *Axin2* transcriptional activation. Pygo2 was weakly acetylated at both two and six hours after LiCl treatment, straddling its association with β-catenin at the 4hr timepoint. These observations suggested that temporal acetylation of Pygo was primarily dependent on the formation of active TCF/β-catenin transcription complexes, however they do not preclude the possibility that Pygo2 may be acetylated in the absence of a detectable interaction with β-catenin.

2.3.2 Pygo2 is acetylated specifically by CBP/p300 family members

The association of Pygo2 acetylation with TCF/β-catenin dependent transcription prompted a further investigation of the interactions of Pygo2 with HATs such as CBP and GCN5. Like that of CBP and GCN5, I found that Pygo2 interacted with both the related family members PCAF (GNAT family) and weakly with p300 (CBP/p300 family; Figure 2.2). The interaction of Pygo2 with the different HAT families raised the possibility that Pygo2 is targeted for acetylation by multiple HATs. Myc-Pygo2 was therefore co-transfected with the HATs: CBP, p300, PCAF and GCN5 (Figure 2.3A). Acetylated Pygo2 was detected at the highest level when CBP was co-transfected, but was also present when p300 was co-transfected. On the other hand, acetylated Pygo2 was undetectable when GCN5 or PCAF was co-transfected, while both GCN5 and PCAF

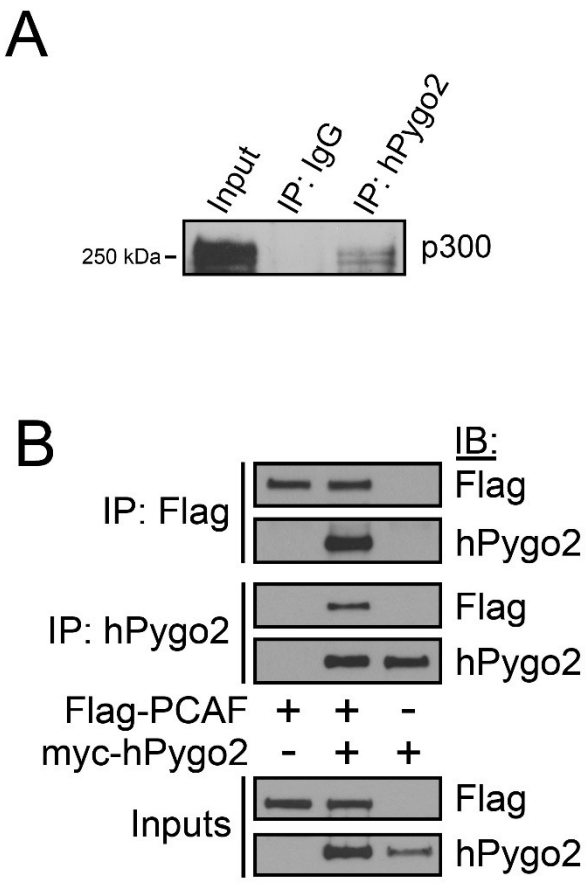

Figure 2.2. Pygo2 interacts with p300 and PCAF. (A) Endogenous Pygo2 was immunoprecipitated from HEK-293 cells and the interaction with p300 was detected by immunoblotting. (B) HEK-293 cells were co-transfected with myc-Pygo2 and Flag-PCAF, immunoprecipitations were performed with myc and Flag and show the interaction between Pygo2 and the HAT PCAF.

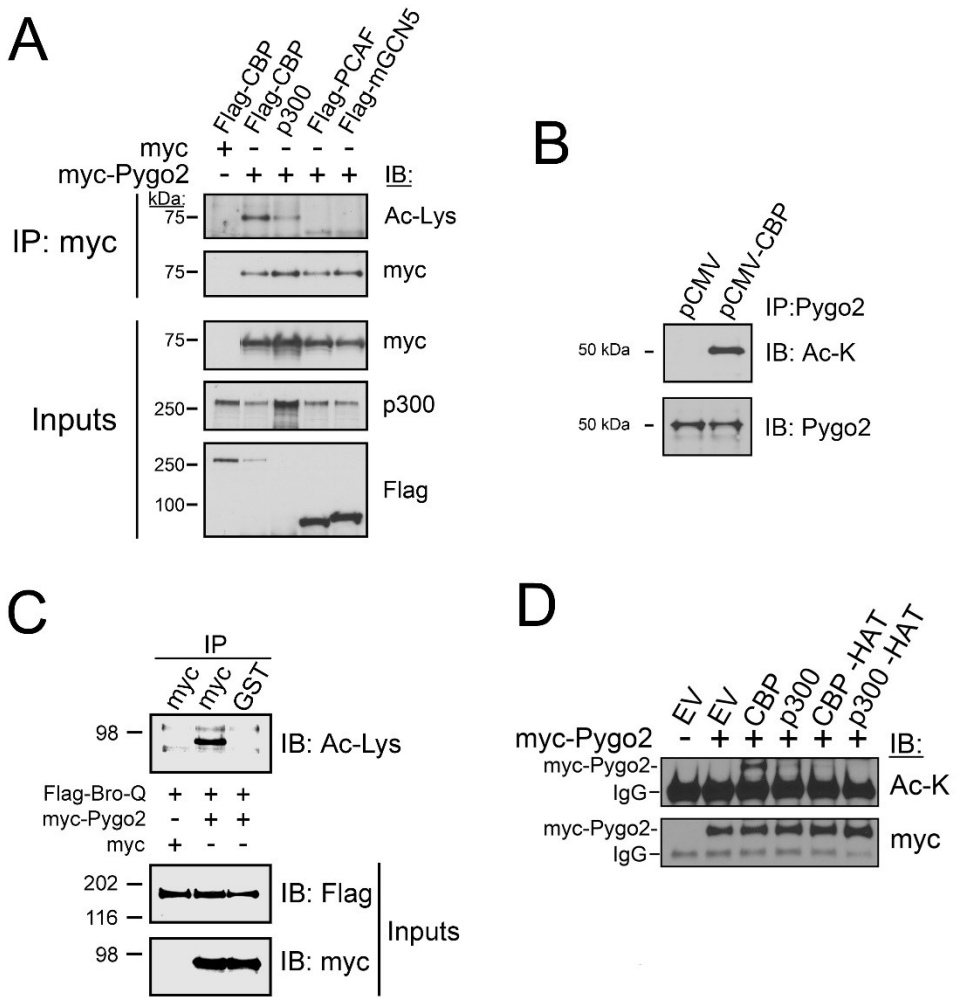

Figure 2.3. Pygo2 is acetylated by the CBP/p300 family of HATs. (A) Immunoprecipitation of myc-Pygo2 from HEK-293 cells that were co-transfected with CBP, p300, PCAF or GCN5, demonstrating that Pygo2 is acetylated by CBP/p300 family members (upper panel). Relative inputs are shown in the lower panel. (B) Immunoprecipitation of endogenous Pygo2 from HEK-293 cells that were transfected with either pCMV or pCMV-CBP, showing the acetylation of endogenous Pygo2 by CBP. (C) HEK-293 cells were co-transfected with myc-Pygo2 and a catalytic fragment of CBP (Flag-Bro-Q), immunoprecipitations were performed with anti-myc or anti-GST as a negative control and probed with an anti-acetyl lysine antibody. (D) Immunoprecipitation of myc-Pygo2 from HEK-293 cells that were co-transfected with either wild-type CBP and p300 or HAT mutated (-HAT) CBP and p300, followed by immunoblotting for Ac-K and myc. IgG denotes the relative position of the IgG heavy chain.

acetylated c-myc (Figure 2.4) as a positive control (Patel *et al*, 2004). Therefore, these results indicated that Pygo2 was specifically acetylated by CBP/p300 family members. Endogenous Pygo2 protein was strongly acetylated when we introduced CBP into HEK293 cells confirming *in vivo*, the foregoing observations (Figure 2.3B). Moreover, when exogenous myc-Pygo2 was introduced along with the catalytic HAT domain-containing fragment of CBP (Bro-Q) in HEK293 cells, acetylated myc-Pygo2 was readily detectable by immunoprecipitation with anti-myc, but not anti-GST as a negative control (Figure 2.3C).

Finally, to show that acetylation of Pygo2 was specific to CBP and p300 family members, catalytic HAT domain mutants of CBP and p300 were co-transfected with myc-Pygo2, resulting in a significant decrease in the amount of detectable Pygo2 acetylation (Figure 2.3D). These results indicated that while it is possible for Pygo2 to bind to multiple HATs, it was acetylated specifically by CBP and p300.

2.3.3 NHD lysine residues of Pygo2 are targeted for CBP and p300 dependent acetylation

To determine the regions of Pygo2 that were acetylated by CBP/p300, two Pygo2 mutants were used in which either the NHD or PHD domain was deleted (Figure 2.5A). The PHD-deleted mutant (ΔPHD) was detectably acetylated, indicating that CBP could acetylate Pygo2 directly, independent of its interaction with Bcl9/β-catenin. Consistent with this observation, acetylation of a Bcl9 binding mutant of Pygo2 was not significantly different compared to wild-type Pygo2 (Figure 2.6A). However, acetylation of ΔPHD

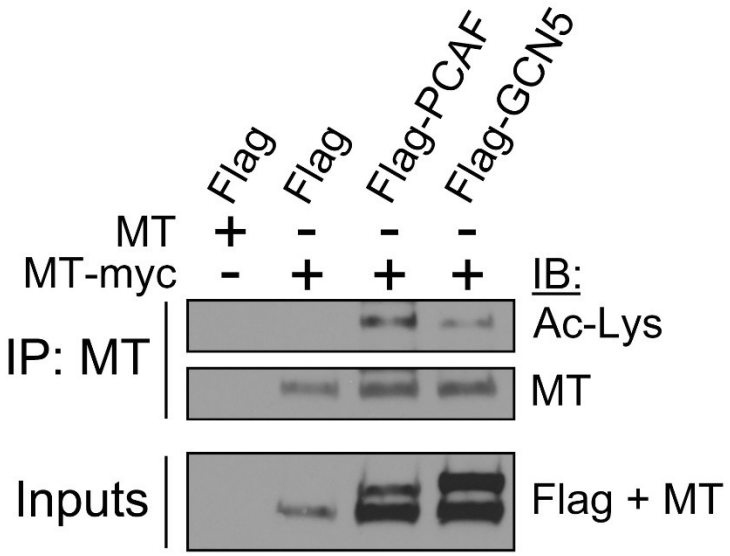

Figure 2.4. PCAF and GCN5 acetylate myc. To demonstrate that overexpressed PCAF and GCN5 constructs are catalytically functional, HEK-293 cells were co-transfected with the bonafide PCAF/GCN5 substrate c-myc. Myc-tagged c-myc (MT-myc) was immunoprecipitated with anti-myc antibodies and immunoblots were performed with anti-acetylated Lysine antibodies to demonstrate acetylation of c-myc by PCAF/GCN5.

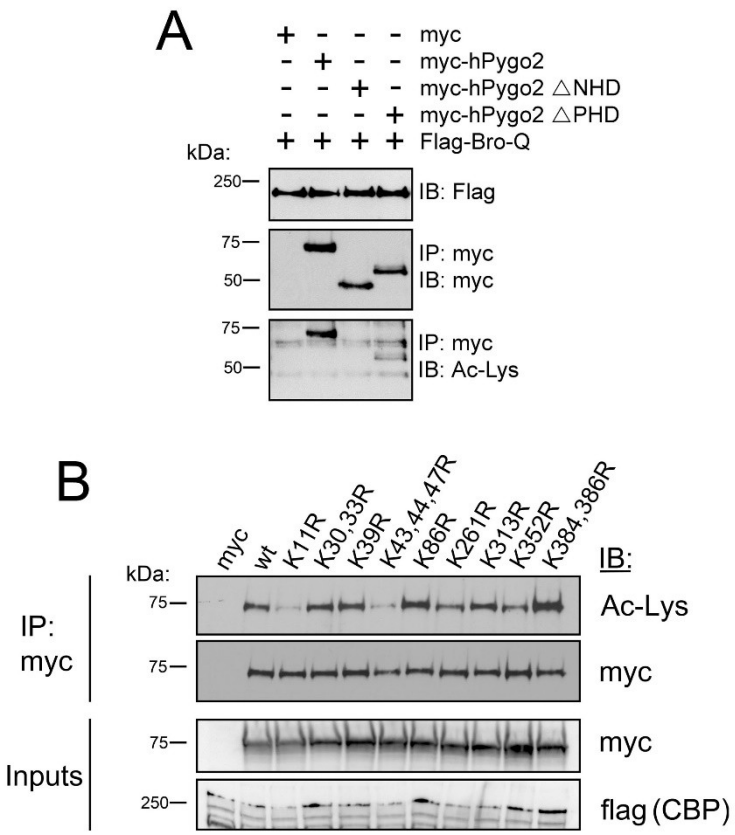

Figure 2.5. Pygo2 acetylation requires the NHD and is acetylated at specific NHD lysine residues. (A) The Bro-Q domain of CBP (Flag tagged) was co-transfected with myc-tagged wild-type Pygo2, Pygo2 lacking the NHD (ΔNHD), or Pygo2 lacking the PHD (ΔPHD), immunoprecipitations were performed with anti-myc and immunoblots were performed with Ac-K and myc. **(B)** Immunoprecipitation of myc-Pygo2 lysine-Arginine (K-R) point mutants from HEK-293 cells that were co-transfected with CBP, followed by immunoblotting for Ac-K.

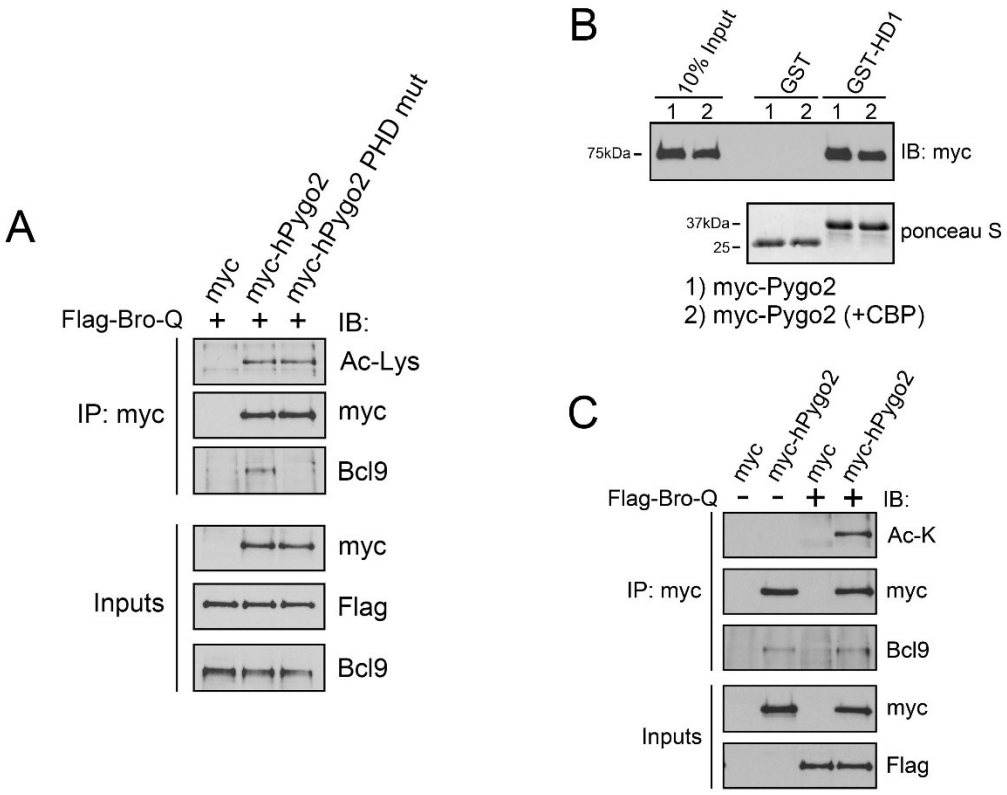

Figure 2.6. **Acetylation of Pygo2 does not affect Bcl9 binding. (A)** Myc-Pygo2 and a Bcl-9 binding mutant of Pygo2 (PHD mut; T363A, A366V) were immunoprecipitated from HEK-293 cells that were co-transfected with CBP Bro-Q, relative Pygo2 acetylation was assessed by immunoblotting. **(B)** GST-pulldown analysis of Pygo2 (with and without CBP) and GST-HD1 of Bcl9, showing no differences in the ability of Pygo2 to bind to the HD1 region of Bcl9 (**C)** Myc or myc-Pygo2 was immunoprecipitated from HEK-293 cell extracts that were co-transfected with either empty vector or CBP Bro-Q and the relative binding of endogenous Bcl9 to Pygo2 or acetylated Pygo was assessed by immunoblot.

was lower compared to its wild-type counterpart, indicating that its interaction with H3K4me2/3 may be important for complete Pygo2 acetylation by CBP. In contrast, the NHD region was essential for direct Pygo2 acetylation by the catalytic fragment of CBP, consistent with the observation that Pygo2 interacts with CBP through its NHD.

To identify the acetylation sites, single point mutants of Pygo2 were constructed substituting Lysine residues with Arginine, which cannot be acetylated, while maintaining the positive charge. When the Pygo2 K-R mutants were co-transfected with full length CBP, acetylation was qualitatively reduced in two Pygo2 constructs. One construct contained a single Arginine substitution at Lysine 11 (K11R), consistent with the findings of a study that identified more than 8100 acetylation sites in HeLa cells (Scholz *et al*, 2015), while the other construct contained three Arginine substitutions at Lysines 43, 44 and 47 (K43, 44, 47R; Figure 2.5B). Together, these results indicated that Pygo2 was highly acetylated at specific residues of its NHD, where it interacts with CBP.

2.3.4 Pygo2 complex formation with Bcl9/β-catenin and HATs occurs independently of Pygo2 acetylation

Since Pygo2 acetylation correlated with binding to β-catenin and transcriptional activation of *Axin2* (Figure 2.1), I hypothesized that Pygo2 acetylation may be a requirement for its association with other components in the active Wnt transcription complex. First the interaction of Pygo2 with Bcl9 was examined, since it is the primary link between Pygo and β-catenin (Kramps *et al*, 2002). LiCl treatment did not result in any change in the ability for Pygo2 to bind Bcl9 (Figure 2.1). To confirm that this interaction was independent of acetylation both *in vitro* GST-pulldowns were performed

using the Pygo binding HD1 domain, as well as immunoprecipitations from cells and I found no difference in the ability of acetylated Pygo2 to bind to Bcl9 (Figure 2.6B and C). This result suggested that Pygo2 acetylation does not affect its interaction with Bcl9 and hence its interaction with β-catenin.

For Wnt-mediated transcriptional activation Pygo2 binds HAT complexes in conjunction with β-catenin to promote chromatin remodeling. Indeed, overexpression of CBP (Figure 2.7A) and p300 (Figure 2.7B) correlated with both Pygo2 acetylation and increased GCN5 binding. Acetylation of Pygo2 and its association with GCN5 were significantly decreased in the presence of both CBP and p300 HAT mutants relative to wild type CBP and p300 (Figure 4.7A and Figure 4.7B). Thus, the interaction between Pygo2 and GCN5 correlated with CBP/p300-dependent HAT acetylation of Pygo2. Paradoxically, while Pygo2 was acetylated in the presence of only the Bro-Q catalytic fragment of CBP, the Pygo2-GCN5 interaction was, on the other hand, inhibited (Figure 2.7C). This suggests the increased interaction of Pygo2 with GCN5 was dependent on its association with full length CBP, rather than indiscriminate Pygo2 acetylation.

To further investigate the nature of its interaction with GCN5, Pygo2 was mutated with three Lysine substitutions (K11R, K43R, K44R; 3K-R) and tested for its ability to be acetylated by CBP and to interact with GCN5. While Pygo2 3K-R showed a significant reduction in CBP-mediated acetylation, the interaction of Pygo2 with GCN5 remained unaffected when immunoprecipitation assays were performed for both Pygo2 (myc) and GCN5 (Flag; Figure 2.8A). Consistently, an acetylation mimic of the same

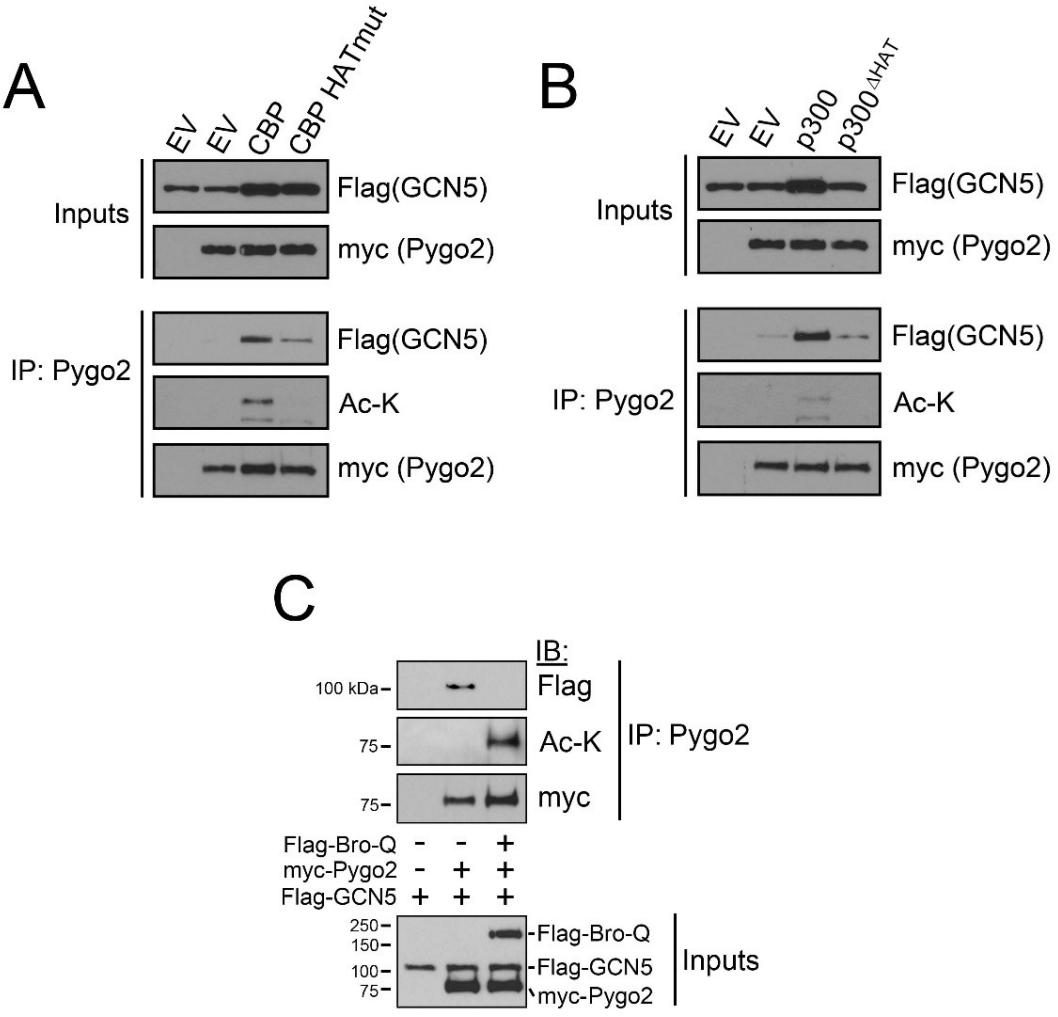

Figure 2.7. **CBP and p300 correlate with an increased binding of Pygo2 to GCN5.** **(A)** Immunoprecipitation of myc-Pygo2 from HEK-293 cells that were co-transfected with CBP or CBP HAT mutant (HAT mut), showing increased binding Pygo2 to GCN5, that requires catalytically active CBP, but is independent of Pygo2 acetylation. **(B)** Immunoprecipitation of myc-Pygo2 from HEK-293 cells that were co-transfected with p300 or p300 HAT mutant (ΔHAT), showing increased binding Pygo2 to GCN5, that requires catalytically active p300, but is independent of Pygo2 acetylation. **(C)** Immunoprecipitation of myc-Pygo2 from HEK-293 cells that were co-transfected with the catalytic C-terminal half of CBP (Flag-Bro-Q), showing the interaction between Pygo2 and GCN5 is inhibited.

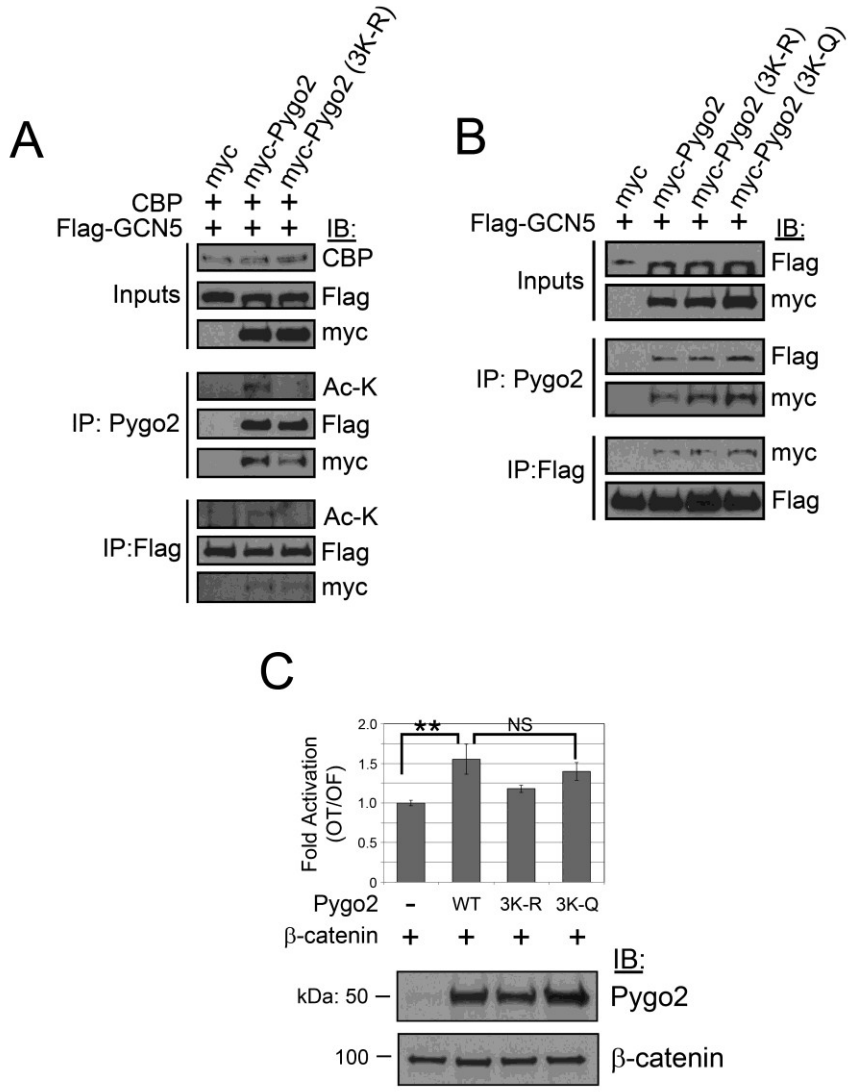

Figure 2.8. GCN5 binds to Pygo2 independent of Pygo2 acetylation. (A) Forward and reverse immunoprecipitations of myc-Pygo2 and a Pygo2 acetylation deficient mutant (3K-R) from HEK-293 cells that were co-transfected with Flag-GCN5 and CBP, showing acetylation of Pygo2 has little effect on its ability to bind GCN5. **(B)** Immunoprecipitation of myc-Pygo2, a Pygo2 acetylation deficient mutant (3K-R) and a Pygo2 acetylation mimic mutant (3K-Q) from HEK-293 cells that were co-transfected with Flag-GCN5, showing little effect on the ability of Pygo2 to bind GCN5. **(C)** Luciferase assay measuring TCF/β-catenin dependent transcription (OT/OF) in HEK293 cells co-transfected with wild-type (WT) and mutant Pygo2 constructs along with β-catenin (Top panel) and a representative immunoblot confirming the overexpression of Pygo2 and β-catenin (Bottom panel; **p<0.01, NS; not significant).

residues of Pygo2 (3K-Q) showed little difference in the ability of Pygo2 to bind to GCN5 (Figure 2.8B).

While acetylation was not required for GCN5 binding, to confirm its functional importance in complex formation, the ability for mutant Pygo2 to activate TCF-dependent transcription was tested in the presence of β-catenin in HEK293 cells. As expected, the acetylation mimic Pygo2 mutant (3K-Q) activated TCF dependent transcription to similar levels as wild-type ($p<0.01$), while acetylation defective Pygo2 (3K-R) showed little activation of TCF dependent transcription, compared to the control (p=NS; Figure 2.8C).

These observations confirmed that GCN5 interacts with Pygo2 independently of its acetylation status, and suggest that while CBP/p300–dependent acetylation of Pygo2 is associated with active Wnt complex formation, it is not specifically required for interaction with individual components of the complex.

2.3.5 Regulation of Pygo2 subcellular localization by p300 mediated acetylation

Mutation analyses revealed that Pygo2 was acetylated by CBP at residues K43, 44 and 47, encompassing the putative Pygo2 nuclear localization sequence (NLS; Figure 2.5). Furthermore, we determined that Lysine 44 was important for Pygo2 nuclear localization, when substituted with Arginine (Figure 2.9). To test whether sub-cellular localization affected Pygo2 acetylation, an unrelated Pygo2 NLS mutant (RRK-AAA) was transfected, which is retained in the cytoplasm (Figure 2.10A), and showed no differences in acetylation compared to wild type Pygo2 (Figure 2.10B). While these

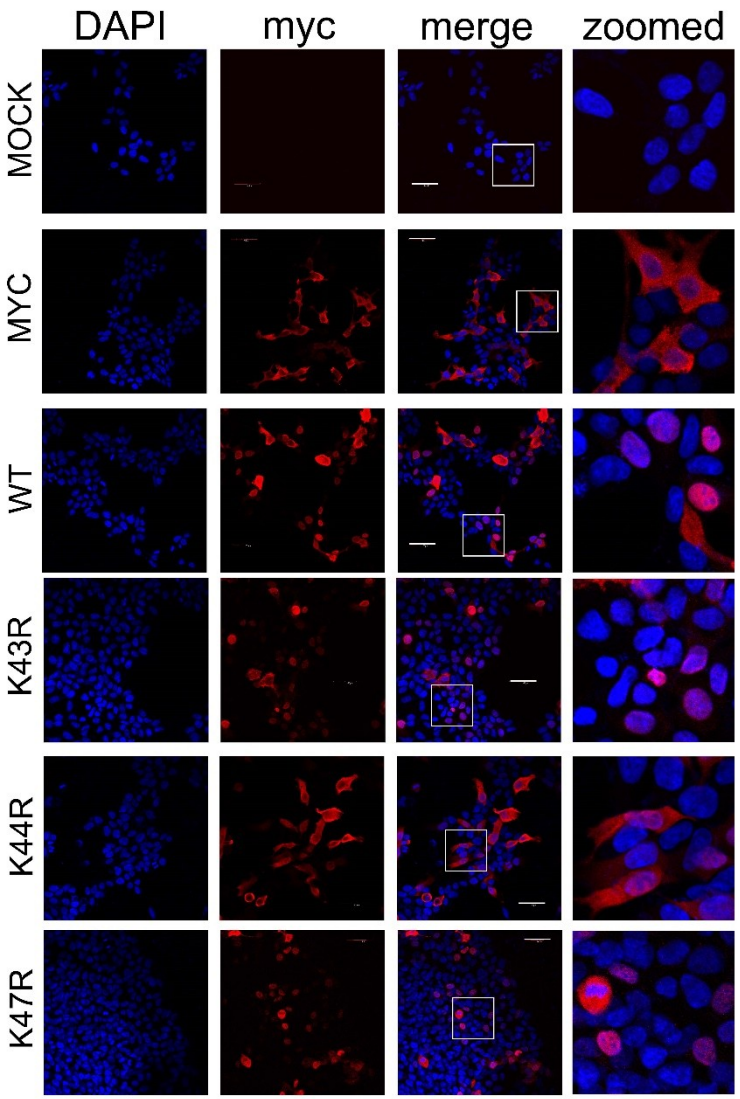

Figure 2.9. Subcellular localization of myc-Pygo2 K->R mutants in HEK-293 cells. 293 cells were transiently transfected with myc-Pygo2 K-R mutants and were visualized by immunofluorescence, revealing that lysine 44 is important for Pygo2 nuclear localization. DAPI was used to stain and visualize the nuclei. Scale bar = 50μm.

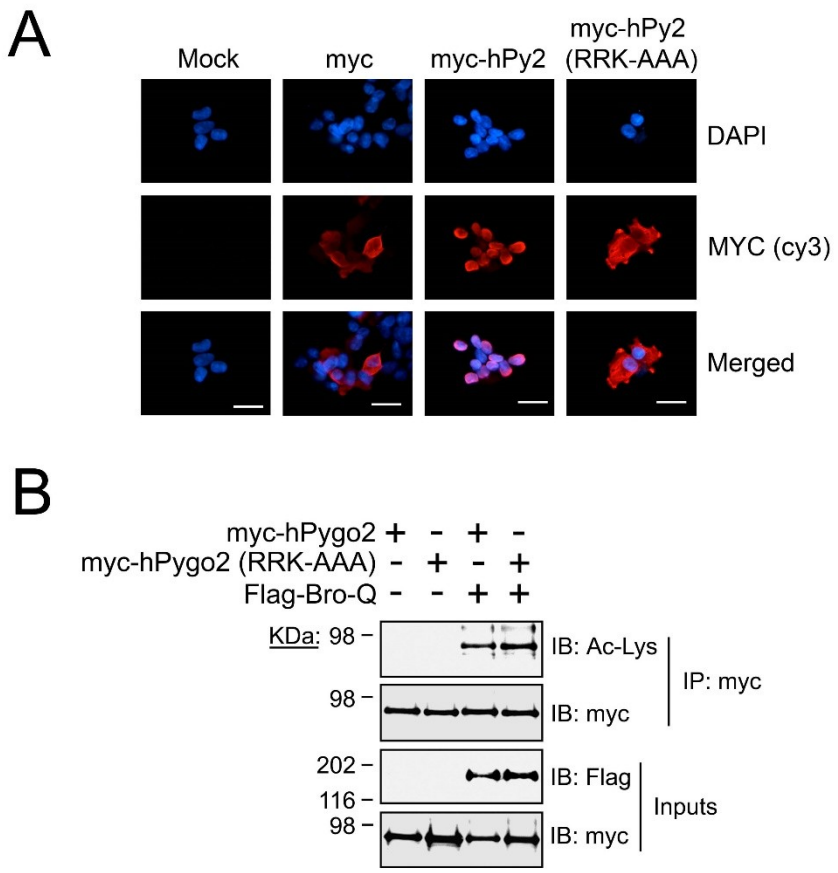

Figure 2.10. **Cytoplasmic Pygo2 can be acetylated by CBP. (A)** HEK-293 cells were transfected with myc-Pygo2 and myc-Pygo2 with an NLS mutation (RRK-AAA), confocal images show cytoplasmic localization of myc-Pygo2 (RRK-AAA), scale bar = 20μm. **(B)** Cytoplasmic Pygo2 is acetylated by CBP. HEK-293 cells were co-transfected with wild type myc-Pygo2 or NLS mutant myc-Pygo2 (RRK-AAA) along with the catalytic region of CBP (Flag- Bro-Q), myc-Pygo2 were immunoprecipitated and immunoblotted using anti-acetyl lysine, showing little difference in acetylation of nuclear or cytoplasmic Pygo2.

results do not indicate in which subcellular compartment Pygo2 is acetylated, they suggest that subcellular localization of Pygo2 may not important for direct CBP mediated acetylation.

On the other hand, I investigated whether acetylation of Pygo2 affected subcellular localization. Initially, I determined whether CBP or p300 could alter the subcellular localization of Pygo2. When wild type myc-Pygo2 was co-transfected with empty vector or CBP, approximately 80% of the cells displayed nuclear retention of myc-Pygo2 protein with the remaining 20% showing distribution to both cytoplasm and nucleus ($p<0.001$; Figure 2.11; lower panel). However, co-transfection of Pygo2 with p300, resulted in a marked increase in the proportion of cells with cytoplasmic Pygo2 ($p<0.001$), suggesting that acetylation of Pygo2 by p300 may promote cytoplasmic Pygo2 subcellular shuttling.

I next tested whether preventing CBP/p300 mediated acetylation of NLS residues could affect Pygo2 subcellular localization. Construction of additional single K-R point mutants revealed that mutation of Lysines 43 and 44 resulted in a reduced acetylation of Pygo2 (Figure 2.12A). Consistent with a potential role in subcellular localization, all three acetylation mimic mutants of the two NLS Lysines (K43Q, K44Q and K43, 44Q) rendered Pygo2 cytoplasmic (Figure 2.12B), thereby suggesting that acetylation of any one of these residues by p300 promotes cytoplasmic localization of Pygo2.

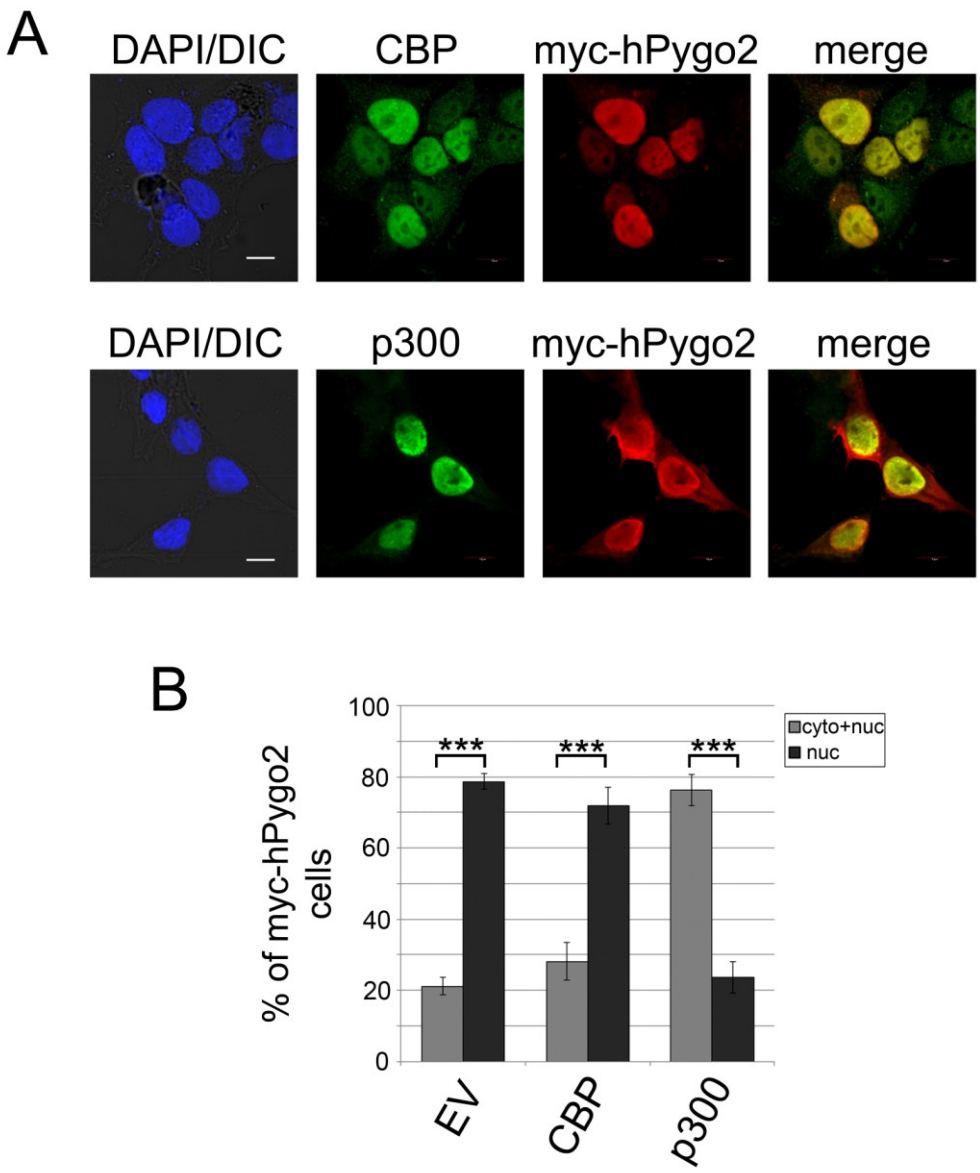

Figure 2.11. p300 targets a fraction of Pygo2 to the cytoplasm. HEK-293 cells were co-transfected with myc-Pygo2 along with empty vector, CBP or p300 and myc cells were scored based on the nuclear or nuclear + cytoplasmic staining, results represent means +/- standard deviation (bottom panel). Representative confocal images showing staining of myc-Pygo2 with CBP or p300 are in the top panel. Scale bar = 5μm (***$p<0.001$).

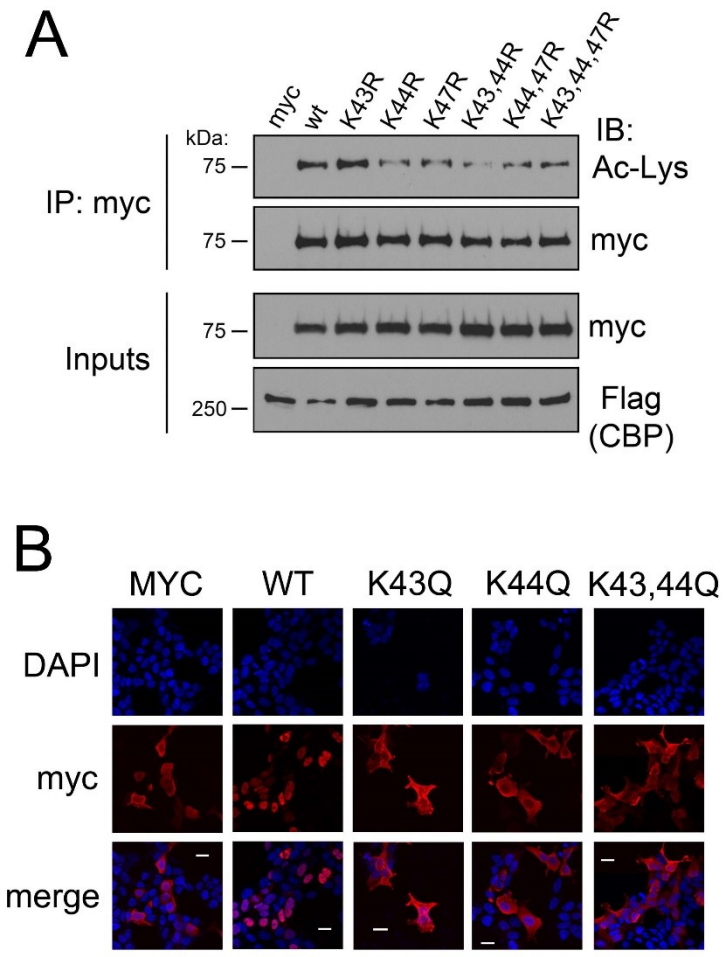

Figure 2.12. Acetylation of Pygo2 NLS lysines. (A) Immunoprecipitation of myc-Pygo2 NLS point mutants from HEK-293 cells that were co-transfected with CBP, immunoblots were performed with anti-Ac-K antibodies. **(B)** Sub-cellular localization of myc-Pygo2 acetylation mimic mutants, showing that K43 or K44 targeted acetylation alone or in combination results in cytoplasmic localization. DAPI was used to stain and visualize the nuclei. Scale bar = 20μm.

2.4 Discussion

Our group previously demonstrated that CBP was associated with Pygo2 dependent transcriptional activation (Andrews *et al*, 2009). In concordance with this finding, I demonstrated that Pygo2 is functionally regulated by CBP/p300 mediated acetylation and is associated with Wnt-dependent *Axin2* gene activation. It is likely that recruitment of CBP/p300 by the β-catenin-Bcl9-Pygo complex is required to promote an amenable conformation necessary to accommodate Pygo2 acetylation. While coupled to active β-catenin, I propose that upon recruitment of CBP/p300, Pygo2 acetylation occurs concurrent with histone acetylation, consistent with widespread histone acetylation associated with CBP observed at Wg target genes (Parker *et al*, 2008). These observations suggest that the association of Pygo2 with CBP/p300 may be required to initiate active β-catenin complex assembly. While Pygo2 acetylation does not appear to be required for complex assembly, it may occur as a result of active complex formation which is likely coupled to histone acetylation (Figure 2.13, panel *i*) and may play a role in subsequent dissociation and shuttling of Pygo2-associated complexes from Wnt target genes following transcriptional initiation (Figure 2.13, panel *ii*).

Non-redundant usage of CBP and p300 by β-catenin can result in different and distinct outcomes (Ma *et al*, 2005; Teo & Kahn, 2010); interestingly, the utilization of CBP by β-catenin can result in cell proliferation, but with p300, in differentiation. Similarly, the alternate acetylation of Pygo2 by CBP and p300 might also be related to different cellular outcomes. For example, Pygo2 acetylation by p300 promoted a fraction

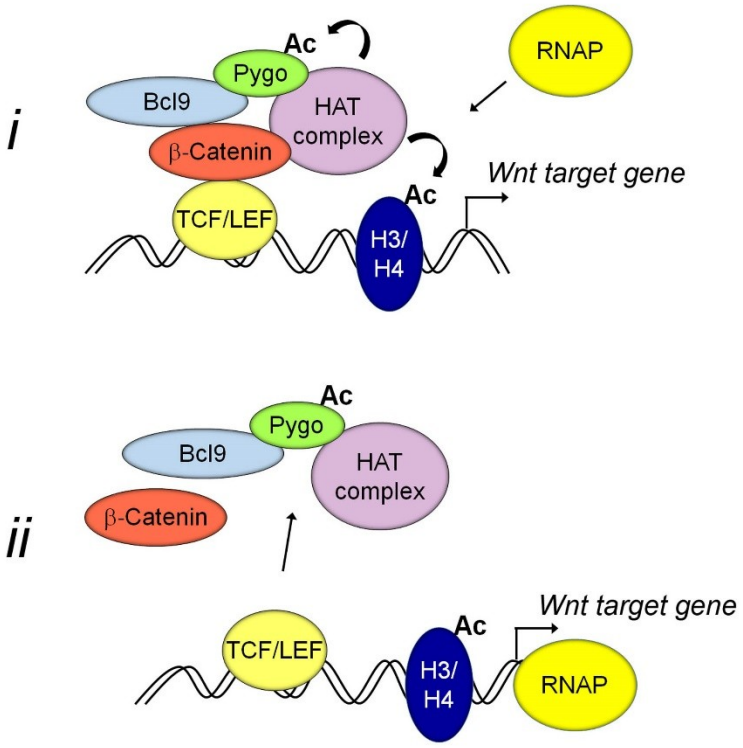

Figure 2.13. Proposed model of Pygo2 acetylation. (*i*) HAT complex recruitment by Pygo2 results in transcriptional initiation/activation, as well as associated Pygo2 and histone acetylation. (*ii*) Acetylated Pygo2 complex dissociates from chromatin immediately following initiation of transcription.

of Pygo2 to localize to the cytoplasm (Figure 2.11), perhaps relating to a differentiation-like phenotype. On the other hand, Pygo2 acetylation by CBP resulted in the nuclear retention of Pygo2 (Figure 2.11), suggesting that nuclear Pygo2 is related to a proliferative phenotype, consistent with a role for Pygo2 in the proliferation of cancer cells where it is localized to nuclei (Andrews *et al*, 2013; Tzenov *et al*, 2015; Andrews *et al*, 2007, 2008; Popadiuk *et al*, 2006; Liu *et al*, 2013; Watanabe *et al*, 2013).

My results support the hypothesis that Pygo2 binds to multiple HATs in the β-catenin transcriptional complex, which is thought to be imperative for promoting histone acetylation and transcriptional activation (Andrews *et al*, 2009; Chen *et al*, 2010). Interestingly, both CBP and p300 promoted an increased association of GCN5 that was dependent on a functional catalytic domain, but not directly on Pygo2 acetylation (Figure 2.7 and 2.8), suggesting the catalytic domain of CBP/p300 is important for the binding of GCN5 to Pygo2. Since β-catenin has been shown to bind to the N-terminal CH1 domain of CBP (Sun *et al*, 2000) and Pygo2 was shown to bind to the C-terminal CH3 domain of CBP (Andrews *et al*, 2009), I propose that the interaction of Pygo with CBP/p300 likely acts in concert with β-catenin to recruit HAT activity required for gene activation. The involvement of a multiprotein complex consisting of many HATs, including CBP/p300 and GCN5 family members, is consistent with findings demonstrating that GCN5/PCAF can directly associate with CBP/p300 (Yang *et al*, 1996; Roth & Iol, 1998). Interestingly, the interaction of Pygo2 with GCN5 required full length CBP, since expression of the C-terminal half (Bro-Q) of CBP resulted in a competition for GCN5 binding, further highlighting the importance of Pygo2 in HAT complex formation.

Acetylation of Pygo2 did not appear to affect Bcl9 binding (Figure 2.1 and 2.6), suggesting that Pygo2 and Bcl9 constitute a functional complex that is independent of, but required for Wnt target gene transcription as was demonstrated previously (Kennedy *et al*, 2010). The correlation of Pygo2 acetylation with transcriptional activation and β-catenin binding suggests a scenario in which Pygo2 is modified only when it is present in a complex with active β-catenin and is quickly de-acetylated upon release from the complex (Figure 2.1). This model is consistent with observations in which the adenomatous polyposis coli (APC) protein was shown to cycle on and off of the c-myc enhancer in response to Wnt activation (Sierra *et al*, 2006), demonstrating the temporal binding of Pygo to chromatin was strongly associated with β-catenin, Bcl9 and p300 and inversely correlated with histone deacetylase binding to the c-myc enhancer.

My results extend previous findings and suggest that Pygo2 acetylation may be important during or after active β-catenin complex assembly. It may play a role in post-transcriptional recycling of the TCF/β-catenin transcription complex via its subsequent displacement to the cytoplasm once transcription initiation has occurred. Most significantly, my results indicate that the association of Pygo2 with HATs and acetylation of Pygo2 by CBP/p300 is important in the regulation of TCF/LEF target gene transcription, further underscoring the importance of the chromatin effector function of Pygo2 in Wnt signalling.

Chapter 3: Evidence of a novel role for Pygopus in ribosomal RNA transcription[2]

[2] A version of this Chapter has been published in: Evidence of a novel role for Pygopus in rRNA transcription. Biochemical Journal 453(1), pp. 61-70, 2013.

3.1 Introduction

Several ribosomes are required for each messenger RNA translated by a eukaryotic cell. Therefore, a significant proportion of cellular resources are devoted to the production of ribosomes, especially during cell growth and division. An important, initial step in ribosome biogenesis is the transcription of the 47S pre-ribosomal (r) RNA by RNA polymerase I (Pol I), a process finely tuned to respond to environmental cues, such as nutrient availability and growth factors (Moss, 2004; Moss *et al*, 2007; Russell & Zomerdijk, 2005). The recruitment of Pol I to sites of rRNA transcription is facilitated by structural and regulatory proteins such as: upstream binding factor (UBF), selectivity factor 1 (SL-1) and Treacle (Prieto & McStay, 2007)**.** Once transcribed, the pre-rRNA undergoes a variety of post-transcriptional (maturation) modifications, before being cleaved into smaller subunits. The cleaved rRNAs are assembled with a number of ribosomal proteins (RPs) into mature ribosomal subunits and exported from the nucleolus to the cytoplasm.

While there are hundreds of tandemly arrayed rDNA gene repeats, about half are normally transcriptionally silent (McStay & Grummt, 2008). Ribosome requirements are met either by adjusting the rate of transcription from active rDNA genes, and/or by increasing the number of active repeats through epigenetic modulation. The mechanisms that form silent, heterochromatic rDNA are well-established, but much less is known about factors such as histone modification, that initiate or maintain actively transcribing euchromatic rDNA (McStay & Grummt, 2008). For instance, how do cells actively engaged in proliferation, such as required for development or malignant growth, epigenetically raise rRNA transcript production?

Pygopus (Pygo) proteins (Kramps *et al*, 2002; Thompson *et al*, 2002) function in chromatin remodeling for transcription at active Wnt target genes via interpretation of the histone code. Pygo binds to histone H3 trimethylated at Lysine 4 (H3K4me3) through its C-terminal plant homeodomain (Fiedler *et al*, 2008; Gu *et al*, 2009), while its N-terminal homology domain (NHD) can recruit histone acetyltransferase (HAT) activity, which can augment target gene activation (Andrews *et al*, 2009; Chen *et al*, 2010). These observations uniquely place Pygo in a position whereby it can read histone marks (H3K4me3) and promote further histone modification such as acetylation, associated with gene activation.

The chromatin remodeling function of Pygo may not be entirely restricted to Wnt signalling, as Pygo proteins have additional uncharacterized Wnt-independent roles in lens development (Song *et al*, 2007) and malignant growth (Popadiuk *et al*, 2006). To elucidate Wnt-independent roles of Pygo2, potential interactions were investigated with cellular proteins using well-established human cancer cell lines. The results presented here suggested a novel requirement for Pygo2 that would address how these proliferating cells adapt to their increased demand for ribosomes. In both *in vivo* and *in vitro* analyses, Pygo2 interacted with Treacle, a nucleolar phosphoprotein required for ribosome biogenesis in neural crest derived craniofacial structures (Sakai & Trainor, 2009). Additionally, Pygo2 was detected interacting with UBF-1, a protein required for rDNA promoter architecture and rRNA transcription (Sanij & Hannan, 2009), in the nucleoli of cancer cells and was associated with Pol I-associated transcription complexes at the rDNA promoters. Using RNA interference, depletion of Pygo2 resulted in a reduction of histone H4 acetylation at rDNA promoters and reduced transcription of the pre-rRNA

transcript in both p53 positive and negative cells. In p53 positive cells, reduction of Pygo triggered the nucleolar stress response, resulting in activation of the ribosomal protein (RP)-mdm2-p53 pathway and subsequent cell cycle arrest. These findings suggest a novel role for Pygopus in ribosome biogenesis, and that Pygopus promotes euchromatin formation at the vicinity of active rDNA genes, a requirement for proliferative growth.

3.2 Materials and methods

3.2.1 Cell lines, plasmids and Antibodies

Cell lines were obtained from the American Type Culture Collection, maintained in Dulbecco's modified Eagle's medium supplemented with 10% FBS (Invitrogen) and cultured at 37°C with 5% CO_2. All GST-Pygo2 constructs have been previously reported (Andrews *et al*, 2009). All constructs were verified by sequencing.

Antisera raised against Pygo2 have been described elsewhere (Popadiuk *et al*, 2006). Treacle (H-90), UBF-1 (F-9), p53 (DO-1), p21 (C-19) and RPA194 (H-300) antibodies were purchased from Santa Cruz; Phospho-cdc2 (Tyr 15), Cyclin A (BF683), p21 (12D1) and Cyclin B1 antibodies from Cell Signalling; Pygo2, H3K4me3, Ac-H3 and Ac-H4 antibodies from Millipore; Treacle, β-Actin and BrdU antibodies from Sigma, and Fibrillarin and RPL11 antibodies from Abcam. Other antibodies used include: β-tubulin (Pharmingen), B23 (Zymed) and Nop56 (Abnova).

3.2.2 GST-pulldowns, immunoprecipitation and proteomics

GST-pulldown and immunoprecipitation analyses were performed using reagents and buffer conditions essentially as described (Andrews *et al*, 2009). Briefly, approximately one mg of purified GST-Pygo2 fusion protein, grown in Rosetta (Novagen) cells, was incubated with 35S-radiolabelled Treacle, washed extensively, separated by SDS-PAGE, stained with Coomassie blue R-250 (Biorad) and exposed to autoradiography film.

3.2.3 Immunofluorescence

Cells were processed and stained for immunofluorescence as previously described (Andrews *et al*, 2009). Detection of Pygo2 was performed using anti-Pygo2 (Millipore; ABE109). For actinomycin D experiments, HeLa cells were treated with 50ng/ml actinomycin D (Sigma) or ethanol carrier for 2 hours at 37°C, 5% CO_2 and immediately fixed in 4% paraformaldehyde and processed.

The bromouridine (BrUTP; Sigma) incorporation assay was performed exactly as described (Sweet *et al*, 2008). Cells were subsequently incubated with BrdU and Pygo2 antibodies (1:100 in PBS with 0.05 units/ml of RNase inhibitor) overnight at 4°C, stained with a mixture of Cy5-conjugated anti-mouse IgG and FITC-conjugated anti-rabbit IgG (Jackson Immunoresearch) and imaged on an Olympus FluoView FV1000 confocal microscope.

3.3.3 Nucleolar fractionation

Nuclei and nucleoli were isolated by sucrose density centrifugation as exactly as described (Andersen *et al*, 2002), imaged using phase-contrast microscopy and immunoblotted for detection of cytoplasmic, nuclear and nucleolar markers. Extracts of whole cells, nuclei and nucleoli were prepared in Laemmli sample buffer.

3.3.4 Chromatin Immunoprecipitation

ChIP assays were performed as previously described (Andrews *et al*, 2008). Briefly, sonication was performed on formaldehyde cross-linked cells to produce genomic DNA fragments approximately 500bp in size. 400 μg of precleared chromatin was subject to immunoprecipitation with 2 mg of antibodies against RPA194, UBF-1,

Treacle, Pygo2, H3K4me3, Ac-H3 and Ac-H4. Normal rabbit and normal mouse IgGs were used as negative immunoprecipitation controls. After washing, formaldehyde crosslinks were reversed at 65°C. Samples were subsequently treated with RNase A and proteinase K. DNA was then purified using the Qiaquick PCR purification kit (Qiagen, Ontario, Canada). For re-ChIP experiments, complexes were first eluted with 10mM dithiothreitol (DTT) for 30 minutes at 37°C, diluted 20X with RIPA buffer supplemented with protease inhibitors and then subjected to a second round of immunoprecipitation. Primer sequences given in Table 3.1 or primers recognizing the rDNA core promoter (Ghoshal *et al*, 2004) and the ITS-1 regions (Gorski *et al*, 2007).

3.3.5 Quantitative (q) PCR

RT-qPCR was performed as described [39], using RT2 SYBR green master mix (SA Biosciences, Mississauga, Canada). Oligonucleotide primers targeting *Pygo2* (Andrews *et al*, 2008) and *47S* (Table 3.1) were used and results were normalized to levels of β-actin mRNA. For ChIP-qPCR analysis, rDNA promoter occupancy was calculated relative to that of the input chromatin. P-values were calculated using one-way ANOVA, using Tukey's multiple comparison test.

3.3.6 RNAi

Cells were grown to approximately 25% confluency and all siRNAs were transfected to a final concentration of 5nM using Lipofectamine RNAiMax (Invitrogen), according to the manufacturers' protocol. The two Pygo2-specific and NTC (a 5 base mismatch control of hpy2-Z, mismatches are underlined in sequence) siRNAs were

Table 3.1 - Primer sequences

Amplicon	5' primer	3' primer	Reference
rDNA promoter	5'-GGTATATCTTT-CGCTCCGAG	5'-GACGACAGGTC-GCCAGAGGA	(O'Sullivan *et al*, 2002)
ITS-1	5'-CGTTCGTTCGC-TCGCTCGTTC	5'-CAAGGGGTCTTT-AAACCTCCGC	(Andrews *et al*, 2013)
Axin2	5'- CTGGCTTTGGT-GAACTGTTG	5'- AGTTGCTCAC-AGCCAAGACA	(Li & Wang, 2008)
Pygo2	5'-GTCCCCCACTCCA-TGGCCGCCTCG	5'-TCGCTTCTTTT-CTGGACTCTTC	(Andrews *et al*, 2008)
p21	5'-GATGTCCGTCA-GAACCCATGC	5'-CAAAGTCGAAGT-TCCATCGCTC	(Andrews *et al*, 2013)
47S	5'-CGTGCGTGTCA-GGCGTTCTC	5'-CCGCAAGTCGA-CAACCACTGG	(Andrews *et al*, 2013)
Actin	5'-ATCTGGCACCACACC-TTCTACAATGAGCTGCG	5'-ATGGCTGGGGT-GTTGAAGGTCTC	(Andrews *et al*, 2008)

designed using the siDESIGN Center (dharmacon.com) and purchased from Dharmacon (The sense strand sequences are: GGAGACAGCUUUAGGGAAUUU (hpy2-X), GGAGUGAGGUGAACGAUGAUU (hpy2-Z) and GGACUGUGGUCAACCAUGUUU (NTC). The Pygo2 siRNAs were analyzed using the Basic Local Alignment Search Tool (BLAST; NCBI) to confirm target specificity. The p53 siRNA was purchased as the TP53 siGENOME SMARTpool (Dharmacon).

3.3.7 Metabolic labeling

HeLa cells were transfected with siRNAs 48 hours prior to metabolic labeling using a modified protocol (Pestov *et al*, 2008). Briefly, cells were washed with 1X PBS and the media was replaced with DMEM containing 5 μCi/ml of ^{3}H Uridine and incubated for 30 minutes at 37°C. The labeling medium was then chased with DMEM containing 1 mg/ml unlabeled Uridine. RNA was extracted 120 minutes later using Tri-Reagent (Ambion). Approximately 10 μg of RNA was separated on MOPS-formaldehyde gels, transferred to nylon membranes, cross-linked, dried and sprayed with En3Hance (Perkin Elmer) and exposed to autoradiography film.

3.3.8 Fluorescence activated cell sorting (FACS)

Initially, HeLa cells were treated with siRNAs for 48 hours. Cells were collected and fixed with 2% formaldehyde for 10 minutes at 37°C and then incubated in 90% methanol/PBS for 30 minutes at 4°C. Cells were then resuspended in 1XPBS treated with 20 μg/ml RNase A for 20 minutes at 37°C, stained with 1mg/ml propidium iodide and

counted in a BD FACS Calibur flow cytometer. P-values were calculated using one-way ANOVA, using Tukey's multiple comparison test.

3.3 Results

3.3.1 Pygo2 interacts with Treacle and UBF-1 and is detected in nucleoli of cancer cells

Previous studies in the lab using tandem mass spectrometry to investigate novel functions of Pygo2 were performed to identify interacting proteins with the NHD of Pygo2 from MCF-7 breast cancer cells. One band in particular at about 205kD matched identically to the primary sequence of Treacle, a protein required for the increase in rRNA production that supports proliferation of anterior neural crest cells (Valdez *et al*, 2004; Jones *et al*, 2008). Therefore, it was hypothesized that previously reported growth requirements for Pygo2 in cancer cells may be related to a potential role in rRNA production.

To confirm the interaction between Pygo2 and Treacle, endogenous Pygo2 was immunoprecipitated with Pygo2 specific antiserum, while pre-immune serum was used as a negative control using MCF-7 cell whole cell extracts (Figure 3.1A). Conversely, Pygo2 was detected in complexes immunoprecipitated using anti-Treacle antibodies (Figure 3.1B).

Since Pol I recruitment to the rDNA genes requires multiple factors including Treacle and UBF-1 (Prieto & McStay, 2007)**,** I tested whether Pygo2 interacted with UBF-1. Similar to Treacle, endogenous UBF-1 was detected in complexes immunoprecipitated using Pygo2 antibodies, but not with control IgG (Figure 3.1C). Conversely, Pygo2 was detected in complexes immunoprecipitated by UBF-1 antibodies (Figure 3.1D).

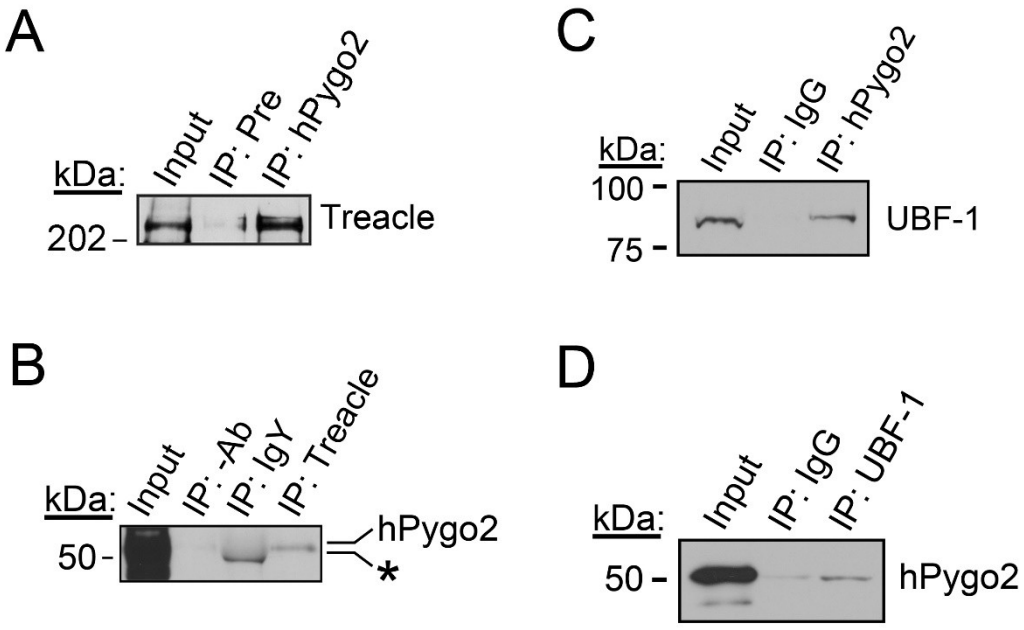

Figure 3.1. Pygo2 protein interacts with the nucleolar factors Treacle and UBF-1. **(A)** Endogenous protein complexes from MCF-7 cell extracts were immunoprecipitated using Pygo2 (Pygo2) antiserum or pre-immune serum, immunoblotting was performed with anti-Treacle antibodies. **(B)** Immunoprecipitations were performed with chicken anti-Treacle antibodies or normal chicken IgY or no antibody (-Ab), immunoblotting was performed with anti-Pygo2 antisera. The asterisk indicates a nonspecific protein associated with normal chicken IgY, which is not present in the control immunoprecipitation without antibody (-Ab). **(C)** Immunoprecipitations were performed using normal IgG or antibodies against Pygo2 from MCF-7 cell extracts and immunoblotted for UBF-1. **(D)** Reverse immunoprecipitations were performed using either normal IgG or antibodies against UBF-1 and blots were probed with anti-Pygo2 antibodies. All input lanes represent approximately 2% of the total extract.

Initially, to ask whether Pygo2 protein was expressed in nuclei, sucrose density gradient centrifugation was performed to enrich both nuclear and nucleolar fractions from HeLa cells (Figure 3.2). Consistent with its observed interaction with Treacle and UBF-1, Pygo2 protein was detected in the enriched nucleolar fraction along with two other well-described nucleolar proteins, UBF-1 and Fibrillarin. To examine the relative purity of the enriched fractions, blots were also probed with β-actin as a control for the nuclear fraction but not the nucleolar fraction (Visa & Percipalle, 2010), while β-tubulin was used as a control which was only present in the whole cell extract, but was not detected the nuclear or nucleolar fractions.

Next, to examine the subcellular localization of Pygo2, indirect co-immunofluorescence was performed for Pygo2 and Treacle (Figure 3.3) in several cancer cell lines. Expression of Pygo2 and Treacle was first examined in breast (MCF-7), cervical (HeLa) and ovarian (SkOv3) cancer cells (Figure 3.3A) and four prostate cancer cell lines (PC3, 22RV1, DU145 and LNCaP; Figure 3.3B). Treacle staining in green showed diffuse localization across the whole cell with strong punctate staining within the nucleus at the presumptive nucleoli. Pygo2, on the other hand, showed diffuse cytoplasmic staining in most cell lines, with distinct nuclear staining in Hela, SkOv3, 22RV1, DU145 and LNCaP. All cell lines showed punctate nuclear staining of Pygo2

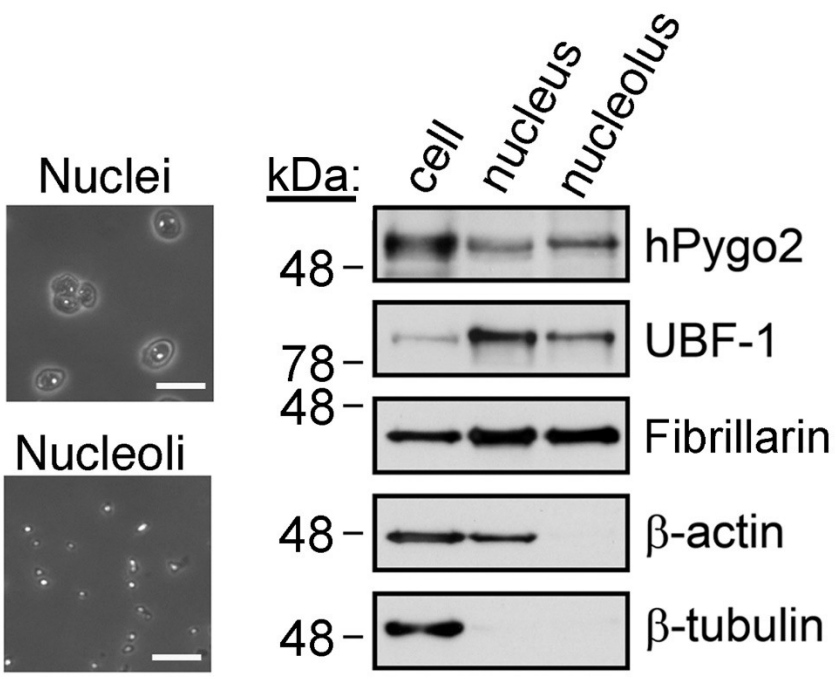

Figure 3.2. Pygo2 protein is detectable in nucleoli. Protein extracts from enriched nuclear and nucleolar fractions (phase contrast images of purified fractions on left) isolated on a sucrose gradient from HeLa cells were separated by SDS PAGE and compared to whole cell extracts. Immunoblots were performed using antibodies against Pygo2, UBF1 and B23. β-actin was used as a negative control for nucleolar fraction and β-tubulin was used as a negative control for both the nuclear and nucleolar fractions. Scale bar = 10 μm.

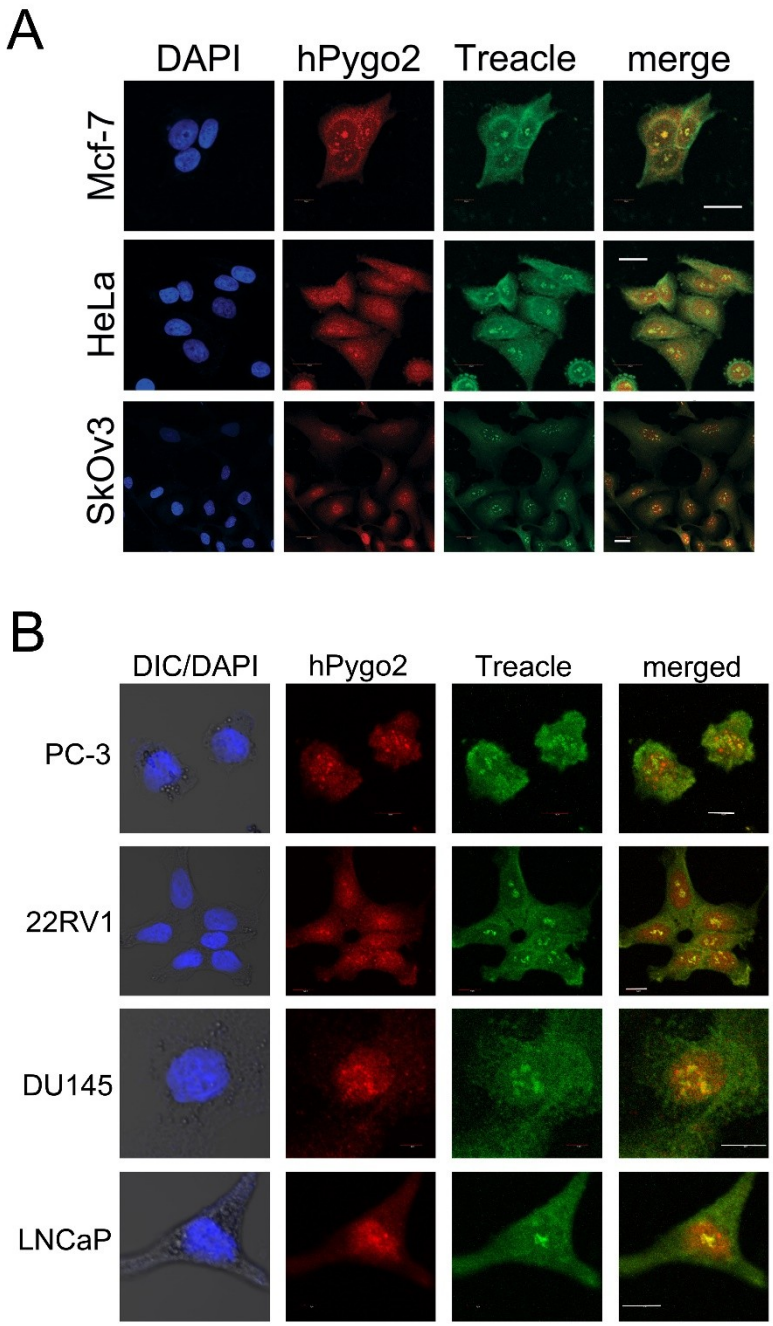

Figure 3.3. Pygo2 co-localizes with Treacle in nucleoli. Confocal microscopy showing Pygo2 (red) co-localizes with Treacle (green) within the presumptive nucleoli of breast (MCF-7), cervical (HeLa) and ovarian (SKOV-1) cancer cells **(A)** and prostate cancer cells (PC3, 22RV1, DU145 and LNCaP; **B)**. DAPI was used to stain DNA and differential interference contrast (DIC) was also used to visualize the cells in **(B)**. Scale bar=20mm in **(A)** and scale bar=10mm in **(B)**.

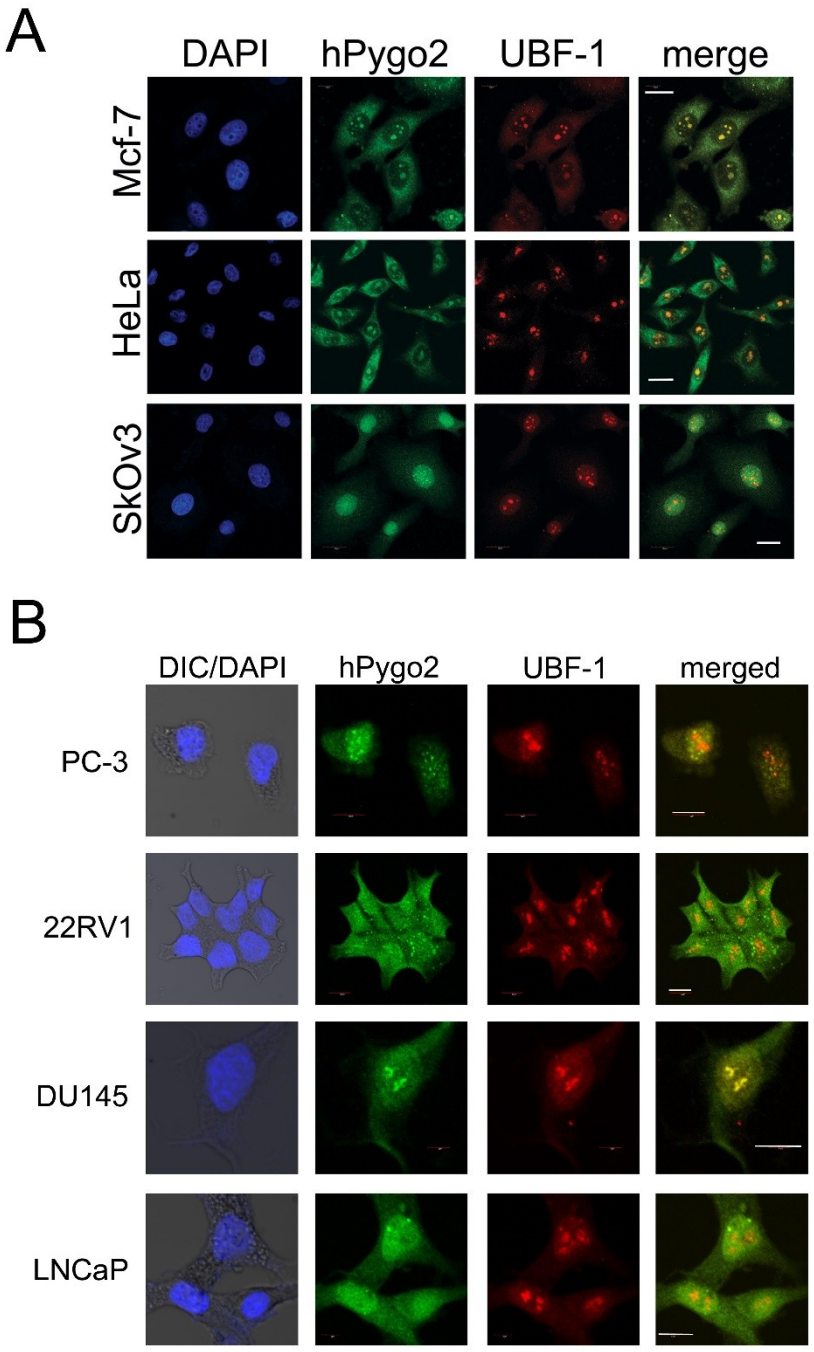

Figure 3.4. Pygo2 co-localizes with UBF-1 in nucleoli. Confocal microscopy showing Pygo2 (green) co-localizes with UBF-1 (red) within the nucleoli of breast (MCF-7), cervical (HeLa) and ovarian (SKOV-3) cancer cells **(A)** and prostate cancer cells (PC3, 22RV1, DU145 and LNCaP; **B)**. DAPI was used to stain DNA and differential interference contrast (DIC) was also used to visualize the cells in **(B)**. Scale bar=20mm in **(A)** and scale bar=10mm in **(B)**.

with some punctate spots overlapping with Treacle at the presumptive nucleoli. Similar patterns of staining were observed between Pygo2 and the nucleolar marker UBF-1 in breast, cervical and ovarian cancer cells (Figure 3.4A) and in prostate cancer cells (Figure 3.4B). These results thereby suggest that at least a fraction of Pygo2 was present at nucleoli in cancer cells. While not shown here, staining was also observed in the primary prostate epithelial cell line PrEC, which showed a lower level of Pygo2 with diffuse staining throughout the nucleus.

To assess whether Pygo2 localized to sites of newly synthesized 47S pre-rRNA at nucleoli, HeLa and SkOv3 cells were incubated with bromouridine triphosphate (Br-UTP), which is incorporated into all cellular RNAs and highly expressed RNAs, such as rRNAs can be visualized by performing indirect immunofluorescence with an anti-bromouridine antibody. As can be seen in Figure 3.5, Pygo2 co-localized with the newly synthesized rRNA at the nucleoli of both HeLa and SKOV-3 cells, therefore suggesting a possible association with *de novo* RNA synthesis.

During mitosis, Nucleolar Organizing Regions (NORs) are transcriptionally silent, but are still bound by core components of the rDNA transcription machinery, such as UBF-1 (Heix *et al*, 1998; Roussel *et al*, 1996; Sirri *et al*, 1999). Staining of mitotic HeLa cells revealed that Pygo2 co-localized with UBF-1 at presumptive NORs during prophase, but then did not appear with NORs during metaphase and telophase, suggesting a transient or dynamic nucleolar association of Pygo2 during cell division (Figure 3.6). Therefore, the association of Pygo2 with nucleoli and newly synthesized rRNA likely occurs during interphase when a cell is growing in preparation for division.

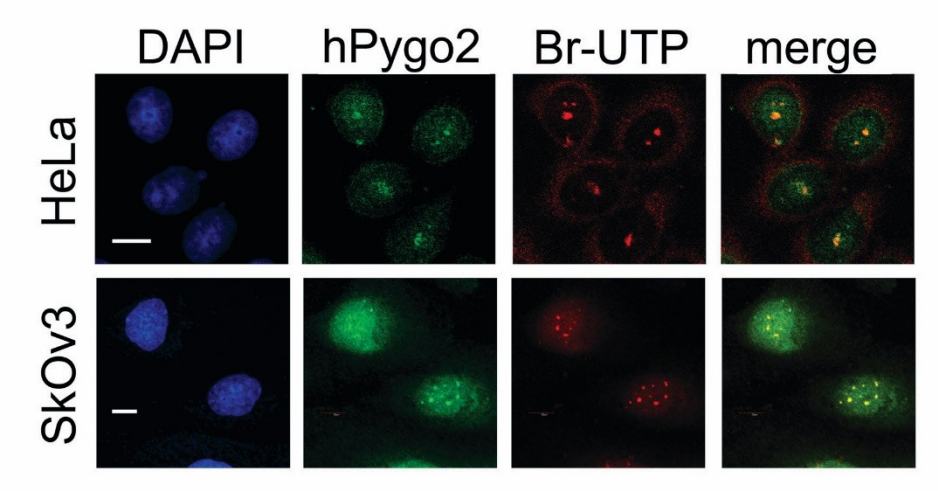

Figure 3.5. Pygo2 is associated with nascent rRNA. HeLa and SKOV-3 cells were incubated for 10 minutes with BrUTP to observe newly synthesized RNA, fixed and stained for Pygo2 and BrUTP and visualized under confocal microscopy. Scale bar = 10μm.

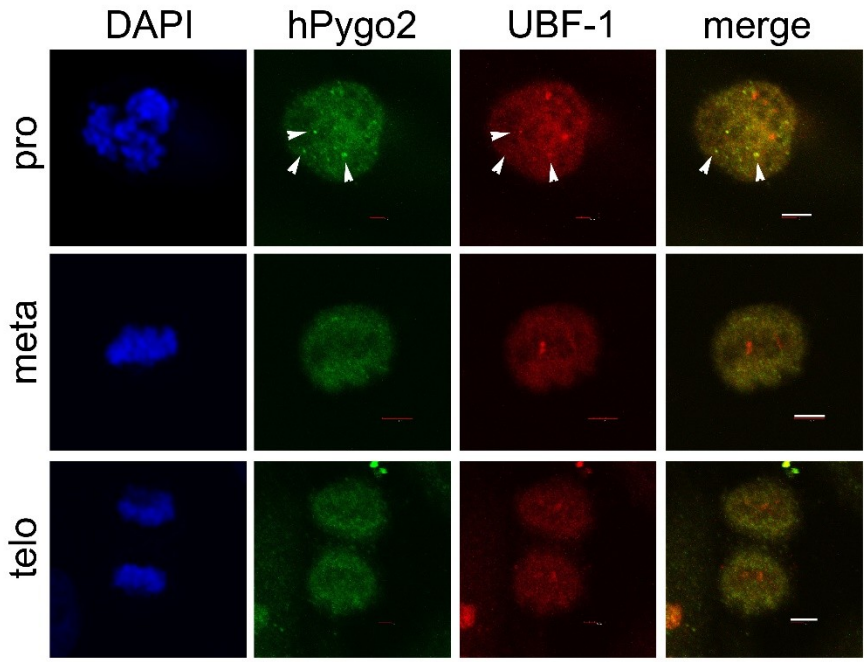

Figure 3.6. Pygo2 dissociates from NORs during mitosis. Images show representative HeLa cells in prophase (pro), metaphase (meta) and telophase (telo). Proteins were detected with antibodies against: Pygo2 (green), UBF-1 (red). DAPI was used to stain DNA (blue). Arrows indicate co-localization between Pygo2 and UBF-1 in prophase. Scale bar = 5 μm.

3.3.2 Pygo2 is dissociated from core transcriptional *rDNA* components in actinomycin D treated cells

Production of the 47S pre-rRNA transcript is followed by its immediate post-transcriptional processing via methylation and pseudouridylation required for maturation and cleavage into the 28S, 18S and 5.8S rRNA subunits. Transcription and processing of the 47S pre-rRNA occurs in distinct nucleolar compartments. To examine this, the Pol I inhibitor, actinomycin D (AMD) was used to disrupt 47S rDNA transcription (Figure 3.7A) and the subcellular localization of Pygo2 was examined. At low concentrations, AMD inhibits actively transcribing rDNA transcriptional complexes and reversibly re-organizes nucleoli according to their functional compartments: the fibrillar centers (FC), composed of the tandemly arrayed rDNA genes, the dense fibrillar component (DFC) and the granular component (GC), which contains rRNA undergoing post-transcriptional modification. This is observed by a restructuring of the FCs and DFCs into "nucleolar caps", which appear as small blebs situated on the central body whose composition is assumed to be derived from the GC (Shav-Tal *et al*, 2005).

In control, ethanol treated HeLa cells, UBF-1 (Figure 3.7B) and Treacle (Figure 3.7C) co-localized with Pygo2 in overlapping regions of the nucleoli. Fibrillarin is a component of small nucleolar ribonucleoprotein complexes (snoRNP) that methylate 47S pre-RNA in a sequence-dependent manner (Reichow *et al*, 2007). B23 is a nucleolar stress sensor required for downstream rRNA processing (Yao *et al*, 2010). In control ethanol treated cells Pygo2 was detected in regions of the nucleolus with Fibrillarin (Figure 3.7D) and B23 (Figure 3.7E). These observations place Pygo2 in the nucleolus along with components of the core transcription machinery and the components involved

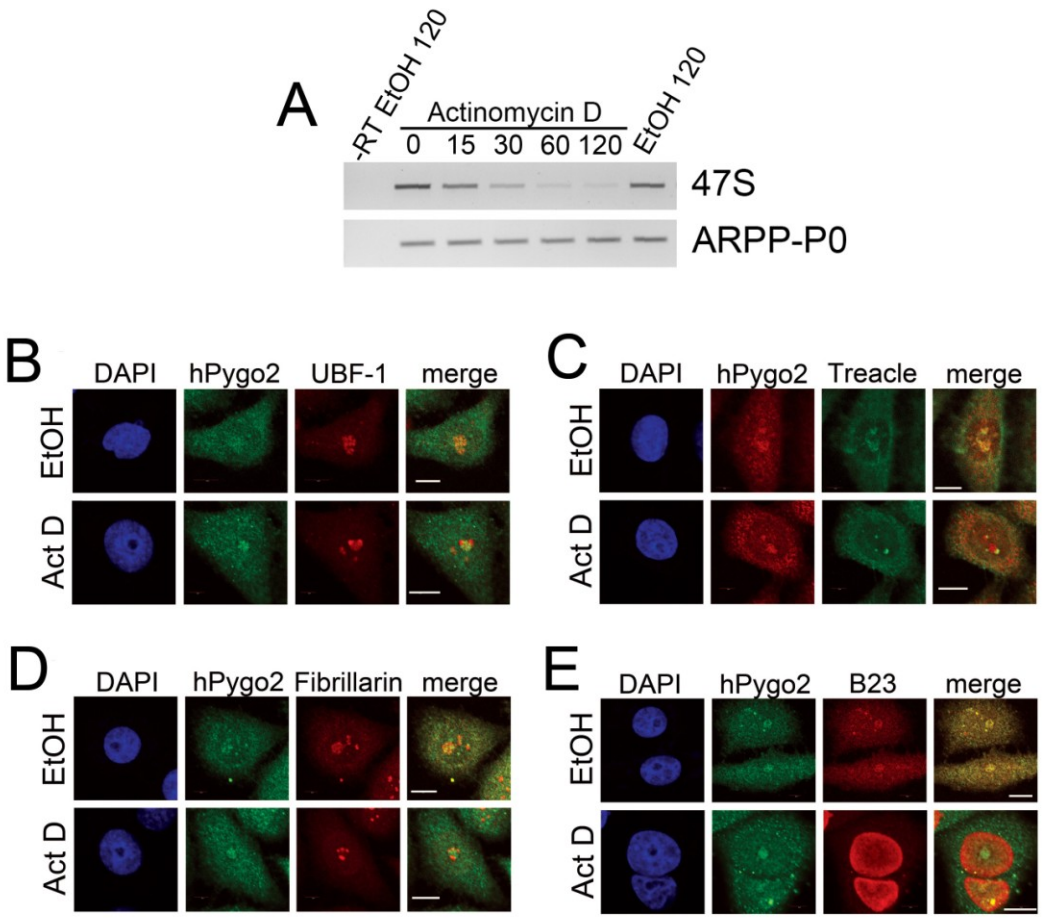

Figure 3.7. Pygo2 is localized to the nucleolus and to the central nucleolar body in cells treated with actinomycin D (AMD). (A) HeLa cells were treated with Actinomycin D for the indicated times in minutes or with solvent alone (EtOH) for 120 minutes. RT-PCR was performed to examine 47S rRNA expression and equal loading was confirmed by examining expression of the RNA Pol II transcribed gene: Acidic ribosomal phosphoprotein P0 (ARPP-P0). **(B-E)** HeLa cells were treated with EtOH or with Actinomycin D (AMD) for 120 minutes, fixed and co-stained with antibodies against Pygo2 and the nucleolar markers UBF-1 **(B)**, Treacle **(C),** Fibrillarin **(D)** or B23 **(E)**. Scale bar = 10μm.

in post-transcriptional processing. In AMD treated cells, Pygo2 was found mainly in the central body, while UBF-1 (Figure 3.7A) and Treacle (Figure 3.7B) localized to the outer nucleolar caps, Fibrillarin was localized to the inner nucleolar caps (Figure 3.7C) and B23 was detected in the nucleoplasm (Figure 3.7D). While Pygo2 was not associated with nucleolar caps, it continued to remain closely associated with the nucleolus after AMD treatment, suggesting it is not likely a core component of the rDNA transcription machinery.

3.3.3 Pygo2 binds to rDNA promoter chromatin

The above observations suggested that Pygo2 is not associated tightly enough with the core complexes to withstand the effects of AMD, even though they co-immunoprecipitated from cells. This is perhaps not surprising as Pygo2 has no DNA binding ability, yet it might still indirectly interact with the promoter through the core complexes, therefore this possibility was tested using chromatin immunoprecipitation (ChIP) assays. Sheared chromatin from HeLa cells was immunoprecipitated using RPA194 (the large subunit of RNA polymerase I), UBF-1, Treacle, β-catenin and Pygo2 antibodies and then subjected to PCR using oligonucleotide pairs complementary to the start of transcription on the rDNA promoter (rDNApro; Figure 3.8A). RPA194, UBF-1, Treacle and Pygo2 immunoprecipitates all contained promoter sequences but not control, internal transcribed sequence 1 (ITS-1; Figure 3.8B). Furthermore, while re-ChIP analysis confirmed the presence of all four proteins at the same region of the rDNA promoter (Figure 3.8C), Pygo2 interacted only with Treacle and UBF-1, but not with Pol I or proteins involved in transcript processing (Figure 3.8D).

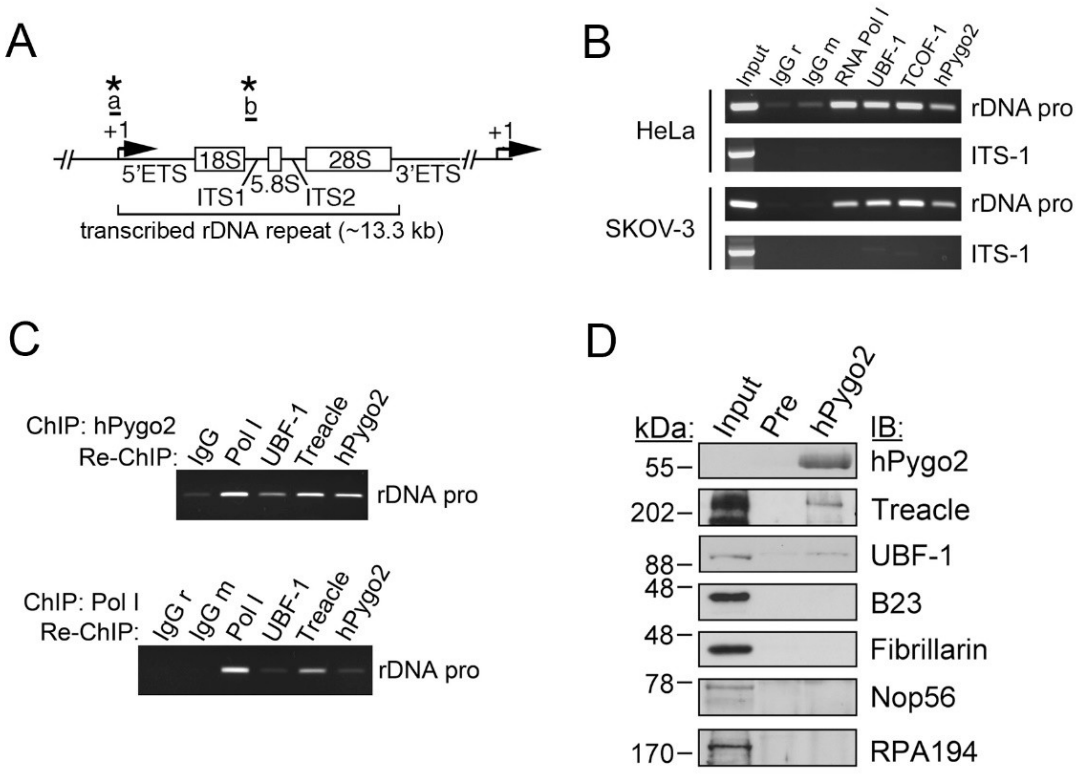

Figure 3.8. Pygo2 is associated with the active rDNA transcription complex *in vivo*. **(A)** Genomic structure of human rDNA repeat indicating regions a, and b corresponding to rDNA promoter and ITS1 regions amplified by sequence-specific primers in chromatin immunoprecipitation assays. The 5' and 3' externally transcribed sequences (ETS), the internal transcribed sequences (ITS1 and 2) and the 18S, 5.8s and 28S rRNA subunits that are cleaved from the transcribed 47S precursor are indicated. **(B)** Chromatin immunoprecipitations from HeLa and SKOV-3 cells using antibodies against RPA194 (RNA Pol I large fragment), UBF-1, Treacle and Pygo2. IgG from rabbit (IgG r) and mouse (IgG m) were used as negative controls. Oligonucleotide primers specific to amplify regions include sequences immediately upstream of the start of transcription (rDNA pro) and the internally transcribed sequence (ITS-1) as a negative control, as indicated in A. **(C)** Samples were subject to a first round of ChIP using Pygo2 antibodies and then subjected to a second round of Chip (re-ChIP) with the indicated antibodies. PCR was performed using primers against the rDNA core promoter. **(D)** Complexes containing Pygo2 were immunoprecipitated and probed for the nucleolar markers: Treacle and UBF-1, which are components of the rDNA transcription complex and B23, Fibrillarin and Nop56, which are components of the rRNA processing machinery, as well as the large subunit of RNA polymerase I (RPA194).

In separate experiments, the rDNA specific primers did not amplify sequence from chromatin precipitated by β-catenin antibodies (Figure 3.9A). Furthermore, while active β-catenin was readily detectable at the Wnt response element of the Axin2 promoter upon LiCl treatment of HeLa cells ($p<0.001$), it was not detectable at the rDNA promoter (p=NS; Figure 3.9B). Finally, an interaction between β-catenin and UBF *in vitro* was not observed (Figure 3.9C). Thus, while Pygo is typically associated with the canonical Wnt transcription complex, it did not appear to rely on β-catenin for its localization to rDNA promoters.

3.3.4 Pygo2 is not sufficient for *rRNA* expression in HeLa cells

Initially, to test whether Pygo2 was sufficient to drive transcription of the 47S pre-rRNA, Pygo2 was overexpressed in HeLa cells which were pulsed with ^{3}H-uridine to label the all the rRNA species (Figure 3.10; top panel). Immunoblots were performed to confirm the expression of Pygo2 protein (Figure 3.10; bottom panel). Expression of wild-type Pygo2 was not sufficient to drive or change the rRNA expression. However, overexpression of a Pygo2 mutant that was previously shown to be required for the transcriptional activity of the Pygo2 NHD (NPF-AAA; Städeli & Basler, 2005), resulted in a reduction in the production of all rRNA species. These results suggested that Pygo2 (NPF-AAA) may possibly act as a dominant negative, thus interfering with rRNA transcription. Finally, a Bcl-9 binding mutant of Pygo2 (L369A) was not sufficient to drive or change the rRNA expression, further suggesting that the possible role of Pygo2 at the rDNA transcription complex does not rely on Bcl-9/β-catenin.

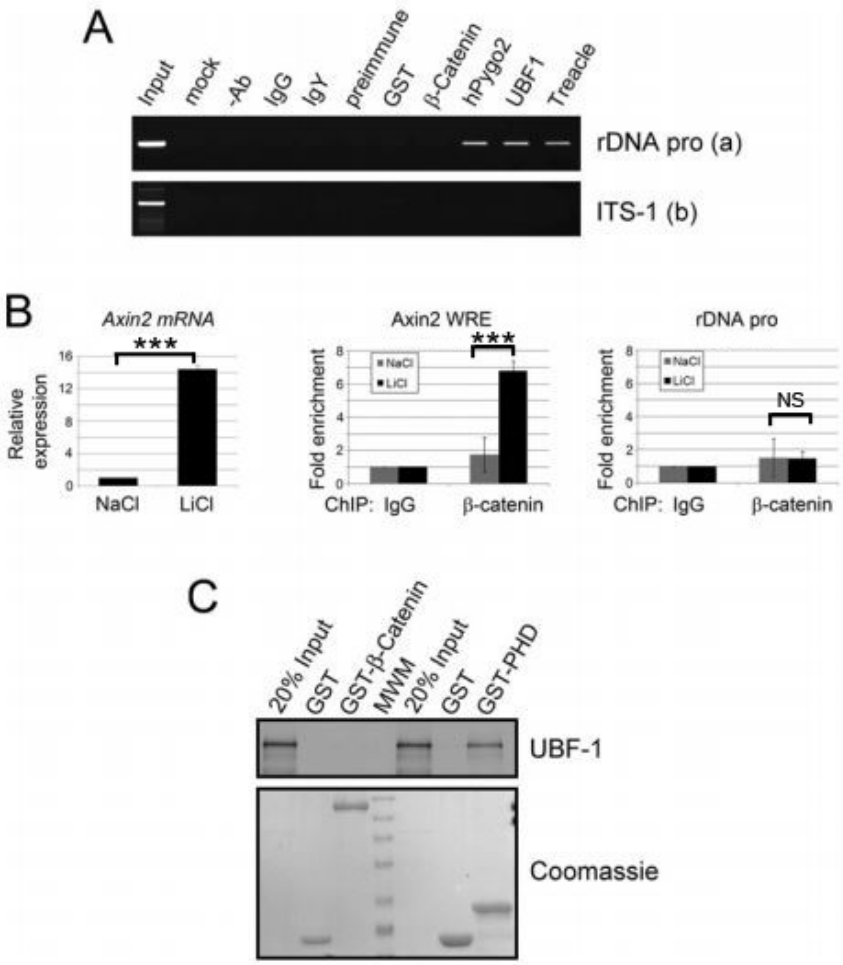

Figure 3.9. β-catenin does not interact with the rDNA promoter *in vivo*. (A) Chromatin was prepared from HeLa cells and subjected to immunoprecipitation with negative controls (mock, -Ab, IgG, IgY, preimmune and anti-GST), positive controls (UBF-1 and Treacle), Pygo2 and β-catenin. PCR was performed on the rDNA promoter and ITS-1 sequences. **(B)** Transcriptionally active β-catenin does not interact with the rDNA promoter. HeLa cells were treated with either 20mM NaCl or 20mM LiCl, RNA and chromatin were extracted after four hours as described. qPCR was performed to assess the relative activation of *Axin2* mRNA expression induced by LiCl (left panel; $p<0.0001$). ChIP analysis was performed to examine the relative amounts of β-catenin binding to both the Axin2 Wnt responsive element (WRE) and to the rDNA promoter (right panels) Primer sequences have been described elsewhere [1]. Error bars represent standard deviation of three independent experiments. (***$p<0.001$, NS; not significant; **C)** UBF-1 interacts with the Pygo2 PHD domain, but not β-catenin *in vitro.* GST fusion proteins of β-catenin and Pygo2 PHD domain were used in an *in vitro* pulldown assay along with radiolabeled UBF-1 (top panel). Gels were stained with coomassie blue to visualize relative amounts of GST proteins (bottom panel).

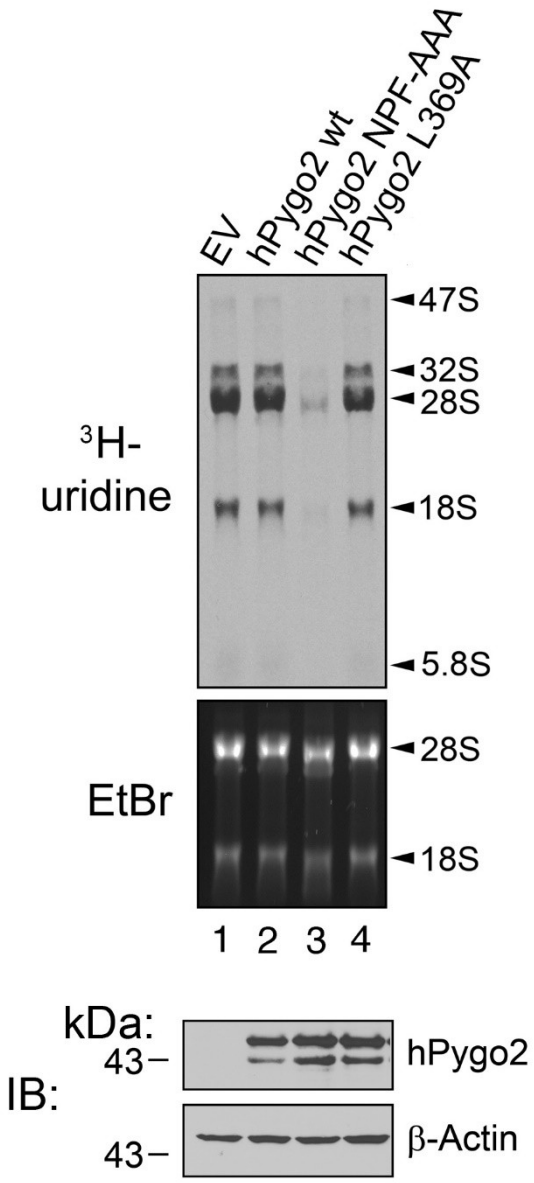

Figure 3.10. Pygo2 overexpression is not sufficient to increase *de novo* rRNA transcription. Hela cells were transfected with pCS2 (EV; lane 1), pCS2-full length Pygo2 (Pygo2 wt; lane 2), pCS2-Pygo2 NPF-AAA (Pygo2 NPF mut; lane 3), pCS2-Pygo2 L369A (Bcl9 binding mutant; lane 4) and assayed for *de novo* rRNA synthesis by ^{3}H-uridine incorporation (^{3}H-uridine; upper panel). Major rRNA species are indicated and relative levels of 28S and 18S rRNAs were assessed by ethidium bromide staining (Etbr; middle panel). Expression of Pygo2 protein was confirmed by immunoblotting for Pygo2 (IB; lower panel), β-actin was used as a loading control.

3.3.5 Pygo2 recruits histone acetyltransferase activity to the rDNA promoter

Pygopus was previously shown, through binding of its PHD to H3K4me3 marks, to recruit histone acetyltransferase activity to its conserved NHD at active Wnt target genes (Fiedler *et al*, 2008; Gu *et al*, 2009; Andrews *et al*, 2009; Chen *et al*, 2010). Pygo2 was present at the rDNA promoter (Figure 3.8) but overexpression was not sufficient to increase rRNA transcription, however an NHD mutant of Pygo2 (NFP-AAA; Figure 3.10) interfered with rRNA transcription, suggesting that Pygo2 may be required for transcription of the 47S precursor rRNA. Therefore, to address a possible requirement of endogenous Pygo2 in rRNA transcription, two Pygo2-targeting siRNAs were selected for loss-of-function studies. First, to test the specificity of the Pygo2 siRNAs, knockdowns were performed in which Pygo2 cDNA was co-expressed and expression of the previously identified Pygo2 responsive gene p21 was analyzed (Gu *et al*, 2009). Transfection of two Pygo2-targeting siRNAs resulted in an increase in p21 expression, as was previously shown. Co-transfection of the Pygo2 cDNA with one of the siRNAs that targeted the 3'-UTR (hpy2-X) of Pygo2, restored the levels of p21 present in the control (NTC + pCS2), verifying the specificity of the knockdown (Figure 3.11A). Depletion of Pygo2 using RNAi also clearly reduced the levels of nucleolar Pygo2 (Figure 3.11B).

Next, I tested whether Pygo2 loss-of-function affected histone modifications at the rDNA promoter by ChIP-quantitative (q) PCR. Transfection of Pygo2 siRNA reduced the amount of Pygo2 bound to the rDNA promoter to approximately 41% compared to the NTC siRNA (Figure 3.12A; $p<0.01$). There was no effect on acetyl (Ac) H3 levels and while not statistically significant (NS; $p=0.1$), there was a detectable increase in H3K4me3 levels at the rDNA promoter, despite a slight decrease in the global levels of

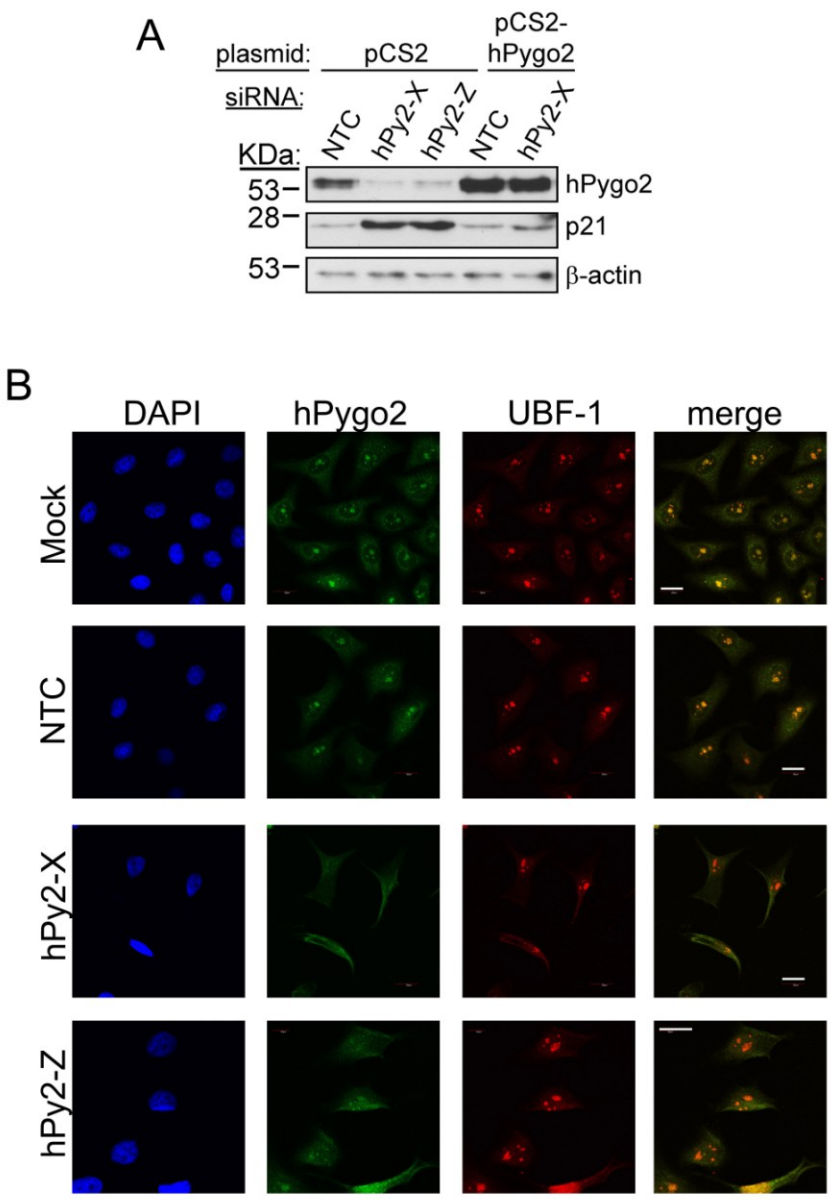

Figure 3.11. Confirmation of Pygo2 siRNA specificity. (A) Knockdown of Pygo2 results in increased levels p21, while co-expression of Pygo2 restored levels of p21. Human endocervical cancer cells were transfected with empty plasmid (pCS2) with either non-targeting (NTC), hPy2-X (targeting 3'untranslated region) or hPy2-Z (targeting coding region) siRNAs. Rescuing Pygo2 cDNA (pCS2-hPygo2) was co-transfected with NTC and hPy2-X (targeting 3'untranslated region) siRNAs. Blots were probed with β-actin to confirm equal loading. **(B)** Knockdown of Pygo2 reduces detectable nucleolar Pygo2 protein. HeLa cells were either mock transfected, or transfected with NTC, hpy2-X or hpy2-Z siRNAs. Cells were then fixed 48 hours later and stained with antibodies against Pygo2 (green) and UBF-1 (red). DAPI was used to stain DNA (blue). Scale bar = 20 μm.

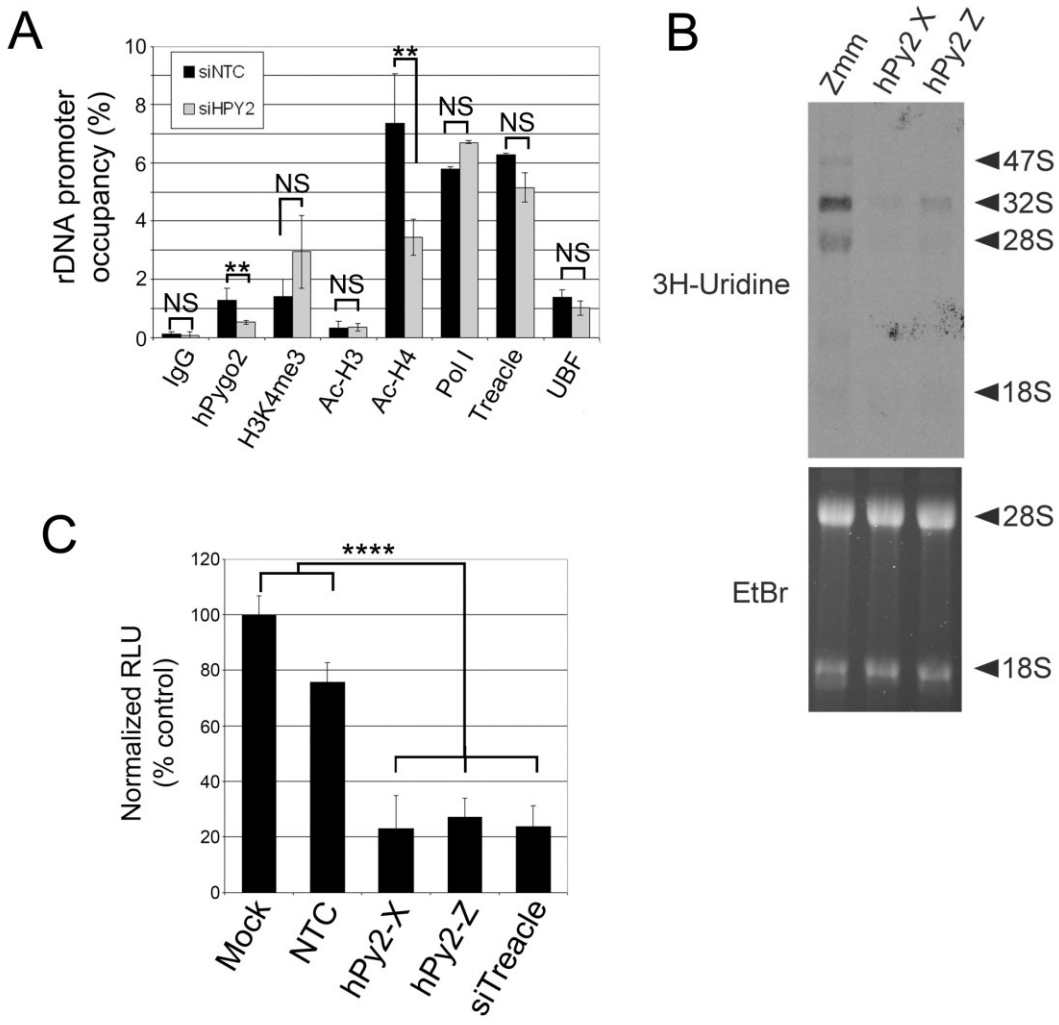

Figure 3.12. Pygo2 depletion decreases histone H4 acetylation at the rDNA promoter. (A) Pygo2 plays a role in H4 acetylation at the rDNA promoter. ChIP-qPCR analysis of HeLa cells treated with NTC (siNTC) and Pygo2 (siHPY2) siRNAs showing rDNA promoter occupancy relative to the input chromatin. **(B)** HeLa cells were transfected NTC, hpy2-X and hpy2-Z siRNAs and assayed for *de novo* rRNA synthesis by ^{3}H-uridine incorporation (^{3}H-uridine; upper panel). Positions of the major rRNA species are indicated on the right and relative levels of 28S and 18S rRNAs were assessed by ethidium bromide staining (Etbr; middle panel). **(C)** Transfection of siRNAs targeting Pygo2 and Treacle reduced transcription from an rDNA promoter reporter. HeLa cells were treated with transfection reagent alone (Mock), NTC, or siRNAs targeting either Pygo2 (X, Z) or TCOF-1 mRNAs (siTreacle). After 48 hours, the cells were transfected with an rDNA luciferase reporter (pHrD-IRES-LUC). Relative luciferase units were normalized to β-galactosidase activity. All data are represented as mean +/- SD from three independent experiments. (**p<0.01, ****p<0.0001, NS; not significant)

H3K4me3 (Figure 3.13A), possibly reflecting a compensatory mechanism for Pygo2 recruitment. Notably, Pygo2 knockdown reduced acetyl histone-H4 levels occupying the promoter region to approximately 47% compared to the NTC siRNA ($p<0.01$) but did not significantly affect the binding of complex(es) containing Pol I or UBF (p=NS; Figure 3.12A). Like H3K4me3, there was a detectable decrease in global levels of acetyl-H4 with Pygo2 siRNA treatment, but this was also accompanied by a decrease in H4 protein as well (Figure 3.13B), consistent with an observed role for Pygo2 in histone gene expression (Gu *et al*, 2012). Thus, while Pygo2 was not necessary for recruitment of transcriptional components, it appeared to be required to maintain acetylation of associated histones at the promoter during rDNA transcription.

To test whether the observed reduction of acetyl-H4 at the rDNA promoter influenced rRNA transcription, further loss of function experiments were performed. Pygo2 knockdown resulted in reductions in the 32S, 28S and 18S rRNAs as measured by ^{3}H-Uridine (Figure 3.12B) incorporation. Similarly, knockdown of Pygo2 significantly reduced transcription from a transfected luciferase reporter gene under the control of the rDNA promoter (pHrD-IRES-Luc; Figure 3.12C). To further confirm and quantitatively assess the transcription of the 47S precursor rRNA, qPCR was performed on Pygo2 siRNA treated cells. Treatment of both HeLa (Figure 3.14A) and SKOV-3 (Figure 3.14B) cells with Pygo2 siRNA showed a significant reduction Pygo2 mRNA levels ($p<0.001$) as well as a significant reduction in the levels of the 47S rRNA ($p<0.01$). Together, these observations provided evidence that Pygo2 is involved in transcription of the 47S pre-rRNA by maintaining levels of acetyl-H4.

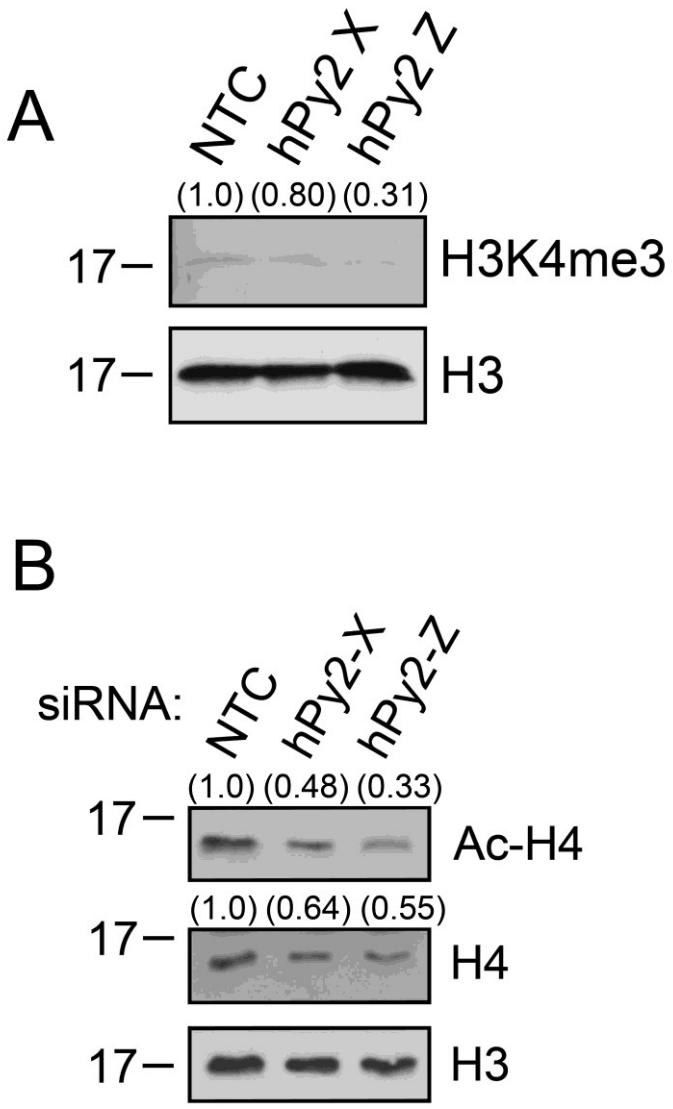

Figure 3.13. Depletion of Pygo2 results in a reduction of H3K4me3, H4 and acetylated H4 levels. (A) Assessment of global levels of H3K4me3 following Pygo2 knockdown using a non-targeting siRNA (siNTC) and two Pygo2 siRNAs (hPy2-X and hPy2-Z), demonstrating a reduction of H3K4me3. **(B)** Assessment of global levels of histone H4 and acetylated histone H4 levels following Pygo2 knockdown. Results demonstrate a reduction in both histone H4 and acetylated H4, relative to histone H3 levels. Relative densitometric values relative to H3 are given in parenthesis for **(A)** and **(B)**.

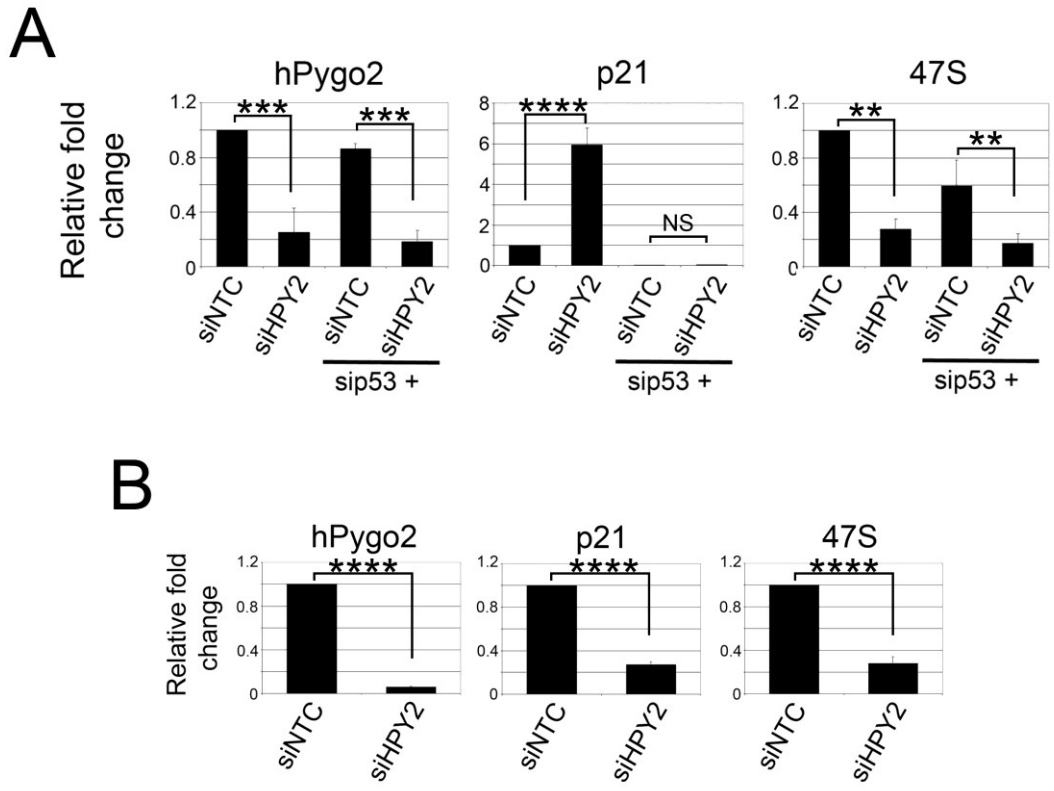

Figure 3.14. Pygo2 depletion resulted in a reduction of 47S pre-rRNA independent of p53. **(A)** p53 independent reduction of the 47S pre-rRNA by Pygo2 knockdown. HeLa cells were treated with either NTC or Pygo2 siRNAs alone or in combination with p53 siRNAs. RT-qPCR was performed and relative levels of Pygo2, p21 and 47S mRNAs are shown. **(B)** RT-qPCR was performed using RNA collected from p53-null SKOV-3 cells treated with NTC and Pygo2 specific siRNAs. Relative expression levels of *Pygo2*, *47S* and *p21* mRNAs were calculated as percentages of the NTC control.
Data are represented as mean +/- SD of three independent experiments. (****p<0.0001, ***p<0.001, **p<0.01, NS; not significant)

3.3.6 Depletion of Pygo2 resulted in growth arrest by activation of the RP-Mdm2-p53 nucleolar stress response in HeLa cells

Nucleolar stress-induced cell cycle arrest is caused by disruptions in ribosome biogenesis resulting in the association of unincorporated ribosomal proteins, such as ribosomal protein (RP) L11, with the E3 ubiquitin ligase HDM2, thereby compromising its ability to inhibit p53 tumor suppressor and apoptotic function (Lohrum *et al*, 2003). I therefore hypothesized that disruption of rDNA transcription by depletion of Pygo2 could possibly trigger the nucleolar stress response.

Notably, it could be argued that the attenuation in rDNA transcription in response to treatment with Pygo2 siRNA was a secondary effect subsequent to disruption of cell cycle progression due to an upregulation of p53. To test this possibility, I first determined the effect of reducing both proteins on rRNA production using both Pygo2 and p53 siRNAs. Depletion of Pygo2 alone resulted in a decrease of 47S rRNA and an increase of p21 (Figure 3.14A). Co-transfection with both Pygo2 and p53 siRNAs resulted in a decrease in the p53 target gene p21 as expected. It did not, however, restore levels of 47S rRNA (Figure 3.14A), suggesting that the reduction in 47S rRNA by Pygo2 depletion was independent of p53 stabilization and activation.

Next, to test whether the observed increase in p53 by depletion of Pygo2 resulted from activation of the nucleolar stress response pathway (Zhang & Lu, 2009), HDM2 was immunoprecipitated from cells treated with Pygo2 siRNAs and the interaction between HDM2 and RPL11 was assessed. In cells treated with Pygo2 siRNA, RPL11 interacted with HDM2, while in untreated (mock) and control (siNTC) siRNA treated cells no interaction between RPL11 and HDM2 could be detected (Figure 3.15A, upper

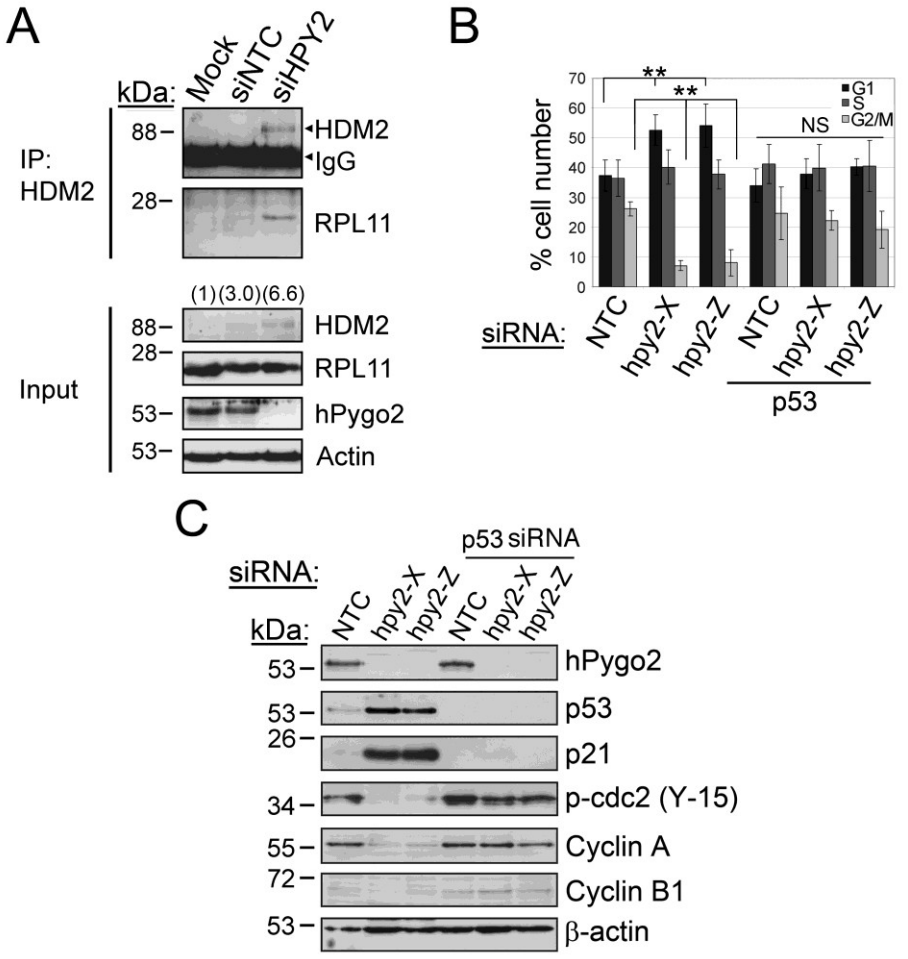

Figure 3.15. Pygo2 depletion results in activation of the nucleolar stress response. **(A)** HDM2 interacted with RPL11 in Pygo2-depleted HeLa cells. Cells were treated with reagent alone (Mock), NTC siRNA (siNTC) or hpy2-X siRNA (siHPY2) and extracts were subject to immunoprecipitation (IP) with an antibody against HDM2. Blots were probed with HDM2 and RPL11 antibodies (top panel). Inputs (5%) were probed with antibodies against HDM2 (relative band densities in parenthesis), RPL11, Pygo2 and the loading control, β-actin (bottom panel). **(B)** HeLa cells were treated with either NTC or Pygo2 siRNA alone and in combination with p53 siRNA. FACS analysis was then performed to show the percentage of cells in each phase of the cell cycle. Treatment of cells with hpy2-X or with hpy2-Z resulted in significant increases in the proportion of cells in G1 compared to the NTC siRNA. Co-treatment of cells with p53 siRNA plus hpy2-X or with p53 siRNA plus hpy2-Z showed no significant increase in the proportion of cells in G1 compared to p53 plus NTC siRNAs. Data are represented as mean +/- SD of three independent experiments. (**$p<0.01$, NS; not significant; **C)** Knockdown of p53 restored cell cycle progression protein expression in cells depleted of Pygo2. Cells were treated with NTC, or Pygo2 siRNAs (X, Z), with or without p53 siRNA. G1 markers include p53 and p21, G2/M markers include p-cdc2 (Y-15), Cyclin A, Cyclin B1. β-actin was used as a loading control.

panel). Interestingly, there was an increase in HDM2 levels in Pygo2-depleted cells (Figure 3.15A, "Input"), which was consistent with previous findings demonstrating HDM2 as a transcriptional target of p53 (Barak *et al*, 1993). The binding of RPL11 to HDM2 suggest that upon depletion of Pygo2, the nucleolar stress pathway was activated.

The increase in p53 levels following Pygo2 knockdown was correlated with cell cycle arrest and a significant increase in the number of cells at G1 ($p<0.01$), accompanied by a decrease in the number of cells at G2/M ($p<0.01$), compared to the NTC siRNA alone (Figure 3.15B). On the other hand, co-depletion Pygo2 and p53 resulted in a rescue of cell growth arrest mediated by Pygo2 depletion, suggesting the growth arrest was p53 dependent (Figure 3.15B; p=NS). Alone, Pygo2 siRNA increased both p53, and the p53 target gene p21 but reduced the levels of the G2/M markers phospho-cdc2, Cyclin A and Cyclin B1 (Figure 3.15C). In contrast, co-depletion of Pygo2 and p53 reduced p21 expression and restored the cell-cycle progression markers phospho-cdc2, Cyclin A and Cyclin B (Figure 3.15C). Together, these results suggested that Pygo2 depletion resulted in the accumulation of p53 and subsequent arrest at G1, consistent with activation of the nucleolar stress response.

3.3.7 Pygo2 knockdown reduced rRNA transcription in p53-null SkOv3 cells

The above-mentioned experiments indicated that while co-transfection of Pygo2 and p53 siRNAs had little effect on cell cycle progression, there was a persistent reduction of 47S rRNA transcription. Therefore, to corroborate this data, Pygo2 depletion was performed in the p53-null ovarian cancer cell line, SKOV-3 (Figure 3.16).

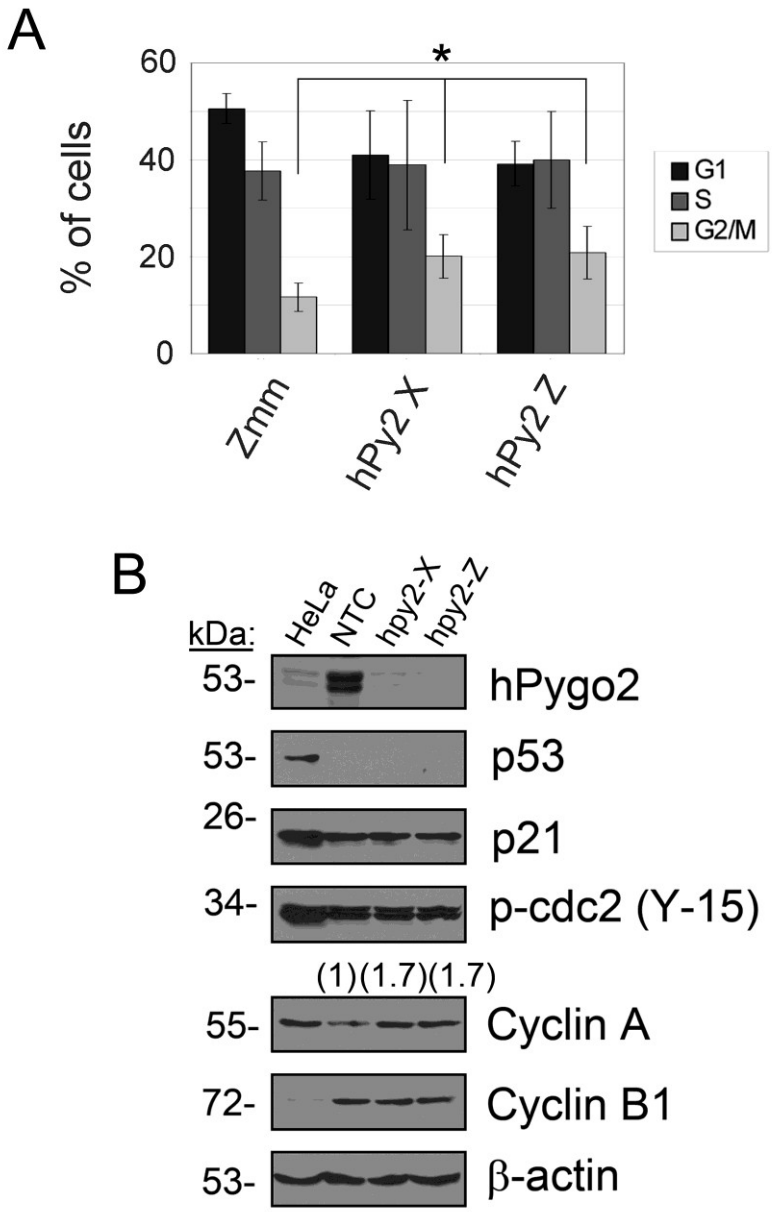

Figure 3.16. Depletion of Pygo2 causes SKOV-3 cells to accumulate in G2/M. (A) FACS analysis of SKOV-3 cells transfected with NTC and Pygo2 siRNAs. Data are represented as mean +/- SD of three independent experiments. (*$p<0.05$; **B)** Immunoblot analysis of SKOV-3 cells transfected with NTC and Pygo2 specific siRNAs. HeLa cell extracts were used as a p53-positive control. G1 markers include p53 and p21, G2/M markers include p-cdc2 (Y-15), Cyclin A, Cyclin B1. Relative Cyclin A band densities given in parenthesis. β-actin was used as a loading control.

Depletion of Pygo2 in SKOV-3 cells, which we previously demonstrated was sensitive to knockdown of Pygo2 (Popadiuk *et al*, 2006), also caused a significant decrease in 47S rRNA (Figure 3.14B). However, cell cycle analysis of Pygo2 depleted SKOV-3 revealed an accumulation of cells in the G2/M phase (Figure 3.16A; $p<0.05$). The only cell cycle marker examined with a detectable change after Pygo2 depletion was Cyclin A, which was consistent with the observed cell cycle arrest at G2/M (Figure 3.16B). It is unclear whether G2/M arrest in p53-null cells was the result of a nucleolar stress response similar to that of p53-positive cells. These observations suggested that a primary effect of Pygo2 depletion was on rRNA production, leading to a subsequent negative effect on cell cycle progression, providing evidence linking Pygo2 function to rDNA transcription.

3.4 Discussion

The association of Pygo2 with ribosomal gene promoters and its participation in rRNA transcription, suggests a function for Pygo2 in ribosomal biogenesis required for proliferative growth. In addition to its demonstrated role in canonical Wnt signalling, I hypothesize that Pygo2 plays a role in ribosomal gene transcription specifically through its previously identified role, the acetylation of histone H4 (Figure 3.12; Andrews *et al*, 2009), but at the rDNA gene promoter in lieu of, or more likely in addition to, Wnt target gene promoters/enhancers. This step would seemingly maintain requisite levels of 47S precursor rRNA, necessary for cell division, and without which would lead to cell growth arrest.

Our data incorporates Pygo2 into models of active ribosomal gene transcription (Denissov *et al*, 2011), perhaps as an adaptor protein for epigenetic modifiers required for histone acetylation (Figure 3.17). I propose that Pygo2 is present at the rDNA promoter through its interaction with both UBF-1 and Treacle. However, the relatively small proportion of the total Pygo2 protein observed in complex with UBF-1 and Treacle suggest that this may not be the primary transcriptional target of Pygo2, hence, these observations will be further discussed in Chapter 4. The fact that Pygo2 does not make direct contact with Pol I is consistent with the idea that Pygo2 functions largely as an adaptor protein, required to induce or promote epigenetic modifications to augment transcription. It is possible that its recruitment to active sites or ribosomal gene transcription and may also depend on H3K4 methylation status at the vicinity of rDNA promoters.

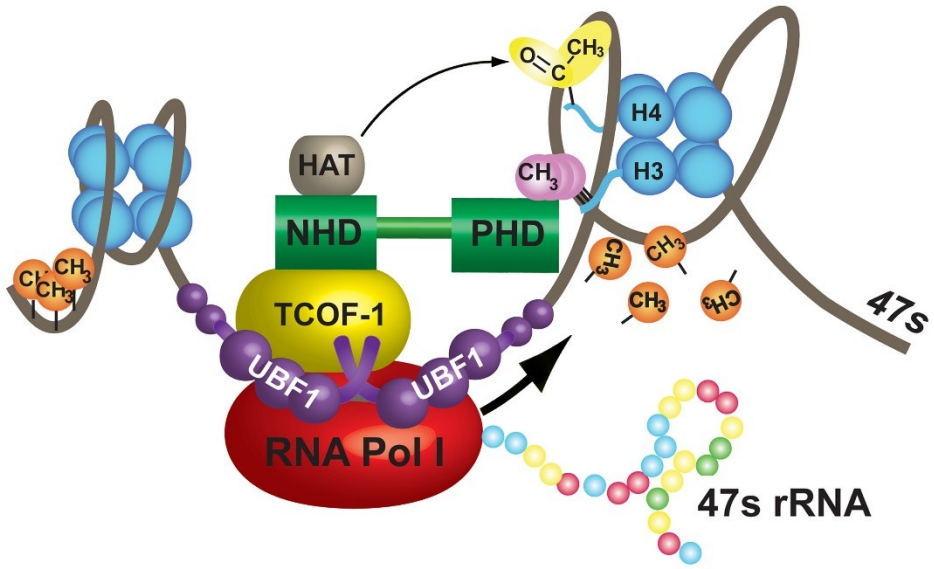

Figure 3.17. Proposed role of Pygopus in ribosomal DNA transcription. Pygopus is required for chromatin remodeling associated with ribosomal gene transcription. The PHD of Pygo (green) binds directly to H3K4me3 histone marks associated with active gene promoters, allowing the recruitment of histone acetyltransferases (HAT) by its NHD to the rRNA transcriptional complex through its interaction with Treacle (TCOF-1), a large phosphoprotein that may serve as a scaffolding function to recruit Pygo2 to the rDNA promoter vicinity. The resulting H4 acetylation, a prerequisite for nucleosomal decondensation and promoter demethylation, is required for transcription of the 47S precursor rRNA by RNA Pol I. For simplicity, not all proteins involved in complex formation are shown.

The diverse requirements for Pygo2 in development suggest that its cellular function is context dependent, as demonstrated by *pygo* loss-of-function studies in mice. Transgenic animals deficient for *mPygo2* die as neonates but display a range of tissue and organ defects, some of which, such as in kidney and mammary gland morphogenesis, have been identified as canonical Wnt-dependent (Li *et al*, 2004, 2007a; Schwab *et al*, 2007). However, the requirement for *mpygo2* in lens formation along with other unattributed defects, such as overall growth agenesis and craniofacial defects including cleft palate was demonstrated as Wnt-independent (Song *et al*, 2007). These observations are consistent with the craniofacial and cleft palate defects observed in a mouse model of Treacher-Collins Syndrome (Sakai & Trainor, 2009) and may possibly be explained by a cooperative role for Treacle and Pygo2 in ribosome biogenesis.

Knock-down of Pygo2 in different cell lines revealed a consistent requirement for rRNA transcription, the cellular responses in different cell lines were strikingly different and appeared to be largely dependent on the tumor suppressor p53. I hypothesize that depletion of Pygo2 results in a p53 dependent cell cycle arrest in G1 in cells that express wild-type p53. Consistently, this was confirmed in other p53 positive cell types, including human endocervical cells, as shown above (Figure 3.11A). When both Pygo2 and p53 were co-depleted in HeLa cells, there were no apparent changes in the proportions of cells in each phase of the cell cycle compared to control treated cells (Figure 3.15), suggesting the observed G1 arrest was p53 dependent. While not explored here, co-depletion of Pygo2 and p53 could possibly result in changes in the relative growth rates, which would be consistent with the observed reduction in 47S rRNA transcription (Figure3.14A). Depletion of Pygo2 in the p53 null SKOV-3 cell line (along

with other p53 null cell lines, such as the prostate cell line PC3, data not shown), resulted in an accumulation of cells in the G2/M phase of the cell cycle (Figure 3.16A). This is a result that is surprising considering the co-depletion of Pygo2 and p53 in HeLa cells resulted in no apparent cell cycle arrest. While there was a decrease in the levels of the 47S pre-rRNA in SKOV-3 cells, I'm not certain that the accumulation of cells in G2/M can be entirely explained by this result. I therefore propose that the accumulation of cells in G2/M is at least partly due to an unknown role of Pygo2, as will be discussed in Chapter 4.

In support of my hypothesis that Pygo2 has an important function in ribosomal RNA transcription are the observations that depletion of Pygo2 triggered the nucleolar stress response, which could be reversed by knocking down p53, mirroring results found in a Treacle knock-out mouse model for Treacher-Collins syndrome (Dixon *et al*, 1997; Jones *et al*, 2008). The parallel between a requirement for Treacle-dependent ribosome biogenesis in normal development and Pygo2-dependent ribosome biogenesis in cancer cells suggests that the interaction we observed between Pygo2 and Treacle may be a conserved adaptation to rapid cell proliferation. Therefore, it would be interesting to examine the role of Treacle in a cancer cell model.

While Pygo2 is required for rRNA transcription, overexpression of Pygo2 was not sufficient to increase rRNA transcription in HeLa cells (Figure 3.10). One possible explanation for this could be that Pygo2 protein in HeLa cells is highly expressed (Andrews *et al*, 2008). Alternate possibilities may include scenarios which are not dependent on Pygo2 levels but on the levels and activities of additional factors. For example, Pygo2 activity could be tightly controlled and/or additional transcriptional

regulatory proteins may be present in limited amounts. Therefore, additional exogenously expressed Pygo2 in these cells may not result in a detectable increase in rRNA transcription. Although not explored here, overexpression of Pygo2 in a low expressing Pygo2 cell line, such as a normal or primary cell type, could possibly render a detectable increase in rRNA transcription. Interestingly, overexpression of a NPF-AAA Pygo2 mutant lacking transcriptional activity when tethered to DNA using a GAL4 DNA binding domain (Städeli & Basler, 2005), resulted in a significant reduction in rRNA transcription (Figure 3.10). These results indicate that the NPF residues of Pygo2 are indeed important for mediating interactions necessary for its role in rRNA transcription and thereby suggest that the transcriptional activity of Pygo2, in addition to its chromatin effector function is likely important for its role in rRNA transcription.

The core components of the rDNA transcriptional machinery localize to nucleolar caps following AMD treatment (Shav-Tal *et al*, 2005). The localization of Pygo2 to the central nucleolar body and not to nucleolar caps after treatment with AMD (Figure 3.7), is not inconsistent with a role in rDNA transcription. Similarly, p14/ARF, which plays a direct role in repressing rRNA transcription (Lessard *et al*, 2010), also co-localizes to the central nucleolar body following AMD treatment (Shav-Tal *et al*, 2005). While Pygo2 and p14ARF are not likely core components of the rDNA transcription machinery, it is possible that as modifiers of the rRNA transcription complex they associate with the central nucleolar body following AMD treatment. Finally, Pygo2 was dynamically associated with the active transcription complex required for rRNA transcription, two observations that are relevant to this are: 1) Pygo is not localized to nucleolar caps after AMD treatment, but is still associated with the nucleolus. 2) Pygo does not co-localize

with UBF at NORs during mitosis, when transcription is silenced (Heix *et al*, 1998; Roussel *et al*, 1996; Sirri *et al*, 1999), but appeared to be associated with the nucleolus during interphase.

The increased demand for ribosomes in cellular growth and proliferation requires that both RP and rRNA synthesis be amplified and precisely coordinated. Pygo2 may serve in this respect to augment or maintain Pol I-dependent transcription to keep in stride with ribosomal protein production in proliferating cells. Since Pygo2 is upregulated in a variety of cancers, these findings suggest that targeting Pygo2 with a small molecule inhibitor, for example JBC117 (Ali *et al*, 2016), represent a broadly applicable strategy would disrupt rDNA transcription, thereby targeting aberrantly growing cells.

Chapter 4: Transcriptional control of cell division by the Pygopus chromatin modulator

4.1 Introduction

During mitosis, equivalent segregation of genetic material to two daughter cells is a precisely coordinated process and depends on mitotic spindle capture of chromosomes. Proper biorientation is required for chromosomal segregation and is thought to occur by a search and capture mechanism in which nucleating spindle microtubules emanate from the centrosomes and make bi-oriented, amphitelic attachments to sister kinetochores, the molecular scaffolds that form the major attachment site to the chromosomes (Monda & Cheeseman, 2015; Tanaka, 2013, 2010; Tanenbaum & Medema, 2010; Foley & Kapoor, 2013). In addition to search and capture, other mechanisms efficiently drive biorientation. For example, the kinetochore contains nucleating microtubules that aid in microtubule-kinetochore capture by a mechanism dependent upon microtubule associated TPX2 (Katayama *et al*, 2008). Another major driver of microtubule-kinetochore interaction and capture is the Regulator of Chromosome Condensation 1 (RCC1) mediated RanGTP concentration gradient that exists around mitotic chromosomes which promotes microtubule nucleation (Kalab & Heald, 2008).

Mitotic spindle formation is controlled largely by the complex actions of several families of serine-threonine kinases that include, but are not limited to, both the Aurora Kinases (AurK) and the Polo-like kinases (Plk). AurKA is associated with mitotic entry, centrosome maturation and mitotic spindle assembly (Carmena *et al*, 2009). AurKB is the catalytic component of the chromosomal passenger complex (CPC) that acts as a master regulator of mitosis at many different levels, including chromosome condensation, kinetochore-microtubule attachments, spindle assembly checkpoint (SAC) activation and cytokinesis (Carmena *et al*, 2012). The Plks are required for several different mitotic

events, such as centrosome and kinetochore maturation, spindle assembly and cytokinesis (Archambault *et al*, 2015). Finally, both AurK and Plk are active in cancer and have gained attention as therapeutic targets (Goldenson & Crispino, 2014; Degenhardt & Lampkin, 2010).

Pygo2 is an emerging target in malignancy since its elevated expression and requirement for growth has been demonstrated in a number of different cancers (Andrews *et al*, 2007; Popadiuk *et al*, 2006; Tzenov *et al*, 2013; Zhang *et al*, 2015a; Liu *et al*, 2013). In addition to its role in Wnt signalling, Pygo2 protein acts broadly as a chromatin effector, linking active H3K4me3 marks to euchromatin formation through its association with histone acetyltransferase activity (Andrews et al, 2009; Chen et al, 2010; Fiedler et al, 2008), especially for expression of highly transcribed RNAs, such as histone mRNAs and ribosomal RNAs, essential for DNA replication and cell cycle progression (Gu et al, 2012; Andrews et al, 2013). These observations raised the possibility that Pygo2 acts epigenetically as a "euchromatic switch" to promote the transcription of key genes required for deregulated cell growth and division, such as in mammary tumor initiation (Watanabe et al, 2013) and prostate cancer (Yang et al, 2013). Therefore, while the role of Pygo2 in cancer growth has been clearly demonstrated, its role in cell division is unknown. In this study, I show that Pygo2 is essential for the proliferation of cancer cells through its epigenetic involvement in a transcriptional program controlling genes directly required for mitosis.

4.2 Materials and methods

4.2.1 Cell lines and antibodies

SKOV-3, PC3 and HeLa S3 cells were obtained from the American Type Tissue Collection (ATCC) and were cultured in Dulbecco's Modified Eagle Medium (DMEM) containing 10% fetal bovine serum. Antibodies used are given in Table 4.1.

4.2.2 RNAi and transfections

Non-targeting (siNTC) and Pygo2 (siPy2) siRNAs (Table 4.2) and concentrations used were previously described (Andrews *et al*, 2013). siRNAs were transfected at 5nM for HeLa S3 and 20nM for PC3 and SKOV-3 cells using Lipofectamine RNAiMAX (Invitrogen), as per the manufacturers' instructions.

4.2.3 Immunoblotting and immunoflourescence

Immunoblotting and immunoflourescence was performed exactly as described (Andrews *et al*, 2013). Confocal images were taken using a FluoView FV1000 confocal microscope (Olympus). For scoring of mitotic cells, three experiments were performed and cells counted from 5 random fields per treatment (siNTC, N=150; siPy2-1, N=196; siPy2-2, N=169) and were classified according to the observed mitotic profiles. Results represent averages for three experiments +/- SEM. P-values were calculated one-way ANOVA, using Tukey's multiple comparison test.

Table 4.1. **Antibodies.**

Antibody	**Clone/Catalogue number**	**Company/Reference**
Normal rabbit IgG	12-370	Millipore
α-tubulin	Ab15246	Abcam
α-tubulin	DM1A	Abcam
γ-tubulin	Ab11317	Abcam
INCENP	58-217	Abcam
H3K9Ac	Ab10812	Abcam
histone H3	Ab1791	Abcam
H3K27Ac	Ab4729	Abcam
Aurora Kinase B	Ab2254	Abcam
Pygo2	S3I4	Tzenov *et al*., 2015
Pygo2	Abe109	Millipore
H3K4me3	07-473	Millipore
H3K14Ac	07-353	Millipore
Aurora Kinase A	1F8	Cell Signalling Technology
Aurora Kinase A (P-T288)	C39D8	Cell Signalling Technology
Survivin	71G4B7	Cell Signalling Technology
Phospho-histone H3	06-570	Upstate Biotechnology
β-actin	AC-15	Sigma Aldrich
Flag	M2	Sigma Aldrich
FITC-CREST	15-235-F	Antibodies Incorporated

Table 4.2. siRNA and oligonucleotide sequences.

	F-primer (5'=>3')	R-primer (5'=>3')	Reference
Gene primer set			
β-actin	ATCTGGCACCACACCTTCTACAATGAGCTGCG	ATGGCTGGGGTGTTGAAGGTCTC	(Andrews *et al*, 2013)
Pygo2	GTCCCCCACTCCATGGCCGCCTCG	TCGCTTCTTTTCTGGACTCTTC	(Andrews *et al*, 2008)
INCENP	AAGCTCATGGAGTTTCTCTGC	CGTCTCTTCTTCCGTCGGTTC	HPB***
RCC1	CGGTGTGATTGGACTGTTGGA	CACCAAGTGGTCGTTTCCTGA	HPB
CEP290	AGATGCTCACCGAACAAGTAGA	ATGAGTCTGTTGAGAAAGGGTTG	HPB
BOD1	AGCCAGCTTACCAAAACCTGA	GCTTCCAACATCCCTGACTGAA	HPB
HAUS8	GGTCGGAAAGGGTGACCTG	GCGTCTTTTTGACGATGCTTTTG	HPB
OIP5	TGAGAGGGCGATTGACCAAG	AGCACTGCGTGACACTGTG	HPB
RAD51	CGAGCGTTCAACACAGACCA	GTGGCACTGTCTACAATAAGCA	HPB
TPX2	TCCTGCCCGAGTGACTAAGG	CTGTTAGGGGTTCGTTTATGGAA	HPB
ASPM	GGCCCTAGACAACCCTAACGA	AGCTTGGTGTTTCAGAACATCA	HPB
CDCA3	ACCTTGGAACCAGACTGAGTT	GGGATCTCCCTAGTACCTTGCT	HPB
CKAP5	TGTGGAAAGCAAGGTTAAGTGG	ACTCTGGGCTCTTTTCATCCT	HPB
SMC3	ATTGGTGCCAAAAAGGATCAGT	GATTGCTTCGAGAAAAACCAGC	HPB
CASC5	CTTCACACCGAGGACTCAAGA	TTTGATGTGTAGAAGAGGCACTG	HPB
BRCA1	ACCTTGGAACTGTGAGAACTCT	TCTTGATCTCCCACACTGCAATA	HPB
AURKA	GAGGTCCAAAACGTGTTCTCG	ACAGGATGAGGTACACTGGTTG	HPB
H4E	CCGTAAGGTCCTGCGAGATAA	AGTCACAGCATCACGAATCAC	(Gu *et al*, 2012)
H4B	AAGGCGGTAAAGGTTTGGGTA	GGAAATTCGCTTAACCCCACC	(Gu *et al*, 2012)
p21	GATGTCCGTCAGAACCCATGC	CAAAGTCGAAGTTCCATCGCTC	(Andrews *et al*, 2013)
KI67	AGAAGAAGTGGTGCTTCGGAA	AGTTTGCGTGGCCTGTACTAA	HPB
ChIP primer set			
INCENP promoter	CCGCCTCTTAGTCCCGCAGATTGC	CTGAAGGCTCAGCCAATCCTCG	
RCC1 promoter	CTGCAGTAGATTCCCAGAAGCCTCAG	GAAGCGACCACTGCGAATCTGTCTCC	

BOD1 promoter	CAGATGGCGTCAACGTTGACCTTTGC	GCGATCACGAGGCCTGCGCCTACAGTTCC	
CEP290 promoter	GATTCTCCGCCGGAGTCCCAGAGC	CCTCCTCTTCTCAGGGACTTCAGTTCC	
AURKA promoter	GGAGTTAAACCCTCTAGCTAGAAAGC	GTTGGCTCCACCACTTCCGGGTTC	
siRNAs			
siNTC	GGACUGUGGUCAACCAUGUUU		(Andrews *et al*, 2013)
siPy2-1	GGAGACAGCUUUAGGGAAUUU		
siPy2-2	GGAGUGAGGUGAACGAUGAUU		

***HPB (Harvard primer bank)

.

4.2.4 RT-qPCR and ChIP-qPCR

RNA was extracted using the RNeasy kit (Qiagen) and was used to make cDNA using MMLV (Invitrogen), as per the manufacturers protocols. For RT-qPCR analysis, primers used are listed in Table 4.2 and reactions used RT2 SYBR Green master mix (Qiagen). Relative values were calculated using the $2^{-\Delta\Delta Ct}$ method normalized to β-actin expression. Briefly, ChIP was performed using nuclei collected from formaldehyde crosslinked HeLa S3 cells. Nuclei were extracted in RIPA buffer (1.1% triton X-100, 0.01% SDS, 1.2mM EDTA, 16.7mM Tris pH8.1 and 167mM NaCl) supplemented with protease inhibitors and phenylmethanesulfonyl fluoride. DNA was sheared using a Sonic Dismembrator 100 (Fisher) to an average size of 300-500bp. Immunoprecipitations were performed using approximately 1mg of chromatin and 3μg of antibody, preblocked protein A agarose beads (Millipore) were used to capture the antibody-protein-DNA complexes. Beads were washed three times in a low salt buffer (1.0% triton X-100, 0.1% SDS, 2mM EDTA, 20mM Tris pH 8.1, 150mM NaCl) followed by one wash in high salt buffer (1.0% triton X-100, 0.1% SDS, 2mM EDTA, 20mM Tris pH 8.1, 500mM NaCl) and one wash in TE buffer. Complexes were eluted in elution buffer (1.0% SDS and 100mM NaHCO3); crosslinks were reversed at 65^{o}C overnight. Samples were RNase A and proteinase K treated before purifying the DNA using the QIAquick PCR purification kit (Qiagen). qPCR was performed using primers in Table 4.2 and values were calculated relative to the input controls. Results represent averages +/- SEM from two experiments.

4.2.5 ChIP-seq, RNA-seq and Bioinformatic analysis

Approximately 10ng of ChIPed DNA and RNA collected from Pygo2 treated cells were sent for high throughput sequencing (approximately 50 million reads per sample) at Seqwright Genomic Services including some data analysis (GE Healthcare, Houston, TX). All other data analyses were performed using SeqMonk v0.33.0 (http://www.bioinformatics.babraham.ac.uk/projects/seqmonk/), excluding non-unique and duplicate reads and mapping them to the reference human genome (GRCH37). Briefly, for the ChIP-seq analysis, significant peaks ($p < 10^{-5}$) were called from mapped reads with Seqmonk running a version of the MACS peak caller using default parameters. Data sets were generated with Pygo2 peaks falling within 1000 base pairs relative to TSS, the data sets were then used to make heat maps and trend plots of Pygo2 binding relative to TSS. For simple RNA-seq analysis, total reads were first normalized between treatments and differences were calculated in Seqmonk running R and compared the results of both Pygo2 targeting siRNAs to the NTC control siRNA using default Seqmonk parameters. Comparative analysis with H3K4me3, p300 and GCN5 was performed using Seqmonk with similar parameters as Pygo2 using the ENCODE Hela S3 ChIP datasets: ENCSR000AOF, ENCSR000ECR and ENCSR000ECV, respectively. Gene ontology analysis was performed using The Database for Annotation, Visualization and Integrated Discovery (DAVID) software using the GO FAT option (Huang *et al*, 2009).

4.3 Results

4.3.1 Depletion of Pygo2 results in an accumulation of cells in metaphase with mitotic chromosome and spindle defects

Our group previously demonstrated that depletion of Pygo2 in the p53 null SKOV-3 epithelial ovarian cancer cell line resulted in growth arrest, independent of Wnt/β-Catenin (Popadiuk *et al*, 2006). Growth arrest of the SKOV-3 cells was accompanied by an accumulation of cells in the G2/M phase of the cell cycle, which could at least be partly explained by a decreased transcription of the 47S rRNA (Andrews *et al*, 2013). Interestingly, similar G2/M accumulations were also obtained in several other p53 null cell lines, including the p53 null metastatic prostate cell line PC3 (Figure 4.1), thereby revealing a possible role for Pygo2 in G2/M phase of the cell cycle.

Under closer scrutiny, Pygo2 appeared to have a more direct role in mitosis. Mitotic profiles of SKOV-3 cells were compared that were treated with two different siRNAs targeting Pygo2 (siPy2-1 and siPy2-2; Figure 4.2A and 4.3) along with a non-targeting siRNA (siNTC) control. Immunofluorescence staining, using antibodies against phospho-histone H3 (p-HH3) and α-tubulin to mark dividing cells, indicated that Pygo2 depletion significantly increased the proportion of cells in metaphase ($p<0.001$) with a corresponding decrease of cells in prophase ($p<0.001$; Figure 4.2B), suggesting that cells may be delayed or arrested in metaphase. Moreover, Pygo2-depleted cells displayed defects in which the mitotic spindles appeared abnormal yet mitotic chromosomes failed to line up at the metaphase plates (Figure 4.2C). The observed defects in Pygo2

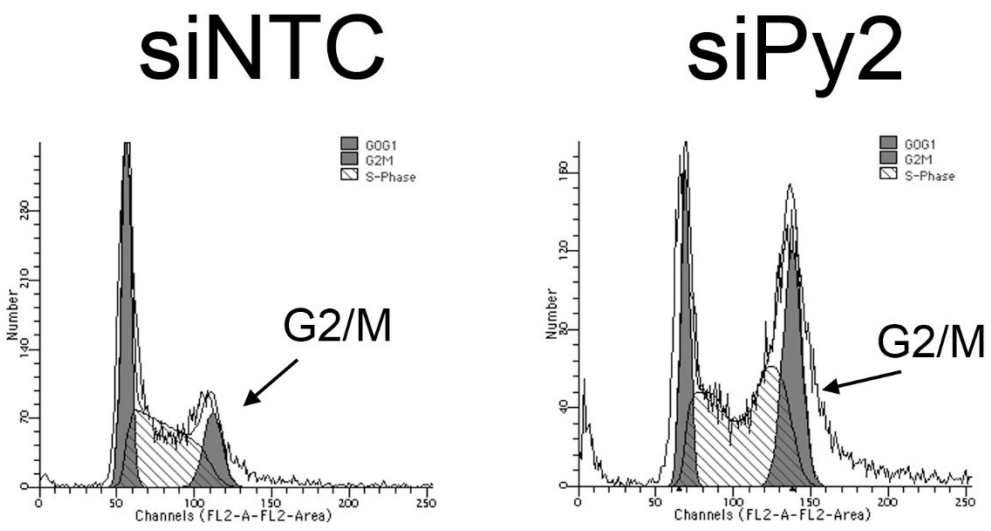

Figure 4.1. Pygo2 depletion results in accumulation of G2/M in p53 null PC3 cells. PC3 cells were treated for 72 hours with non-targeting (siNTC) or Pygo2 (siPygo2) siRNAs, cells were then fixed and stained with propidium iodide and the relative DNA content was examined using flow cytometry.

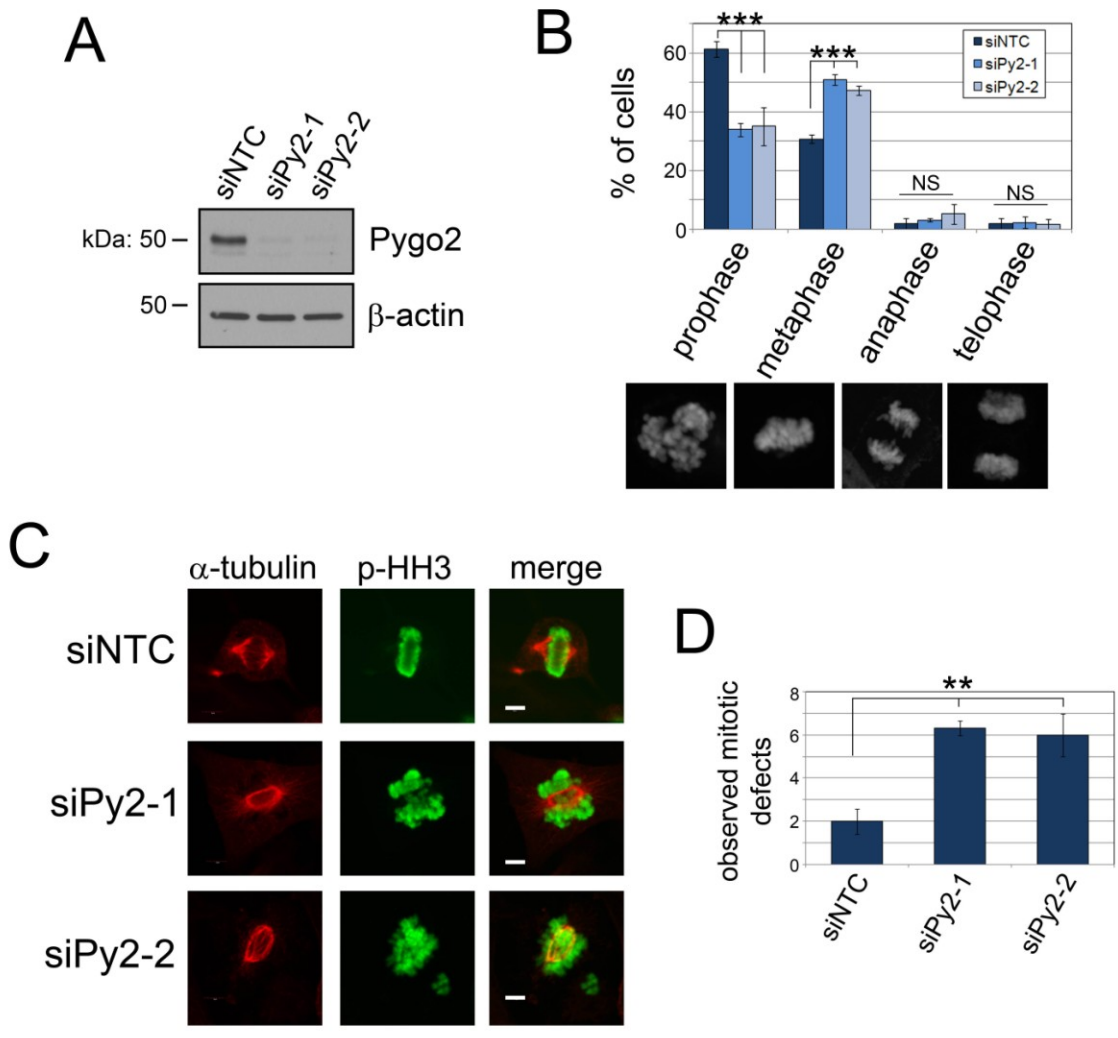

Figure 4.2. Depletion of Pygo2 results in mitotic defects. (A) Immunoblot showing a reduction of Pygo2 protein in SKOV-3 cells that were treated with a non-targeting siRNA (siNTC) or two Pygo2 specific siRNAs (siPy2-1 and siPy2-2), β-actin was used to as a loading control. **(B)** Pygo2 was depleted from SKOV-3 cells and cells were co-stained with α-tubulin and phospho-histone H3 (p-HH3) to visualize and score various mitotic stages. Pygo2 depleted cells resulted in a significant accumulation of cells in metaphase, consistent with a mitotic delay. Representative images of p-HH3 positive cells in each phase shown in the lower panel. **(C)** Confocal images of SKOV-3 cells co-stained with α-tubulin and p-HH3 from experiments performed in (B) showing chromosome and mitotic spindle defects (scale bar=5μm). **(D)** Quantification of observed mitotic defects, showing an increase number of defects in Pygo2 depleted SKOV-3 cells. Bar graphs represent averages +/- SEM. (**p<0.01, ***p<0.001, NS; not significant)

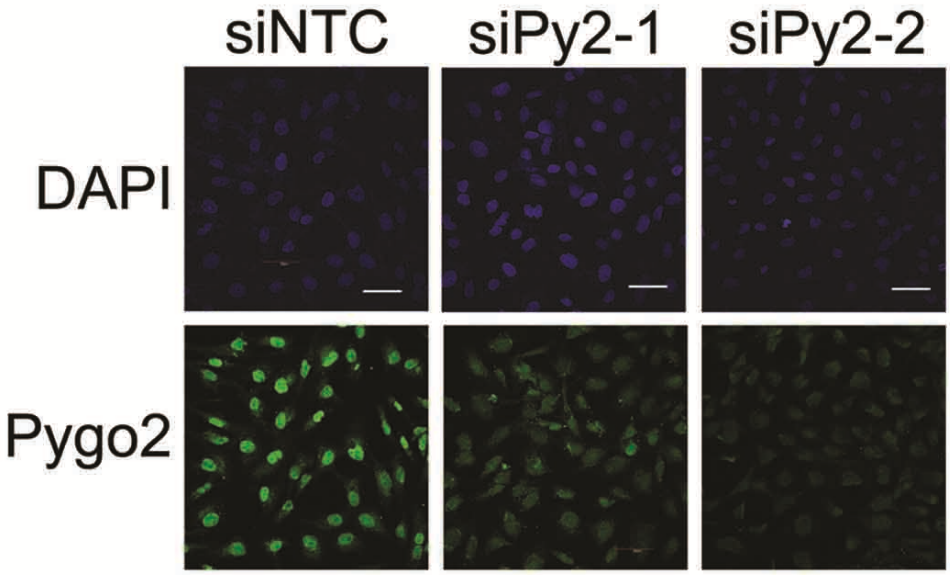

Figure 4.3. Depletion of Pygo2 with siRNA reduces nuclear Pygo2 protein. Confocal images of Pygo2 depleted SKOV-3 cells stained with Pygo2 and α-tubulin antibodies showing a reduction in nuclear Pygo2 levels. Scale bar = 50μm.

depleted cells were significantly higher as compared to cells treated with the non-targeting control (Figure 4.2D; $p<0.01$). Together, these results suggested that Pygo2 depletion resulted in mitotic spindle/chromosome defects, resulting in an accumulation of cells in metaphase.

4.3.2 Pygo2 is required for spindle-kinetochore recognition and chromosome biorientation

To investigate potential deficiencies in mitotic spindle function, γ-tubulin expression, which is required for proper centrosome formation and spindle microtubule nucleation, was examined (Kollman *et al*, 2011). In Pygo2 depleted cells, γ-tubulin appeared to be largely unaffected compared to the control-treated cells. However, in Pygo2 depleted cells the chromosomes appeared to be misaligned with the presumptive metaphase plates and the mitotic spindle microtubules appeared to circumnavigate the misaligned chromosomes (Figure 4.4).

To examine the alignment of the chromosomes and spindle microtubules, the localization of spindle microtubules was assessed with respect to the centromeres using α-tubulin and anti-centromere (CREST) antibodies/antiserum (Figure 4.5). Pygo2 depletion caused spindle related defects in which the centromeres were oriented in a parallel manner to the spindle microtubules, suggesting the chromosomes were not being efficiently captured by spindle microtubules. Similar results were obtained upon examination of the inner kinetochore protein INCENP (Figure 4.6), a component required for targeting and function of the CPC, which plays key roles in the capture of the mitotic spindle by the kinetochore during mitosis (Carmena *et al*, 2012). Next, two other CPC

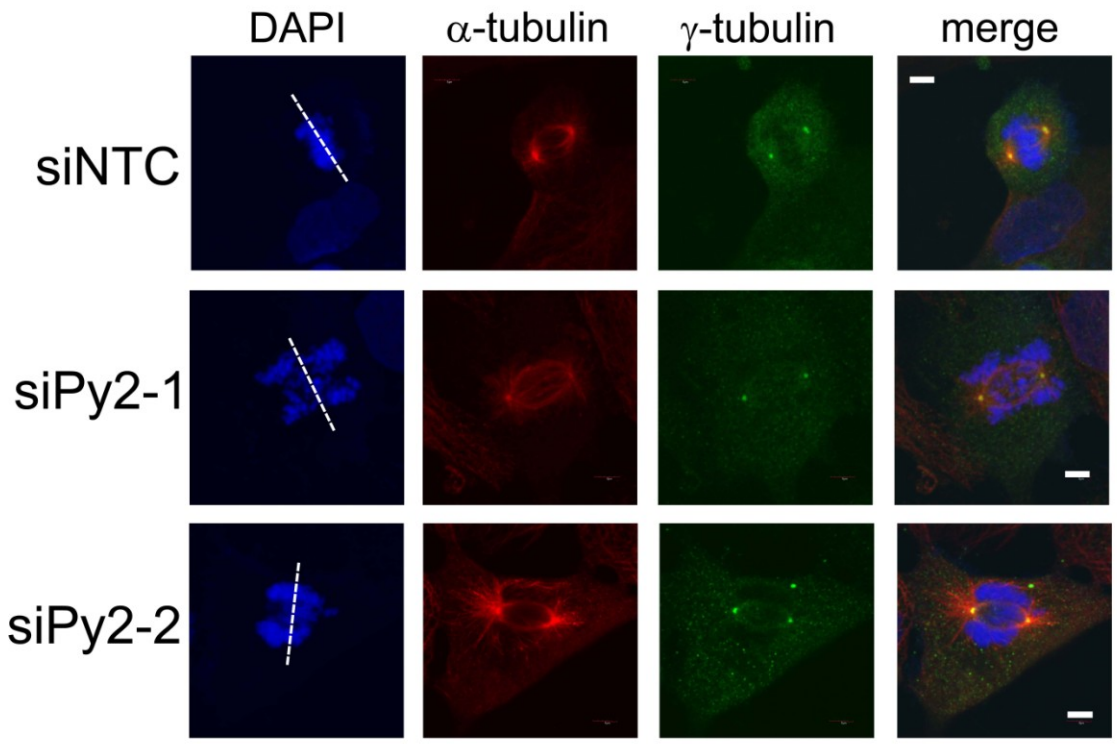

Figure 4.4. Depletion of Pygo2 does not appear to affect γ-tubulin and the centrosome. Confocal images of Pygo2 depleted SKOV-3 cells in metaphase stained with α-tubulin to visualize mitotic spindles and γ-tubulin to visualize centrosomes, showing little change in microtubule nucleation or centrosome localization. The dashed line indicates the plane of cell division and the presumptive metaphase plates. Scale bar = 5μm.

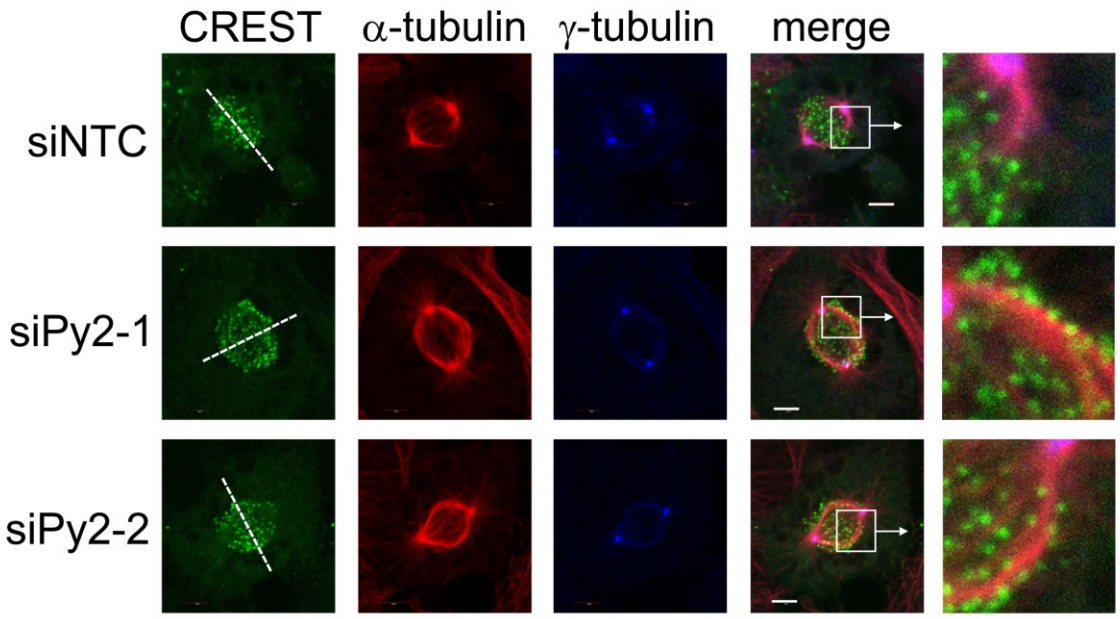

Figure 4.5. Pygo2 is required for proper spindle-kinetochore alignment in early metaphase cells. Confocal images of Pygo2 depleted SKOV-3 cells during early metaphase that were co-stained with anti-centromere antisera (CREST) to visualize centromeres and α-tubulin and γ-tubulin to visualize the mitotic spindles and spindle poles, respectively. The dashed line indicates the plane of cell division and the presumptive metaphase plates. Zoomed panels show misalignment of mitotic spindle microtubules and the centromeres and kinetochores. Scale bar = 5μm.

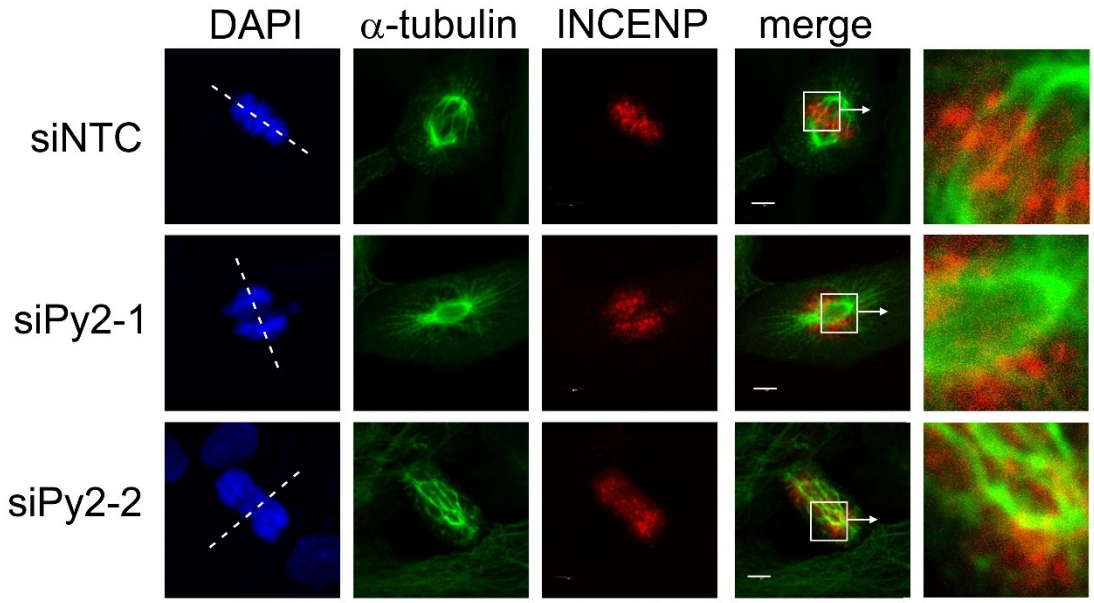

Figure 4.6. Pygo2 is required for spindle alignment with INCENP. Confocal images of Pygo2 depleted SKOV-3 cells during early metaphase that were co-stained with α-tubulin and INCENP to visualize the mitotic spindles and kinetochores, respectively. Zoomed panels show misalignment of mitotic spindle microtubules and the centromeres and kinetochores. The dashed line indicates the plane of cell division and presumptive metaphase plates. Scale bar = 5μm.

components: AurKB (Figure 4.7) and Survivin (Figure 4.8) were examined revealing a similar pattern of disorganized chromosomal- associated staining. However, both AurKB and Survivin co-localized weakly with INCENP at kinetochores, suggesting that the localization of CPC components to kinetochores was not greatly affected by Pygo2 depletion.

AurKA plays key roles in cell division, by controlling centrosome formation and also kinetochore microtubule attachment (Nikonova *et al*, 2013; Katayama *et al*, 2008). We found no change in the centrosomal localization of AurKA but a decrease in staining intensity as compared to control-treated cells (Figure 4.9). Similar decreases were observed with an antibody that recognizes active phosphorylated AurKA (AurKA P-T288; Figure 4.9), resulting from autophosphorylation of Threonine 288 (Nikonova *et al*, 2013). While we could not detect AurKA at kinetochores (Katayama *et al*, 2008), the reduction of AurKA at centrosomes suggests that its overall expression is likely decreased and could contribute to the observed changes in chromosome biorientation. These results therefore suggested that overall levels of centrosomal AurKA were affected by Pygo2 depletion, while there was little effect on subcellular localization or autophosphorylation.

4.3.3 Pygo2 is required for the expression of genes involved in cell division mechanics

Since Pygo2 protein appears to be excluded from mitotic chromatin (Andrews *et al*, 2013) and the expression of at least one candidate, AurKA, appeared to be affected by

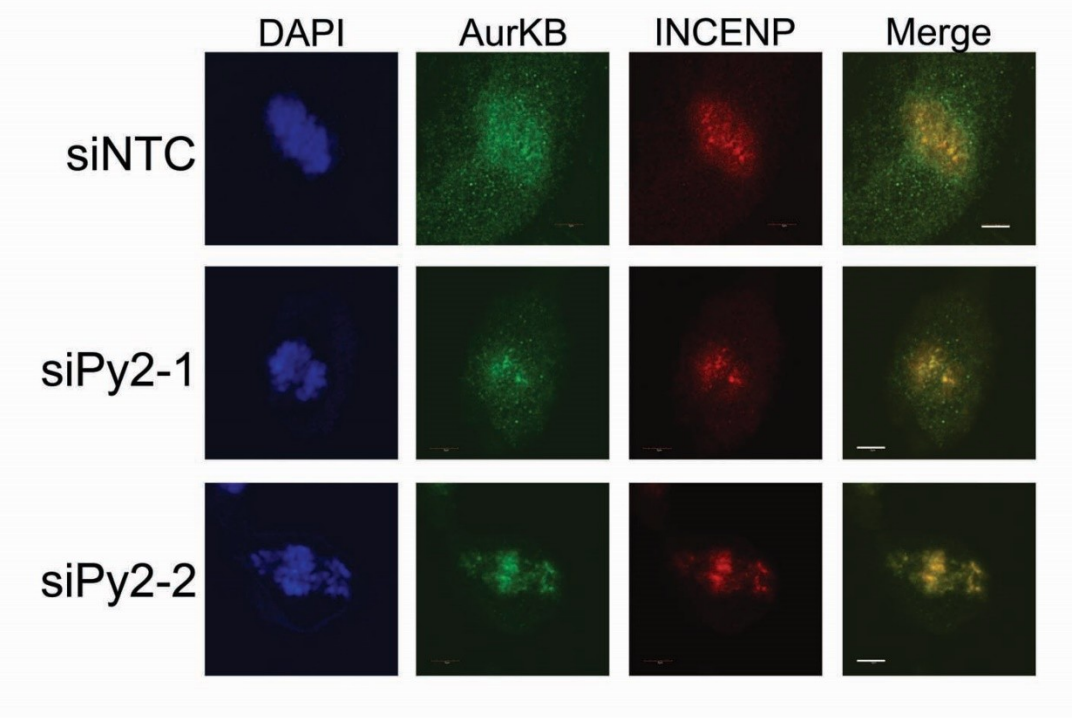

Figure 4.7. Pygo2 depletion does not affect the association of CPC components AurKB with INCENP. Confocal images of Pygo2 depleted SKOV-3 cells showing the localization of CPC components AurKB and INCENP. Scale bar = 5μm.

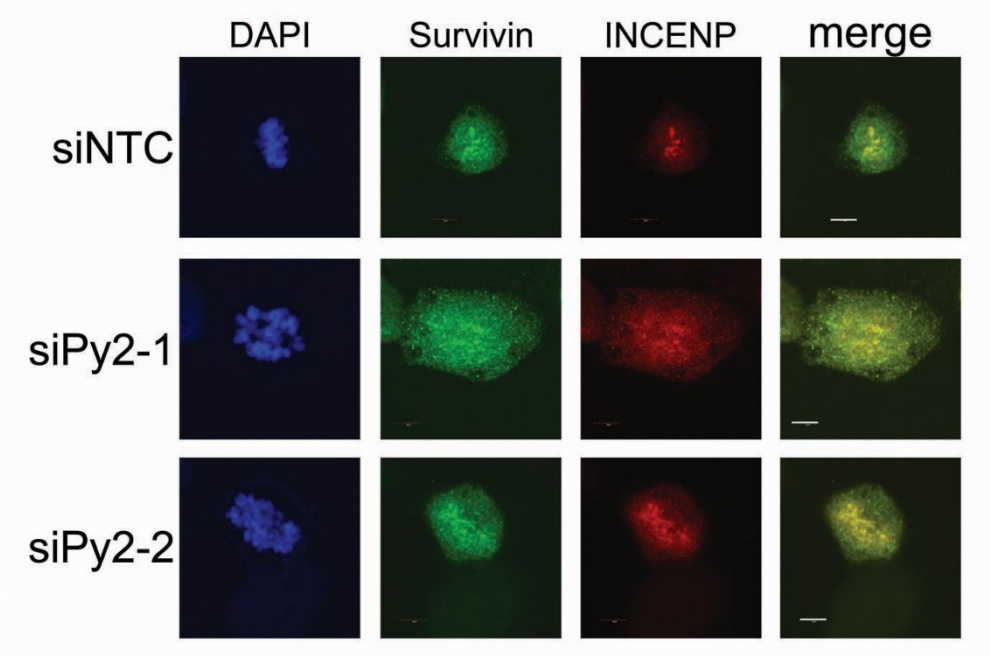

Figure 4.8. Pygo2 depletion does not affect the association of CPC components Survivin with INCENP. Confocal images of Pygo2 depleted SKOV-3 cells showing the localization of CPC components AurKB and INCENP. Scale bar = 5μm.

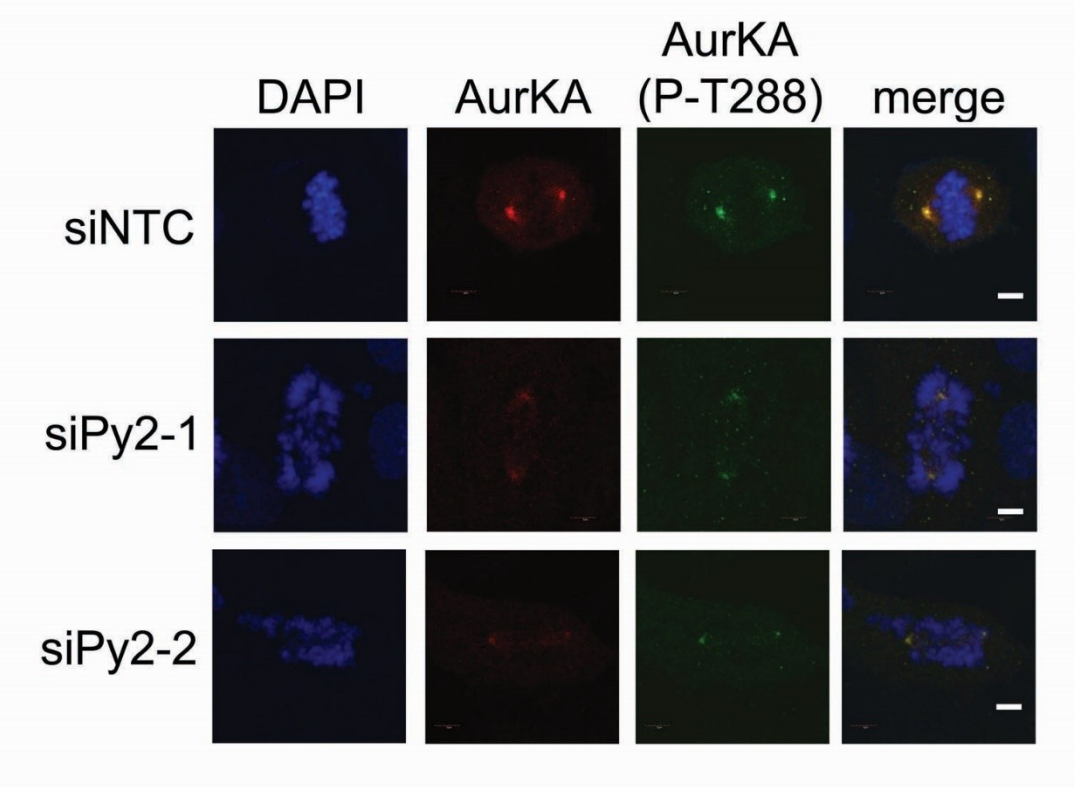

Figure 4.9. Depletion of Pygo2 leads to decreases levels of AurKA and active AurKA at centrosomes. Confocal images of Pygo2 depleted SKOV-3 cells stained with Aurora kinase A (AurKA) and activated phosphorylated AurKA (P-T288), showing a decrease in overall AurKA and AurKA (P-T288). For comparative purposes to show differences in intensities, confocal images were taken with the same exact settings. Scale bars=5μm.

loss of Pygo2, I hypothesized that it may function as a chromatin effector involved in the transcription of genes either directly or indirectly required for mitosis. To this end, Pygo2 was depleted from HeLa S3 cells (Figure 4.10A) and massively parallel RNA-sequencing (RNA-seq) was performed (Seqwright) on extracted RNA to identify mitotic candidate genes.

Using RNA-seq analysis, I identified a total of 379 mRNAs that significantly changed using both Pygo2-targeting siRNAs compared to the control (siNTC; Figure 4.10B). Out of the 379 mRNAs, 287 were upregulated and 92 were downregulated (Figure 4.10C and 4.10D). Gene ontology (GO) analysis was performed on both up- and down-regulated genes using DAVID (Huang *et al*, 2009). GO analysis of upregulated genes revealed functional ontologies in primarily cell proliferation and cell adhesion, while GO analysis of downregulated genes revealed functional ontologies, with significantly high scoring groups related to mitosis and cell cycle (Figure 4.11), consistent with our previous results.

4.3.4 Pygo2 associates with promoter proximal regions adjacent to TSS

In an attempt to identify direct Pygo2 target genes, the genome wide association of Pygo2 with TSS on HeLa S3 chromatin was interrogated using ChIP followed by high throughput massively parallel sequencing (ChIP-seq) of chromatin DNA (Seqwright) precipitated by two Pygo2 antibodies; one from a commercial source (ABE109, Millipore) and one (S3I4) that was previously generated and characterized in our lab (Tzenov *et al*, 2015). High confidence peaks were calculated using a version of the

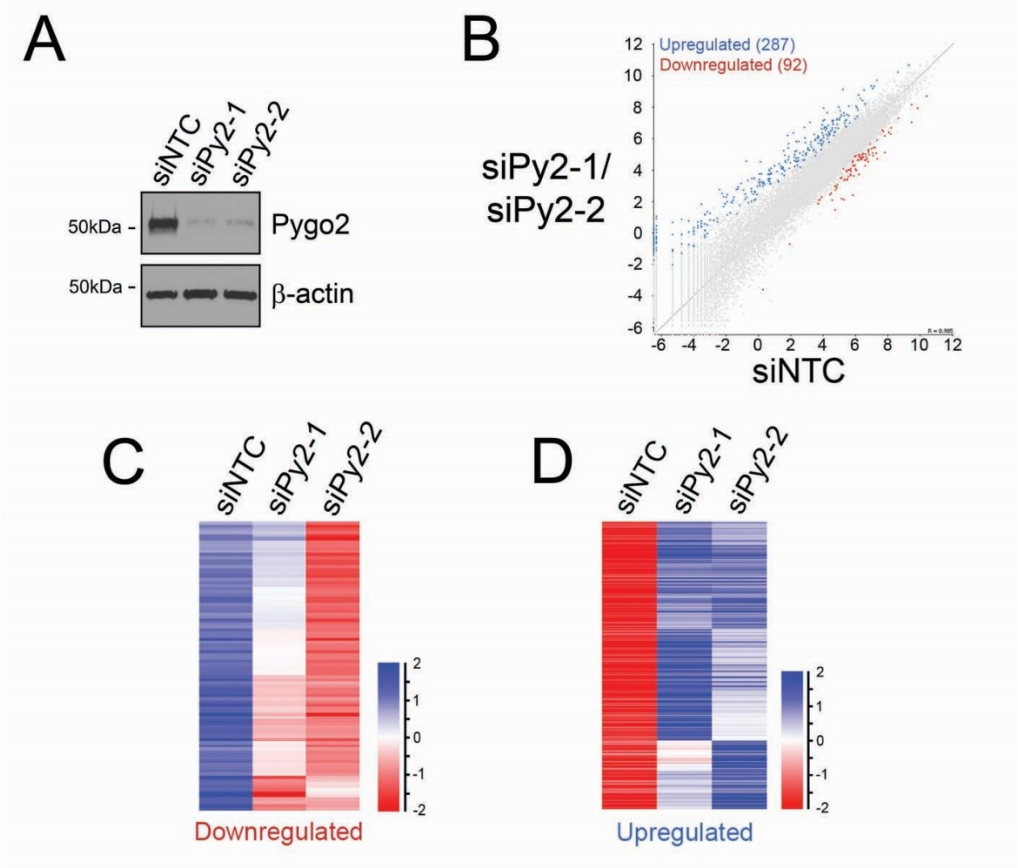

Figure 4.10. Genome wide analysis of Pygo2 responsive genes. (A) Immunoblot analysis using a Pygo2 specific antibody to confirm Pygo2 knockdown in HeLa S3 cells, prior to performing RNA-seq. **(B)** Scatter plot highlighting upregulated and downregulated genes from all genes analyzed by RNA-seq. **(C and D)** Heat maps illustrating the relative expression of the 92 downregulated and 287 upregulated genes resulting from Pygo2 depletion, respectively.

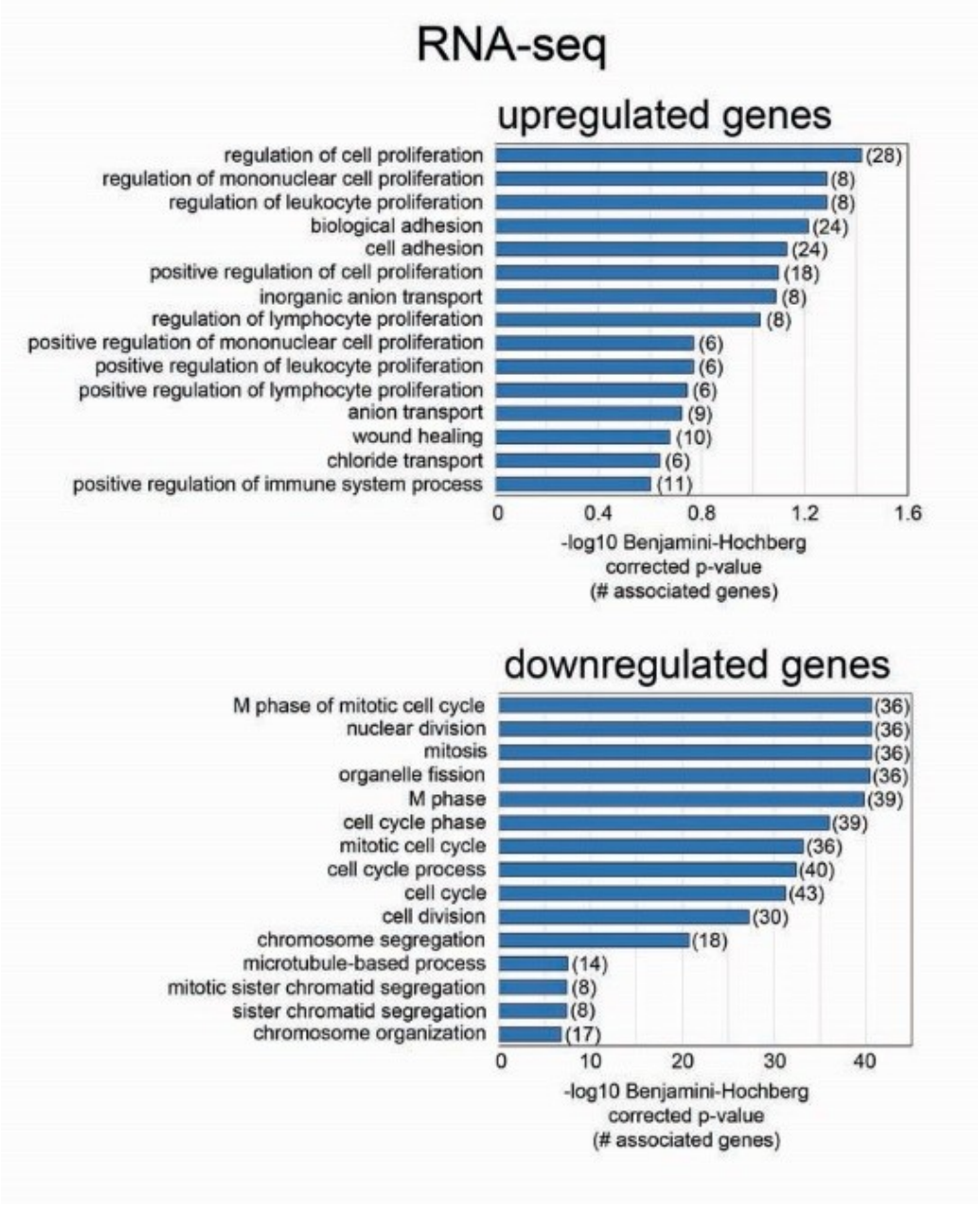

Figure 4.11. Pygo2 responsive genes are associated with genes involved in cell cycle and mitosis. DAVID GO analysis of 287 upregulated (upper panel) and 92 downregulated (lower panel) genes from RNA-seq analysis. Total number of genes in each category are in parenthesis. Benjamani-associated p-values represent a measurement of false discovery rate.

Model-based Analysis for ChIP-seq (MACS) peak caller using a p-value cut-off of 10^{-5}. This analysis revealed an enrichment of the most robust peaks (lowest p-values) approximately 74 base pairs upstream of transcription start sites (TSS)s for both Pygo2 antibodies used (Figure 4.12A and 4.12B), indicating that Pygo2 binding was enriched around TSSs. Motif analysis of the binding sites associated with Pygo2 revealed a correlation with sites that are similar to the FOXP1 consensus sequences and loosely correlated with sites that resemble Tcfcp2l1 binding sites (Figure 4.12C). GO analysis of common ChIP-seq sites using both Pygo2 antibodies revealed functional ontologies related to complex assembly, chromatin, transcription, cell cycle and mitosis (Figure 4.13).

Pygo2 is hypothesized to induce euchromatin formation at transcriptionally active target genes by recruiting and promoting histone acetyltransferase (HAT) and methyltransferase activity (Gu *et al*, 2012; Andrews *et al*, 2009; Chen *et al*, 2010). I therefore compared the genome wide enrichment of Pygo2, H3K4me3, p300 and GCN5 using available ChIP datasets from ENCODE performed on HeLa S3 cells. I found the genome-wide association of Pygo2 on chromatin relative to TSS was correlated with the position of p300 binding and it also showed a positive correlation with the HAT GCN5 and active H3K4me3 marks at promoters (Figure 4.14).

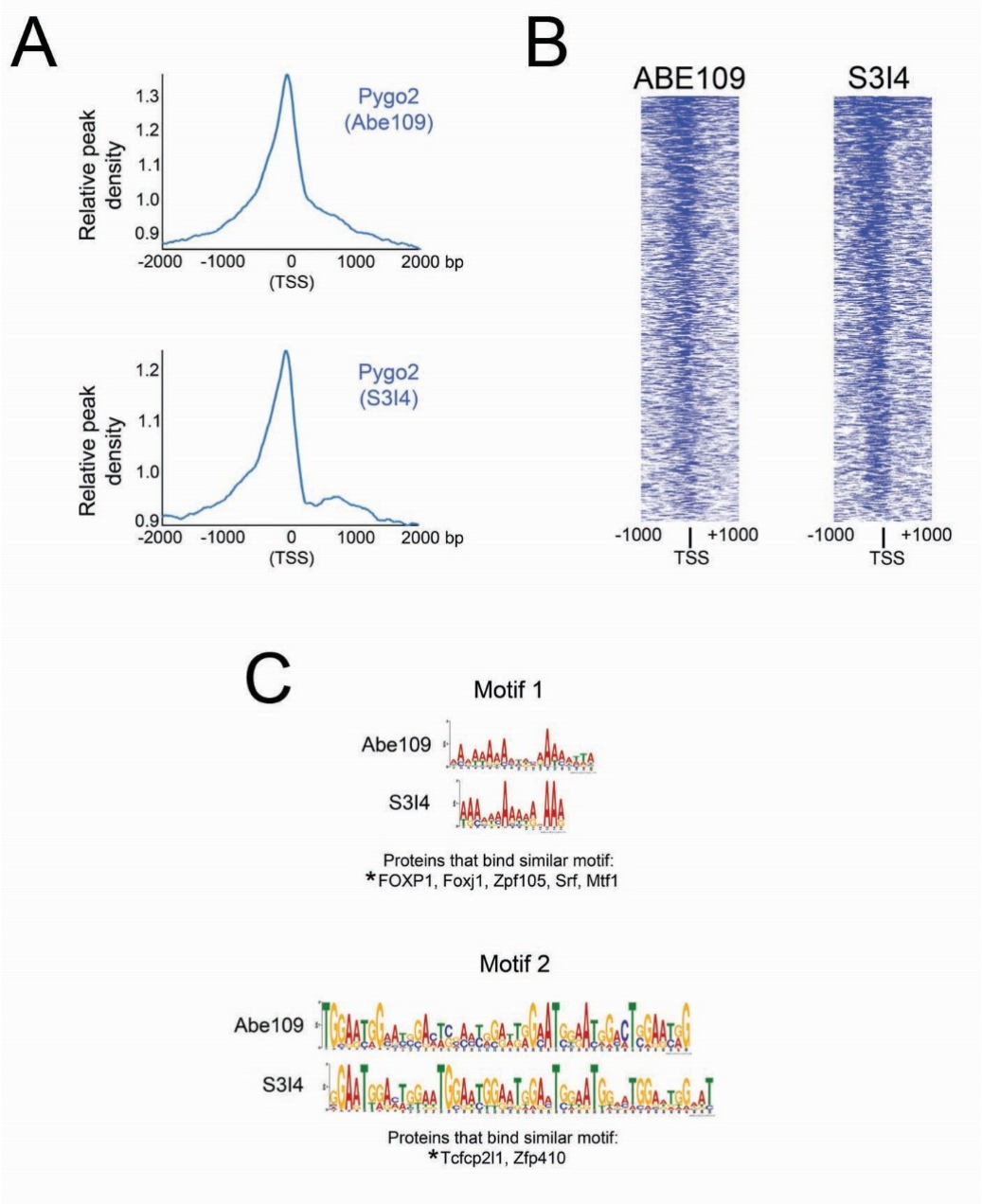

Figure 4.12. Genome wide analysis of Pygo2 enrichment with chromatin. Probe trend plots **(A)** and aligned probe plots **(B)** generated from HeLa S3 ChIP-seq data using two different Pygo2 antibodies (Abe109 and S3I4) indicating the average enrichment of Pygo2 from -2000 to +2000 relative to transcriptional start sites (TSS), with the maximum enrichment occurring approximately 74 bp upstream of TSS. **(C)** Peak motif analysis of Pygo2 peaks revealing between 30-50 FOXP1 binding sites (motif 1; upper panel) and between 7-9 Tcfcp2l1 binding sites (motif 2; lower panel).

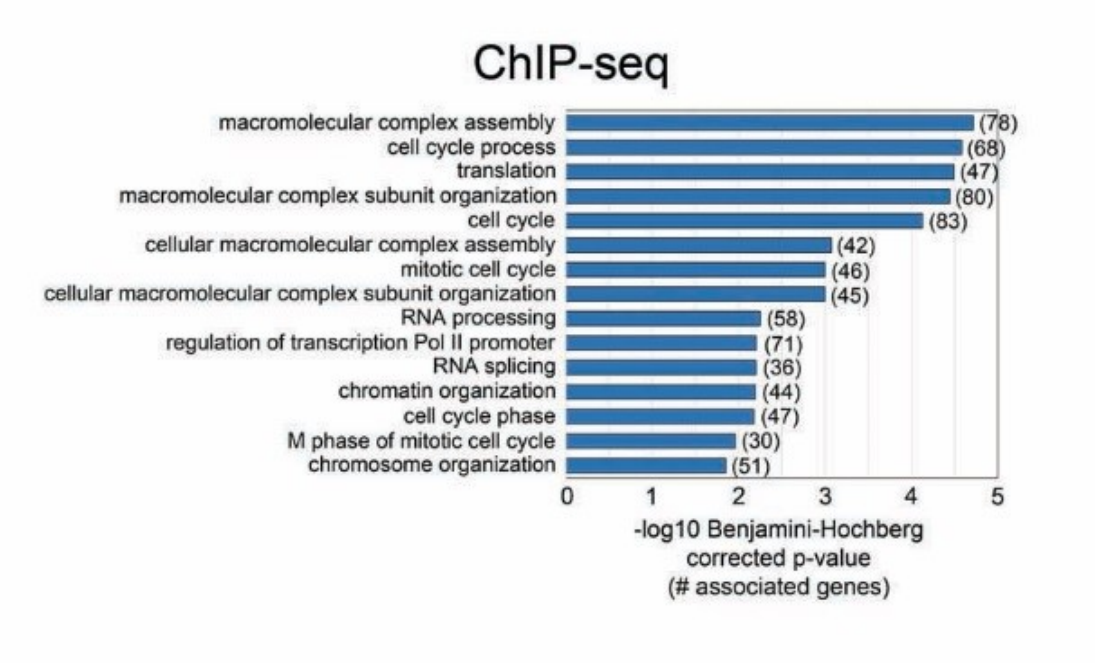

Figure 4.13. DAVID GO analysis of the common 1341 ChIP-seq genes using two different Pygo2 antibodies. The total number of genes in each category is in parenthesis. Benjamani-associated p-values represent a measurement of false discovery rate.

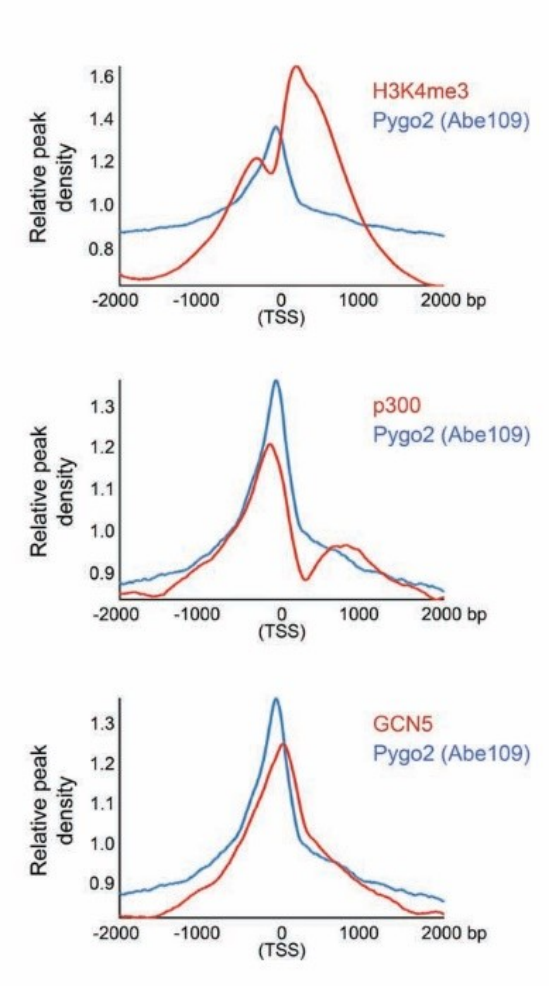

Figure 4.14. Pygo2 enrichment at TSS correlates with H3K4me3 and HATs. Probe trend plots showing correlation of enriched Pygo2 binding (Abe109) with the active histone mark H3K4me3 and the HATs p300 and GCN5, with respect to TSS in HeLa S3 cells.

4.3.5 Pygo2 directly regulates a subset of genes involved in mitotic cell division control

To reduce false positives and identify *bona fide* functional Pygo2 target genes I examined 1341 genes that showed enriched Pygo2 binding common to both Pygo2 antibodies used in the ChIP-seq analysis. To expand our downregulated gene list to all functionally downregulated Pygo2 target genes, I compared the relative expression of the 1341 genes with those analyzed by RNA-seq and found that 210 of the 1341 genes showed a reduction in RNA expression to less than 75 percent with two Pygo2-targeting siRNAs compared to the non-targeting control (Figure 4.15A).

Among the 210 genes were several histone gene targets that were previously identified to be directly regulated by Pygo2 (Gu *et al*, 2012), providing independent validation of my ChIP-seq and RNA-seq analysis (Figure 4.16; $p<0.001$). While not direct Pygo2 target genes, I observed an increase in *p21* expression ($p<0.01$), consistent with previous results (Gu *et al*, 2009; Andrews *et al*, 2013) and a concomitant decrease in the proliferation marker *KI-67* (Figure 4.16; $p<0.001$). Gene ontology (GO) analysis was performed on the 210 identified Pygo2 target genes using DAVID (Huang *et al*, 2009). This analysis revealed a significant association of GOs related to mitotic cell division and spindle assembly (Figure 4.15B), which correlated with the independent RNA-seq and ChIP-seq analysis.

To confirm expression of the subset of genes identified by RNA-seq with GOs related to mitotic cell division, I performed RT-qPCR analysis for 15 candidate genes,

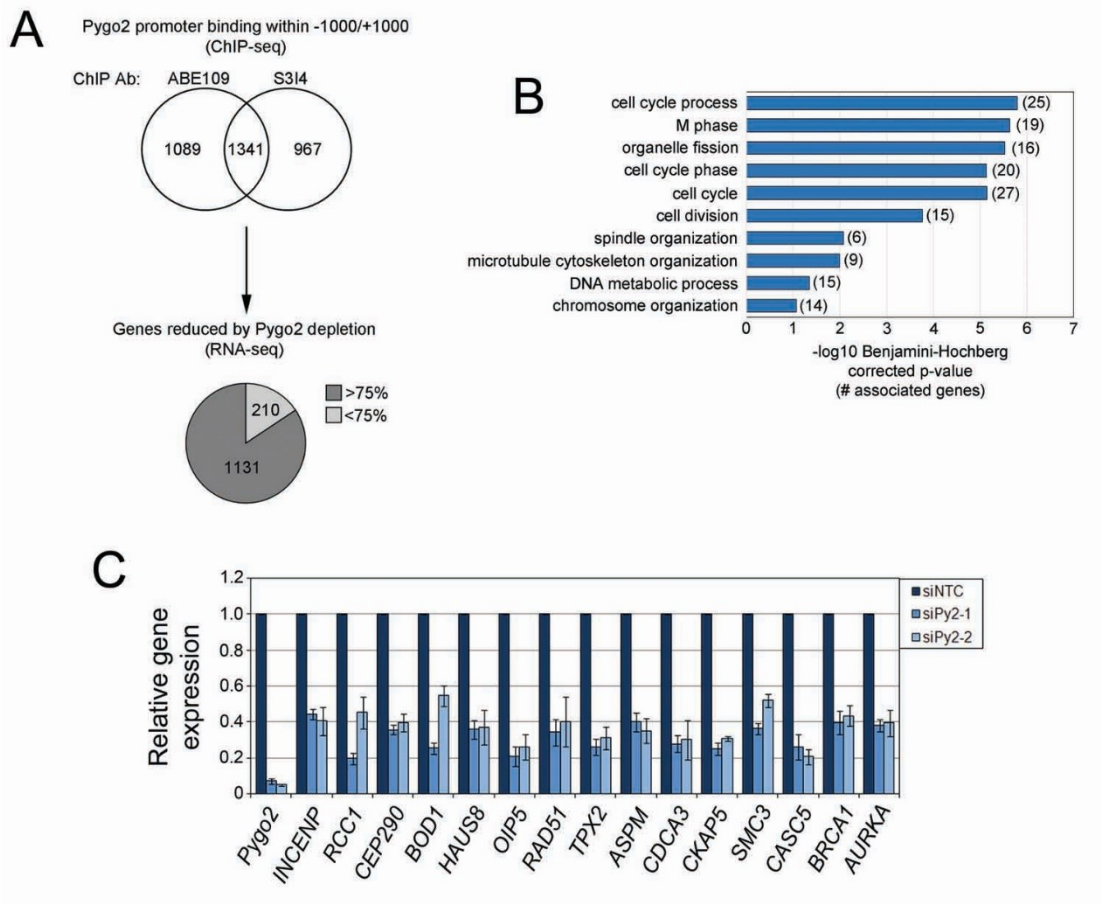

Figure 4.15. Pygo2 is directly involved in controlling the transcription of a subset of genes involved in mitotic cell division. (A) Workflow of whole genome analysis using ChIP-seq and RNA-seq to identify 210 functionally relevant Pygo2 target genes. Expression of 1341 common genes that showed Pygo2 enrichment within 1000bp of TSS using two Pygo2 antibodies was analyzed by RNA-seq data of HeLa S3 cells that were treated with two Pygo2 targeting siRNAs, compared to a non-targeting siRNA control. 210 of 1341 genes whose expression were downregulated lower than 75 percent compared to the control were identified. **(B)** Top functional GO categories using DAVID software to analyze the 210 genes identified by ChIP-seq and RNA-seq (parenthesis indicate number of associated genes in each category). **(C)** Depletion of Pygo2 in HeLa S3 cells followed by RT-qPCR to examine and validate the RNA expression of Pygo2 and 15 candidate Pygo2 target genes with ascribed function in cell division. Reduced expression of all genes, $p<0.001$.

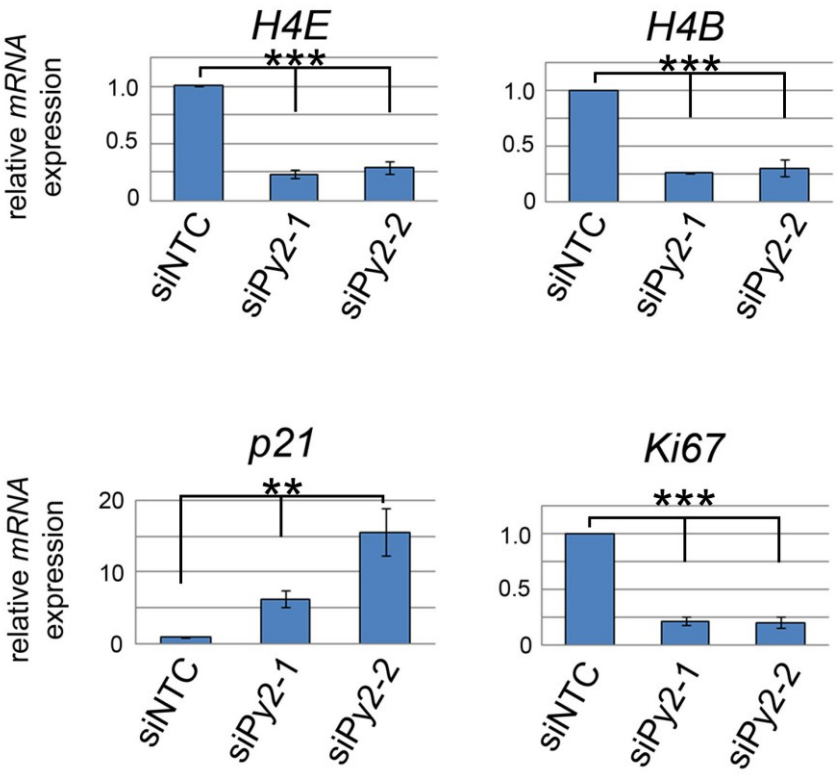

Figure 4.16. Pygo2 is required for histone and cell cycle gene expression. RT-qPCR of histone genes (*H4E and H4B*), *p21* and proliferation marker *KI-67* normalized to β-actin expression in Pygo2 depleted HeLa S3 cells. Bar graphs represent mean +/- SEM. (***p<0.001, **p<0.01)

which showed function in mitotic spindle-kinetochore assembly, following Pygo2 depletion (Figure 4.15C). Depletion of Pygo2 resulted in a significant reduction to less than 50 percent compared to that of the controls for all the mitotic candidate genes analyzed ($p<0.001$). Interestingly, among these were genes directly required for microtubule attachment to the kinetochores, such as *RCC1*, *INCENP, AurKA* and *TPX2*, consistent with the mitotic defects observed (Figure 4.2).

4.3.6 Pygo2 plays a role in H3K27Ac at genes required for mitosis

To assess whether Pygo2 plays a role in euchromatin formation at mitotic target genes, the status of H3K4 trimethylation and H3K9, K14 and K27 acetylation was examined at the promoters of five randomly chosen target genes identified from Figure 4.15C (Figure 4.17). As a control, depletion of Pygo2 resulted in a reduction of Pygo2 bound to the promoters of all genes analyzed ($p<0.05$). While not statistically significant ($p>0.05$/p=NS), Pygo2 depletion resulted in an observed decrease of both H3K9 acetylation and H3K4 trimethylation compared to the control treated cells at the *BOD1*, *RCC1* and *INCENP* promoters, consistent with a role for Pygo2 in functionally binding to MLL2 and GCN5 (Chen *et al*, 2010). While there was no observed difference in H3K14 acetylation (p=NS), Pygo2 depletion on the other hand, resulted in decreased H3K27 acetylation at all the promoters analyzed ($p<0.05$), consistent with a required role in their expression (Figure 4.15C), highlighting the role of Pygo2 as a chromatin effector.

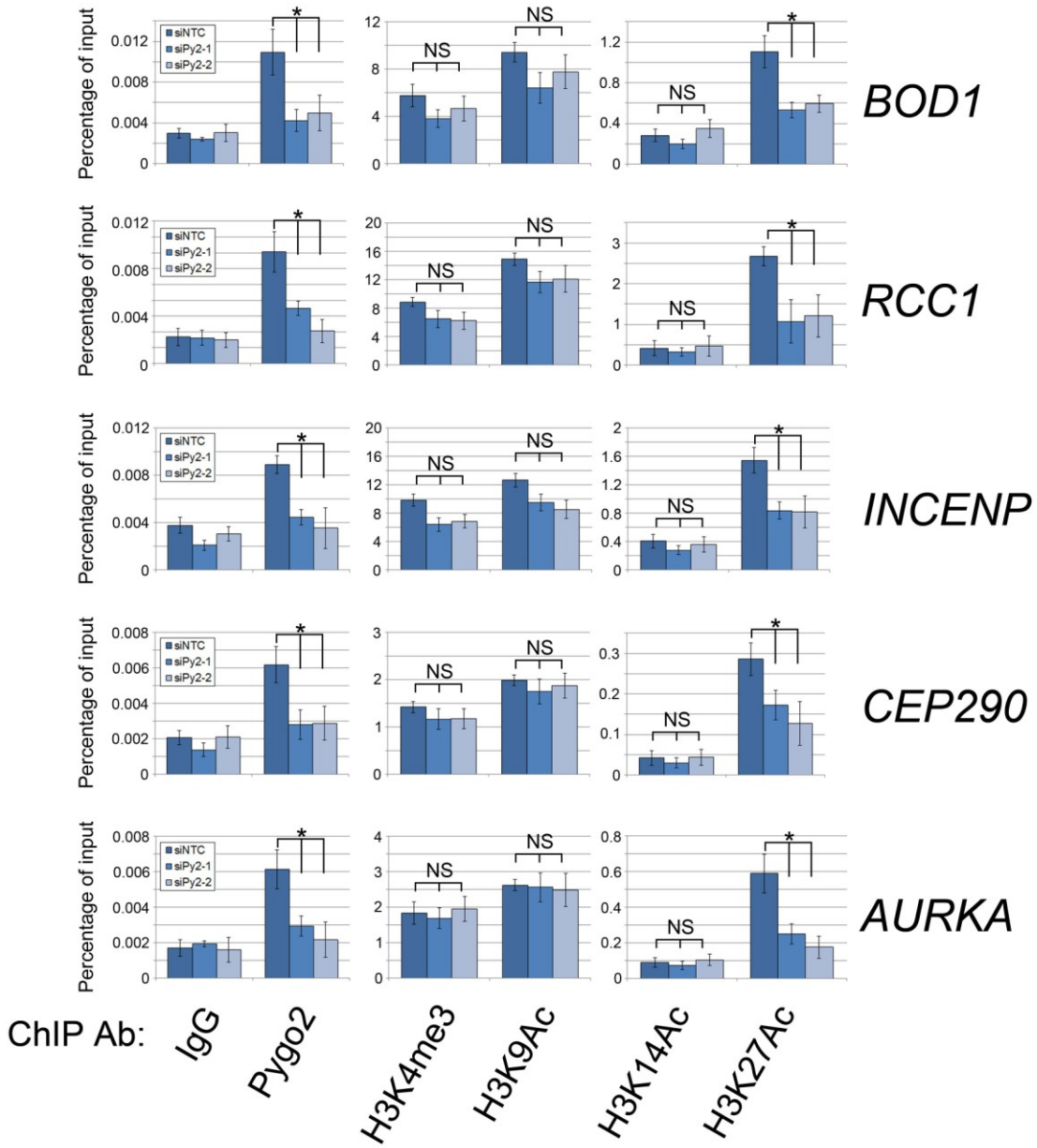

Figure 4.17. Pygo2 plays a role in H3K27Ac at gene promoters involved in the regulation of mitosis. Examination of the relative enrichment of Pygo2, H3K4me3, H3K9Ac, H3K14Ac and H3K27Ac in Pygo2 depleted HeLa S3 cells, at the BOD1, RCC1, INCENP, CEP290 and AurKA promoter regions by ChIP-qPCR. Bar graphs represent averages +/- SEM. (*$p<0.05$, NS; not significant)

4.3.7 Association between Pygo2 and the c-myc proto-oncogene

The foregoing results suggested an essential role for Pygo2 in promoting a transcriptional program required for cell division. Interestingly, some of the critical Pygo2 target genes identified, such as *AurKA* and *RCC1*, were also targets of the c-myc proto-oncogene (Den Hollander *et al*, 2010; Tsuneoka *et al*, 1997). This prompted the hypothesis that Pygo2 and c-myc may be present in a complex and may regulate similar sets of genes. Therefore, ChIP-seq public-domain (ENCODE) data for c-myc binding in HeLa S3 cells were compared with the data obtained for Pygo2 to ascertain an *in silico* association. Strikingly, I found that approximately 50% of the identified Pygo2 ChIP-seq and functional target genes were also occupied by c-myc (Figure 4.18A), thereby suggesting the proteins may target similar sets of genes. Analysis of the 117 functional Pygo2 and c-myc genes revealed ontologies mainly related to mitotic cell division (Figure 4.18B)

Interestingly, the accumulating evidence for Pygo2 in malignant growth parallels the oncogenic potential of c-myc. For example, the growth promoting activity of c-myc, and as we have shown for Pygo2, partly depends on its requirement for rDNA gene expression (Grandori *et al*, 2005; Arabi *et al*, 2005). Therefore, to test the existence of a Pygo2/c-myc interaction, both Pygo2 and myc tagged (MT) c-myc were co-transfected into HEK-293 cells and forward and reverse immunoprecipitations were performed and confirmed an interaction between the two proteins (Figure 4.19A). The interaction between Pygo2 and c-myc was confirmed in HeLa S3 cells using Pygo2 antisera to immunoprecipitate Pygo2 and by performing immunoblots for c-myc (Figure 4.19B). Finally, Pygo2 and c-myc showed a similar pattern of localization in the nuclei of HeLa

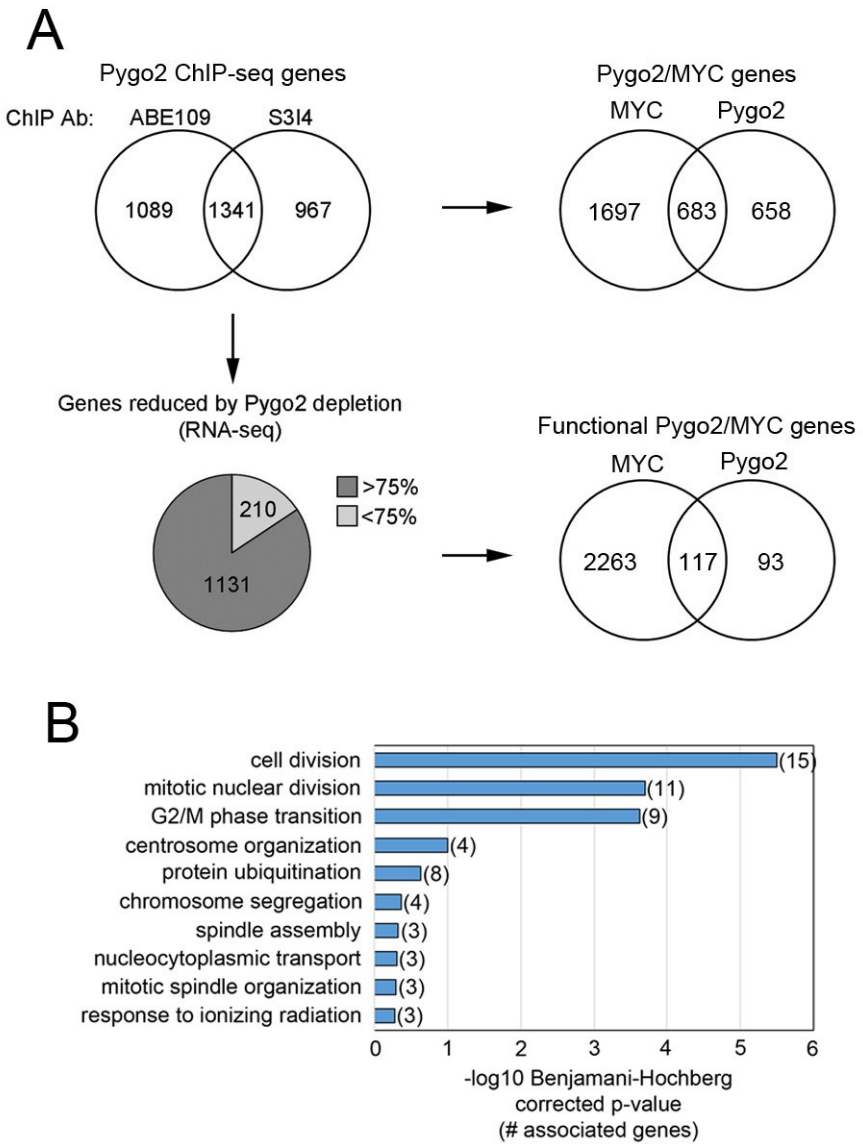

Figure 4.18. *In silico* analysis of Pygo2/c-myc (MYC) genes in HeLa S3 cells. (A) Left panels represent Pygo2 target genes and functional Pygo2 target genes that were identified in Figure 4.15. Right panels show the association of the Pygo2 target genes that are shared with c-myc. **(B)** Gene ontologies associated with 117 "functional" Pygo2/c-myc genes.

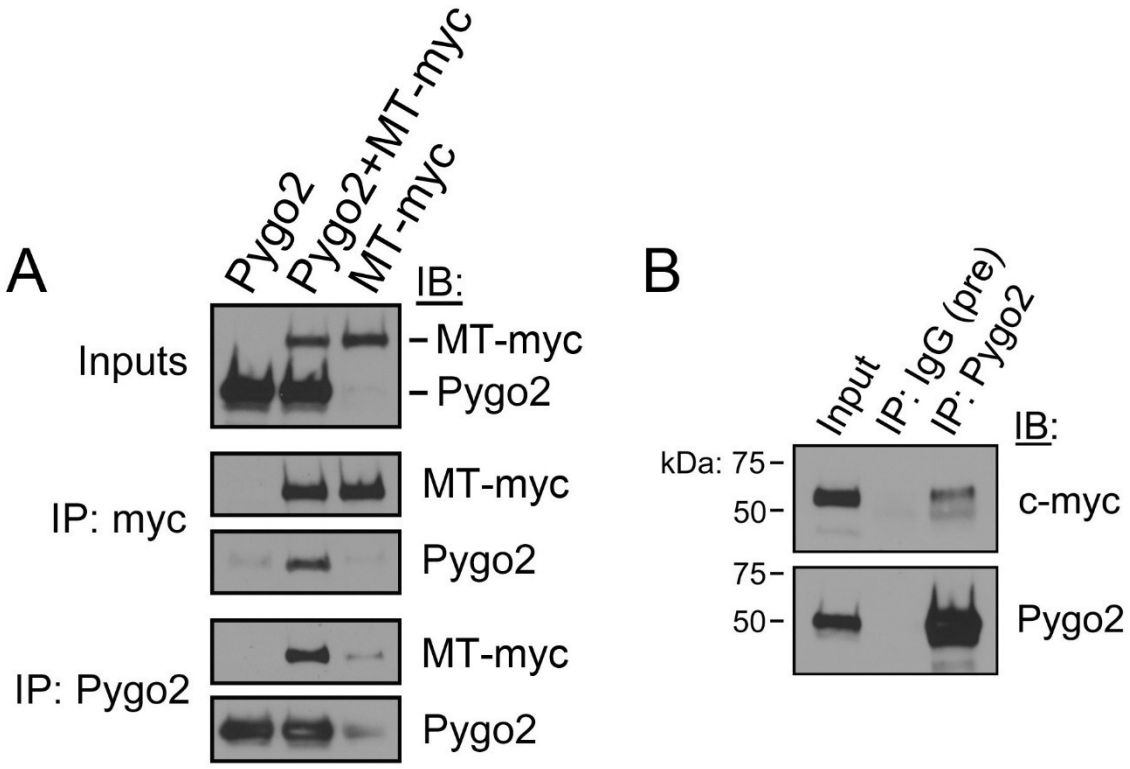

Figure 4.19. ***In vivo*** **association between Pygo2 and c-myc. (A)** Pygo2 and c-myc interact in HEK-293 cells that were co-transfected and immunoprecipitated (IP) with MT-myc and Pygo2. Immunoblots (IB) were performed with myc and Pygo2 antibodies. **(B)** Pygo2 and c-myc interact in HeLa S3 cells. Cells were co-transfected with Pygo2 and c-myc, immunoprecipitations were performed with either pre-immune sera or Pygo2 antisera.

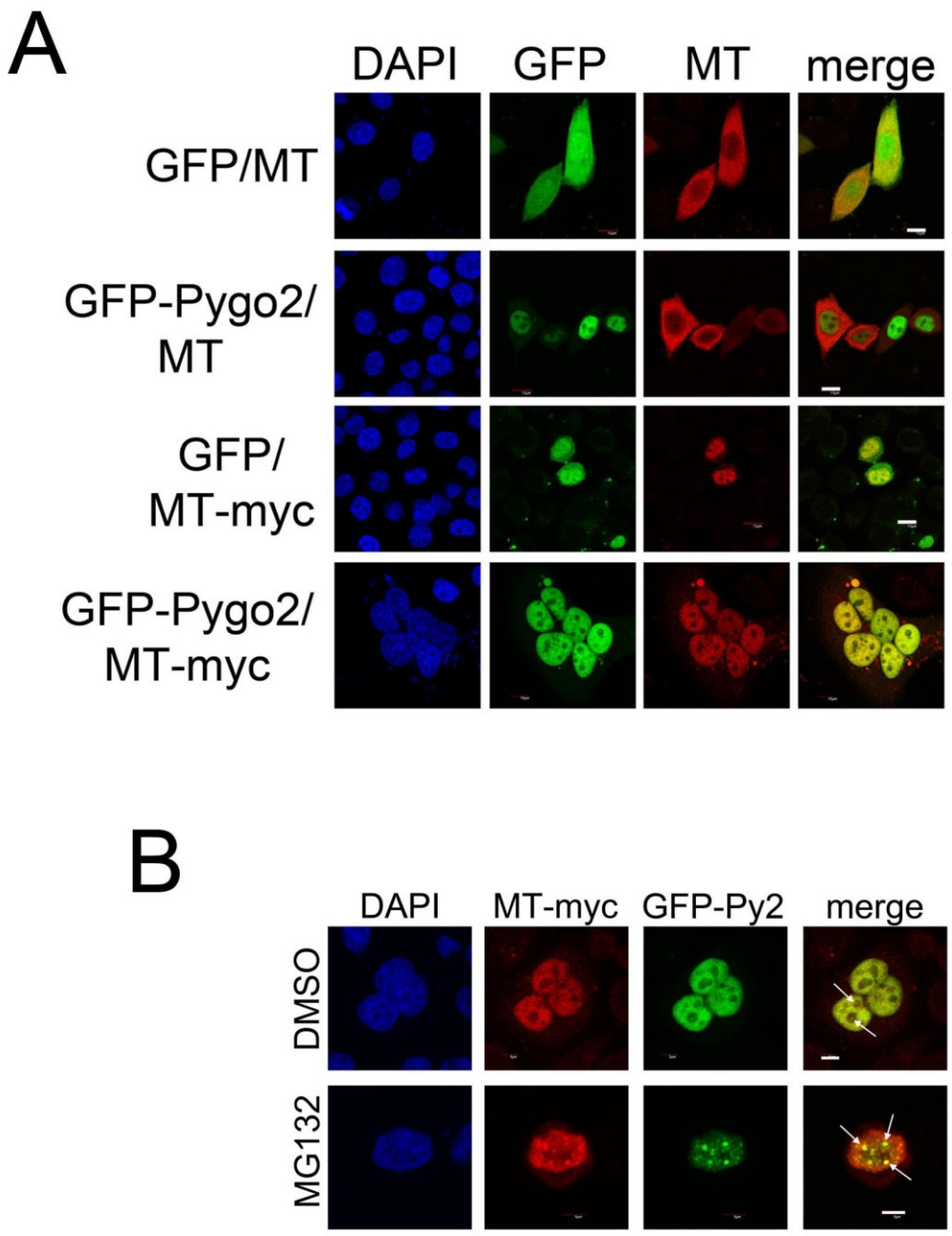

Figure 4.20. Pygo2 and c-myc co-localize in the nuclei of HeLa S3 cells. (A) Confocal images of cells that were co-transfected with different combinations of GFP, GFP-Pygo2 (GFP-Py2), MT and MT-myc, cells were stained with antibodies recognizing MT and DAPI to visualize nuclei. Scale bar = 10μm. (B) Pygo2 and c-myc co-localize in the nucleus of DMSO and MG132 treated HeLa S3 cells. Arrows indicate co-localization in presumptive nucleoli. Scale bar = 5μm.

S3 cells that were co-transfected with green fluorescent protein (GFP) tagged Pygo2 and MT-myc (Figure 4.20A).

The c-myc protein is rapidly turned over by proteasomal degradation, resulting in a relatively short half-life. Nucleolar localization of c-myc was observed in cells expressing elevated levels of c-myc or when proteasome inhibitors were used to increase its expression (Arabi *et al*, 2003). In HeLa S3 cells both endogenous c-myc and Pygo2 appear to localize mainly to the nucleoplasm and chromatin, with punctate co-localization in the nucleoli in untreated or vehicle treated (DMSO) cells (Figure 4.20B).

These results suggested that in addition to the Pygo2/c-myc target genes outlined above, Pygo2/c-myc containing complexes may also play a role in ribosomal RNA transcription. Upon treatment of cells with the proteasome inhibitor MG132, there was an increased co-localization of both Pygo2 and c-myc to the presumptive nucleolar regions of the nuclei of HeLa S3 cells (Figure 4.20B), thereby suggesting the possibility of Pygo2/c-myc complexes in ribosomal RNA transcription, consistent with previous findings (Andrews *et al*, 2013; Grandori *et al*, 2005; Arabi *et al*, 2005).

4.4 Discussion

Here, my findings suggest that the chromatin effector Pygo2 controls a transcriptional program required for mitosis. Consistently, Pygo2 was required to maintain levels of H3K27 acetylation at promoters and expression of genes involved in microtubule-kinetochore interactions facilitating chromosome biorientation (Figure 4.21). Pygo2 was also associated with H3K4 trimethylation at select promoters (Figure 4.17), consistent with a role for Pygo2 in promoting H3K4me3 through a histone methyltransferase dependent mechanism (Chen *et al*, 2010). Examination of functional genome-wide Pygo2 binding sites revealed that more than half of the promoters occupied by Pygo2 were also occupied by the proto-oncogene c-myc. Finally, identification of a novel interaction between Pygo2 and c-myc, thereby suggests the existence of a Pygo2/c-myc dependent transcriptional program that is involved in cell division control.

My results suggest at least one possible explanation for the observed chromosome segregation defects is dependent on a transcriptional program regulated by Pygo2. During mitosis, Pygo2 appears to dissociate from the condensed mitotic chromatin (Andrews *et al*, 2013), however it is possible that Pygo2 may also play a direct role in kinetochore organization. Centromeric chromatin is unique, composed of repetitive α-satellite DNA which is recognized and organized by the histone H3 variant, Centromere Protein A (CENP-A; Ohzeki & Larionov, 2015). Using human artificial chromosomes, it was demonstrated that CENP-A assembly is dependent on acetylation by PCAF or p300 (Ohzeki *et al*, 2012). Since Pygo2 is associated with PCAF and p300 HATs (Chen *et al*, 2010; Andrews *et al*, 2009; Andrews & Kao, 2016), raising the possibility that

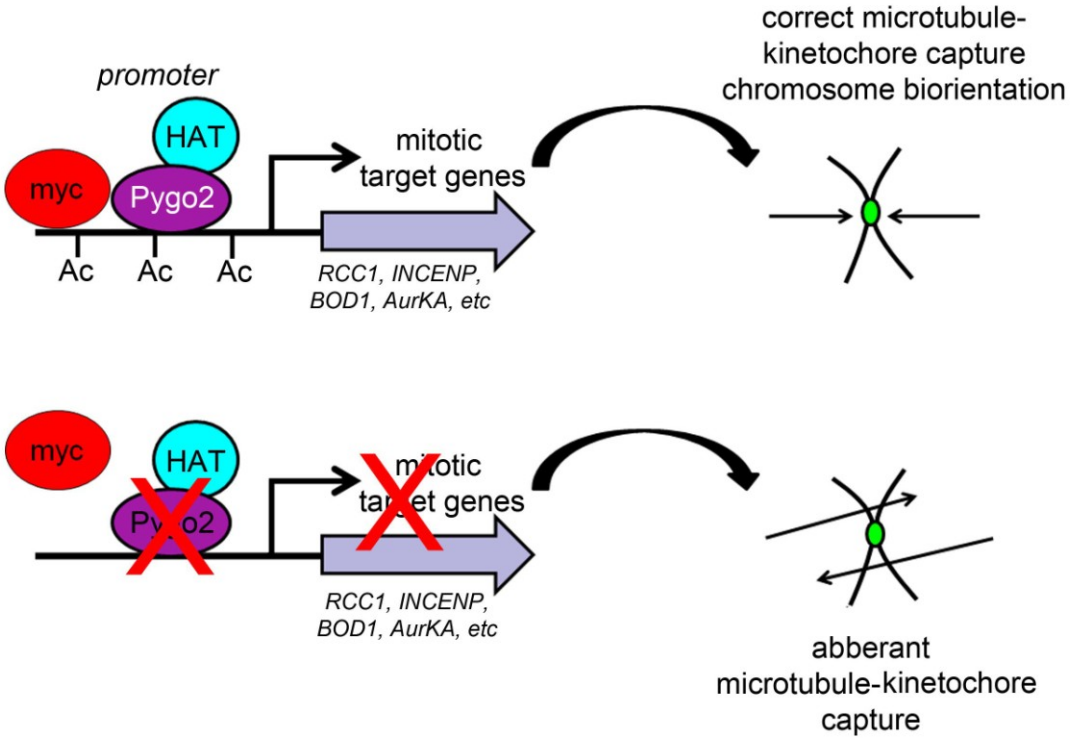

Figure 4.21. Proposed mechanism of the transcriptional control of cell division by Pygo2. Complexes of Pygo2 and c-myc may be required for the recruitment of HATs to genes involved in cell division required for H3K27 acetylation and normal kinetochore capture by spindle microtubules (top panel). Depletion of Pygo2 results in lower amounts of H3K27 acetylation causing a reduction in expression of genes involved in cell division, resulting in aberrant capture of kinetochores by spindle microtubules.

Pygo2 may be involved in centromere assembly by promoting CENP-A acetylation.

Little change was observed in the centrosomes and mitotic microtubules in Pygo2 depleted cells (Figure 4.4), indicating proper centrosome function and bipolar spindle assembly. Further examination revealed defects in in spindle-kinetochore recognition (Figure 4.5 and 4.6), similar to chromosome alignment defects in cells deficient in a kinetochore protein known as biorientation of chromosomes in division 1 (BOD1), required for the detection of syntelic attachments by the mitotic spindle (Porter *et al*, 2007).

Additionally, we identified Regulator of Chromosome Condensation 1 (RCC1) as a direct Pygo2 responsive gene and Pygo2-dependent spindle defects resemble spindle defects resulting from overexpression of a dominant negative RCC1 (Moore *et al*, 2002). Kinetochore associated RCC1 required for the binding of GTP to Ras-related nuclear protein (RanGTP), is necessary to form a concentration gradient of RanGTP, required for kinetochore proximal microtubule nucleation and kinetochore recognition (Kalab & Heald, 2008). While not explored here, the Pygo2 dependent reduction of RCC1 expression may also reduce the gradient of RanGTP, thereby affecting spindle-kinetochore interaction.

Depletion of Pygo2 resulted in the reduction in expression of TPX2 and AurKA. Both of which are involved in the formation of kinetochore-derived microtubule nucleation that aids in spindle-kinetochore interactions (Katayama *et al*, 2008). While AurKA could not be detected at kinetochores, the general reduction of AurKA and activated phospho-AurKA at centrosomes suggests a reduction of active AurKA at

kinetochores is likely. Overall, these results suggest that Pygo2 plays a role in the expression of key genes involved in directing mitotic spindle-kinetochore interaction.

It is already well established that Pygo binds directly to H3K4me3 (Fiedler *et al*, 2008). In stride with this, on a global scale with respect to TSS, Pygo2 preferably binds to proximal promoter regions, which strongly correlated with H3K4me3 enrichment (Figure 4.14). In malignant and transformed cells Pygo2-H3K4me3 binding is important for cell growth and expansion (Gu *et al*, 2009), but a recent study revealed that Pygo2 binding to H3K4me3 through its PHD motif was dispensable for normal development and target gene transcription (Cantù *et al*, 2013). Here, I hypothesize that Pygo2 is likely targeted to active gene promoters through a mechanism that could be either directly or indirectly through H3K4me3 marks, as evidenced by the strong correlation with HAT enrichment (Figure 4.14).

The canonical binding of c-myc to specific E-box enhancer elements on DNA, which lie upstream of TSS, occurs in cooperation with its partner MAX. However, the genome wide association of c-myc with DNA revealed that it was strongly associated at active TSS lacking canonical E-box motifs, thereby suggesting that c-myc may be targeted to active promoters, independent of MAX (Kress *et al*, 2015). While the association between Pygo2 and MAX is unknown, its association with c-myc offers the interesting possibility that Pygo2 may be involved in recruiting c-myc to active promoters through the direct binding to H3K4me3 marks to activate specific transcriptional programs including cell division and ribosome production. It is also possible that Pygo2/c-myc could be targeted by other promoter bound factors to promote histone

acetylation (Figure 4.12C), such as the oncogene FOXP1 (Fox *et al*, 2004; Choi *et al*, 2015).

The interaction between c-myc and Pygo2 raises the possibility of an interaction between Pygo2 and other myc family members, such as n-myc, which has been shown to play roles in both normal development and cancer. In normal development, n-myc expression is restricted to certain developing tissues, such as neural progenitor cells, hair follicles, retinas and lenses (Hirning *et al*, 1991), closely mirroring the expression and function of Pygo2 in normal development. Furthermore, n-myc can functionally substitute for c-myc during normal development (Malynn *et al*, 2000) and has been associated with a variety of cancers, such as neuroblastoma (Westermark *et al*, 2011). These observations suggest the interesting possibility that Pygo2 and n-myc complexes could play important roles in both normal development and cancer.

Its documented overexpression and requirement for growth suggests that Pygo2 is an important biomarker and possible therapeutic target in a number of different cancers (Liu *et al*, 2013; Andrews *et al*, 2007; Watanabe *et al*, 2013; Popadiuk *et al*, 2006; Andrews *et al*, 2008; Gu *et al*, 2012; Zhang *et al*, 2015a; Andrews *et al*, 2013; Tzenov *et al*, 2013; Yang *et al*, 2013; Sun *et al*, 2014; Zhang *et al*, 2015b; Zhou *et al*, 2014; Li *et al*, 2015). Furthermore, Pygo2 plays key roles in cell growth by facilitating euchromatin formation at genes required for both nucleosome and ribosome biogenesis (Gu *et al*, 2012; Andrews *et al*, 2013). While these processes clearly link Pygo2 function to the demands of a growing cell, these results demonstrate that the chromatin modulator Pygo2 is similarly involved in a transcriptional program essential for mitotic cell division,

suggesting that Pygo2 function may be important to coordinate cell growth with mitotic division.

Chapter 5: Summary

5.1 Pygo2 as a permissive Wnt chromatin effector in cancer

Over the past few decades there has been mounting evidence highlighting the importance of chromatin remodeling events that drive proliferative growth. In this thesis, I presented Pygo2 as an emerging player in the epigenetic control of cell growth and division, thereby identifying Pygo2 as an important therapeutic target in cancer. I hypothesized that Pygo2 acts as an adapter or "docking" protein required for HAT binding and euchromatin formation at active gene promoters driving cancer cell growth and division. Pygo2 is targeted to active gene promoters primarily through H3K4me3 marks, however, more complex interactions with transcription factors at both gene enhancers and/or promoters are conceivably required to dictate the sets of genes that get turned on. For example, the interaction of Pygo2 with complexes containing Bcl9/β-catenin (Chapter 2) or with UBF/Treacle (Chapter 3) likely dictates its chromatin effector function in either Wnt signalling or ribosomal RNA transcription, respectively. However, the interaction of Pygo2 with c-myc only partially explains its requirement in transcription of genes involved in mitosis, since approximately half of the Pygo2 enriched genes showed a co-enrichment for c-myc (Figure 4.18), indicating that Pygo2 may also co-operate with other unknown transcriptional complexes to fulfil its role in transcription and chromatin remodeling.

Pygo2 is expressed in almost all developing tissues and evidence from Pygo2 null mice support the idea that it may be relevant in all cells to promote proliferation. Pygo2 is clearly required to promote the development of certain tissues such as the lens and kidney (Song *et al*, 2007; Schwab *et al*, 2007). In addition, Pygo2-null fetuses are significantly smaller than wild-type littermates (Li *et al*, 2007a; Schwab *et al*, 2007; Song *et al*, 2007),

suggesting that it may be important for development of many different tissues. Pygo2 is also expressed in normal human cells, albeit at lower levels compared to immortalized and malignant cells (Popadiuk *et al*, 2006; Andrews *et al*, 2007; Tzenov *et al*, 2013).

Collectively, these data suggest that Pygo2 function may be important to promote the growth of normal cell types, consistent with a model of cell growth and division regulation by Pygo2 (Figure 5.1). Here, cell growth and division driven by Wnt signalling, for example, results in the recruitment of the active β-catenin transcriptional complexes to target genes, such as *cyclin D1* and *c-myc*. Transcriptional activation requires HAT recruitment by the Pygo2/β-catenin complex to promote necessary euchromatic changes necessary for transcriptional initiation. In the active β-catenin complex, Pygo2 becomes acetylated, which likely occurs concurrently with histone acetylation and promotes the dissociation of active complexes (Chapter 2).

Cyclin D1 is required for phosphorylation of the Retinoblastoma (Rb) protein and cell cycle progression though the G1/S checkpoint of the cell cycle. Inactivation of Rb by phosphorylation activates a transcriptional program, primarily mediated by the activation of E2F (Dick & Rubin, 2013; Ren *et al*, 2002) and Elf-1 (Wang *et al*, 1993), resulting in an increase in Pygo2 expression (Tzenov *et al*, 2013; Andrews *et al*, 2008). I hypothesize that the increase in c-myc and Pygo2 expression results in the activation of gene expression program(s) promoting cell growth and biomass accumulation through both histone (Gu *et al*, 2012) and ribosome production (Chapter 3; Andrews et al., 2013). It is possible that this activity is coupled to a consequent or subsequent activation of cell division machinery by Pygo2/c-myc complexes (Chapter 4). Therefore, the chromatin

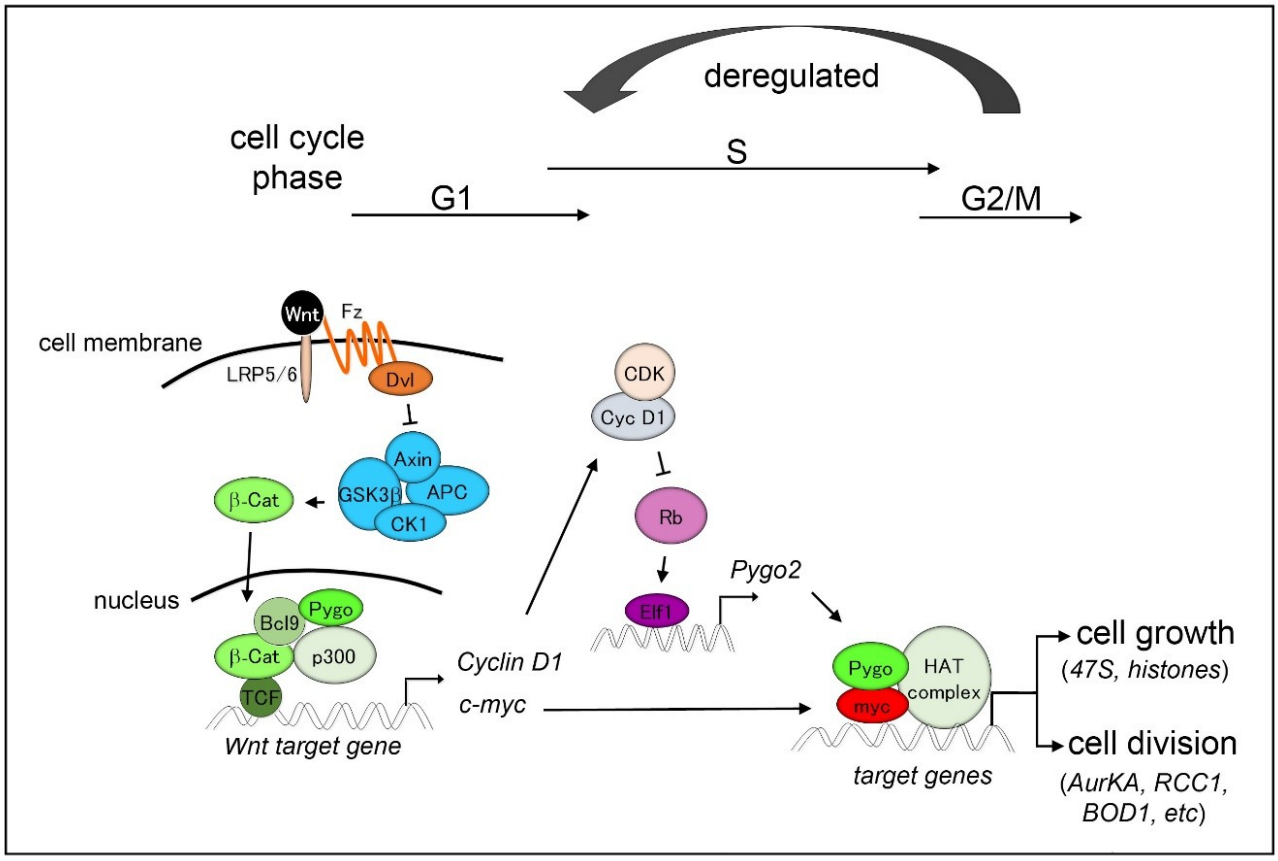

Figure 5.1. Proposed model of normal and aberrant growth regulation by the chromatin effector Pygo2. (For description see text in section 5.1)

remodelling function of Pygo2 may be required in multiple contexts, in an overall theme of promoting cell growth and division.

In normal cells the function of Pygo2 as a general effector of cell expansion would require careful regulation and at each cell cycle, newly minted daughter cells would be competent to respond to additional waves of growth promoting Wnt signals. I speculate that if this proposed function were abnormally hyper-stimulated in normal cells, feedback tumor suppressor programs would become activated to attenuate the growth response, similar to the p14ARF dependent activation of p53 by mitogenic c-myc activation (Zindy *et al*, 1998).

In cancer, it is likely that Pygo2 activity is hijacked during tumorigenesis and takes on a role as an oncogenic accessory protein, promoting open chromatin structure to facilitate gene expression, an idea worthy of further discussion. The probable functional interaction between Pygo2 and c-myc offers a convenient avenue addressing this interesting possibility. Importantly, the myc genes and proteins lie downstream of many pro-growth related signaling pathways and act as master regulators of the growth response (Dang, 2012; Califano & Alvarez, 2016). The overall outcome of aberrant myc expression results in transcriptional amplification necessary to drive cancer cell growth (Nie *et al*, 2012; Lin *et al*, 2012). To date, there is no evidence suggesting Pygo2 alone plays a role in cellular transformation, suggesting that its role in tumorigenesis could be dependent on c-myc. The involvement of Pygo2 in growth and division related transcriptional programs parallels the requirement of c-myc in promoting cell proliferation related to cancer (Dang, 2012). I therefore hypothesize that Pygo2 and c-

myc constitutes a functional unit required for cell proliferation, whether c-myc hijacks Pygo2 or vice versa, remains to be determined.

Cancer cells, whose uncontrolled growth phenotypes are partly dependent on the loss of tumor suppressors, bypass the G1/S phase checkpoint and undergo continuous growth (Figure 5.1; "deregulated"). Here, aberrant growth signalling cascades converge and result in the over expression of c-myc as well as additional proto-oncogenes and master regulators to supercharge cell proliferation. Moreover, the coupled inactivation of Rb results in the overexpression of Pygo2 at the mRNA and protein levels. I propose that the deregulated expression of both c-myc and Pygo2 and their cooperative roles in promoting aberrant gene expression increases cellular capacity to both grow and divide, likely through the recruitment of chromatin remodelling machinery.

5.2 The chromatin effector Pygo2 as a druggable molecule in cancer.

It is not surprising that targeting chromatin-remodeling proteins in cancer has garnered much recent attention. For example, inhibition of c-myc gene expression has been achieved in a number of cancers with the small molecule inhibitor JQ1, which binds and inhibits the epigenetic function of the bromodomain-containing protein Brd4 (Filippakopoulos *et al*, 2010). Recently, there have been attempts to target Pygo2 with small molecules that bind to the PHD motif disrupting its interaction with H3K4me3 and Bcl9 (Miller *et al*, 2014; Ali *et al*, 2016). Moreover, the small molecule targeting Pygo2 called JBC117, identified by Ali and coworkers was shown to display anti-cancer properties in both colorectal and lung cancer cells (Ali *et al*, 2016). Since the PHD domain of Pygo2 is largely dispensable for normal development (Cantù *et al*, 2013),

while it appears to be important for cancer growth (Ali *et al*, 2016), targeting the Pygo2 PHD finger in cancer may be therapeutically feasible with reduced side effects in normal cells. Furthermore, there are several studies that provide direct evidence for the requirement of Pygo2 in tumor formation and its association with disease progression and clinical outcome (Watanabe *et al*, 2013; Zhang *et al*, 2015a), bolstering Pygo2 as a potential therapeutic target. However, since Pygo2 functions in adult stem cell maintenance, further studies are needed to assess the efficacy of targeting the Pygo2 PHD domain.

Although the crystal structure of the full Pygo2 protein or the NHD remains to be solved, targeting the NHD with a small molecule inhibitor may also prove to be useful. The NHD region of Pygo family members is highly conserved and shares little homology with other proteins, therefore making it an attractive region for small molecule targeting. Thus far, the Pygo2 NHD appears to be required for the transcriptional activity of Pygo2, by mediating the binding of HATs, HMTs, H3K4me3 and the mediator complex (Andrews *et al*, 2009; Chen *et al*, 2010; Carrera *et al*, 2008). While the exact amino acid sequences that mediate Pygo2 binding to the abovementioned proteins is unknown, our group and others (Andrews *et al*, 2009; Chen *et al*, 2010; Andrews *et al*, 2013) have identified a short sequence comprising the first 47 amino acids within the NHD region of Pygo2 likely constitutes a multi-protein-protein interaction interface. Therefore, future studies will be needed to analyze the structure and the binding of this functional unit to HATs and HMTs.

5.3 Future endeavors

I believe that I made my most interesting observations toward the end of this thesis, regarding the existence of a Pygo2/c-myc complex that may control gene expression. Preliminary studies in both cultured cervical and prostate cells suggest that there is a positive correlation between the number of Pygo2/c-myc complexes present in cancer cells compared to "normal" primary cells. These results suggest that Pygo2 and c-myc may indeed be linked to the cancer phenotype and this interaction may be of clinical value in cancer diagnostics. Since both Pygo2 and c-myc likely converge on target genes involved in cell growth and division, future work regarding a functional Pygo2/c-myc interaction may represent an important perspective for targeted cancer therapies.

Chapter 6: References

6.1 References

Alabert C & Groth A (2012) Chromatin replication and epigenome maintenance. *Nat. Rev. Mol. Cell Biol.* **13:** 153–167

Ali F, Yamaguchi K, Fukuoka M, Elhelaly AE & Kuwata K (2016) Logical design of an anti-cancer agent targeting the plant homeodomain in Pygopus2. *Cancer Sci.* **107:** 1321-8

Andersen JS, Lyon CE, Fox AH, Leung AKL, Lam YW, Steen H, Mann M & Lamond AI (2002) Directed proteomic analysis of the human nucleolus. *Curr. Biol.* **12:** 1–11

Andrews PGP, He Z, Popadiuk C & Kao KR (2009) The transcriptional activity of Pygopus is enhanced by its interaction with cAMP-response-element-binding protein (CREB)-binding protein. *Biochem. J.* **422:** 493–501

Andrews PGP, He Z, Tzenov YR, Popadiuk C & Kao KR (2013) Evidence of a novel role for Pygopus in rRNA transcription. *Biochem. J.* **453:** 61–70

Andrews PGP & Kao KR (2016) Wnt / β -catenin-dependent acetylation of Pygo2 by CBP / p300 histone acetyltransferase family members. *Biochem. J.* **473:** 4193–4203

Andrews PGP, Kennedy MW, Popadiuk CM & Kao KR (2008) Oncogenic activation of the human Pygopus2 promoter by E74-like factor-1. *Mol. Cancer Res.* **6:** 259–66

Andrews PGP, Lake BB, Popadiuk C & Kao KR (2007) Requirement of Pygopus 2 in breast cancer. *Int. J. Oncol.* **30:** 357–63

Arabi A, Rustum C, Hallberg E & Wright APH (2003) Accumulation of c-Myc and proteasomes at the nucleoli of cells containing elevated c-Myc protein levels. *J. Cell Sci.* **116:** 1707–17

Arabi A, Wu S, Ridderstråle K, Bierhoff H, Shiue C, Fatyol K, Fahlén S, Hydbring P,

Söderberg O, Grummt I, Larsson L-G & Wright APH (2005) c-Myc associates with ribosomal DNA and activates RNA polymerase I transcription. *Nat. Cell Biol.* **7:** 303–310

Archambault V, Lépine G & Kachaner D (2015) Understanding the Polo Kinase machine. *Oncogene* **34:** 4799–4807

Bannister AJ & Kouzarides T (2011) Regulation of chromatin by histone modifications. *Cell Res.* **21:** 381–395

Bannister AJ, Schneider R & Kouzarides T (2002) Histone methylation: Dynamic or static? *Cell* **109:** 801–806

Bannister AJ, Zegerman P, Partridge JF, Miska E a, Thomas JO, Allshire RC & Kouzarides T (2001) Selective recognition of methylated lysine 9 on histone H3 by the HP1 chromo domain. *Nature* **410:** 120–124

Barak Y, Juven T, Haffner R & Oren M (1993) Mdm2 Expression Is Induced By Wild Type P53 Activity. *EMBO J.* **12:** 461–8

Belenkaya TY, Han C, Standley HJ, Lin X, Houston DW, Heasman J & Lin X (2002) pygopus Encodes a nuclear protein essential for wingless/Wnt signaling. *Development* **129:** 4089–101

Bernstein BE, Humphrey EL, Erlich RL, Schneider R, Bouman P, Liu JS, Kouzarides T & Schreiber SL (2002) Methylation of histone H3 Lys 4 in coding regions of active genes. *Proc. Natl. Acad. Sci. U. S. A.* **99:** 8695–8700

Brembeck FH, Wiese M, Zatula N, Grigoryan T, Dai Y, Fritzmann J & Birchmeier W (2011) BCL9-2 promotes early stages of intestinal tumor progression. *Gastroenterology* **141:** 1359–1370

Brücher BLDM & Jamall IS (2016) Somatic Mutation Theory - Why it's Wrong for Most Cancers. *Cell. Physiol. Biochem.* **38:** 1663–1680

Byvoet P, Shepherd GR, Hardin JM & Noland BJ (1972) The distribution and turnover of labeled methyl groups in histone fractions of cultured mammalian cells. *Arch. Biochem. Biophys.* **148:** 558-67

Cadigan KM & Peifer M (2015) Wnt Signaling from Development to Disease : Insights from Model Systems. *Cold Spring Harb Perspect Biol.* **1**:a002881

Califano A & Alvarez MJ (2016) The recurrent architecture of tumour initiation, progression and drug sensitivity. *Nat. Rev. Cancer* **124:** 116-130

Cantù C, Valenta T, Hausmann G, Vilain N, Aguet M & Basler K (2013) The Pygo2-H3K4me2/3 interaction is dispensable for mouse development and Wnt signaling-dependent transcription. *Development* **140:** 2377–86

Cao R, Wang L, Wang H, Xia L, Erdjument-Bromage H, Tempst P, Jones R & Zhang Y (2002) Role of Histone H3 Lysine 27 Methylation in Polycomb-Group Silencing. **298:** 1039–1043

Carmena M, Ruchaud S & Earnshaw WC (2009) Making the Auroras glow: regulation of Aurora A and B kinase function by interacting proteins. *Curr. Opin. Cell Biol.* **21:** 796–805

Carmena M, Wheelock M, Funabiki H & Earnshaw WC (2012) The chromosomal passenger complex (CPC): from easy rider to the godfather of mitosis. *Nat. Rev. Mol. Cell Biol.* **13:** 789–803

Carrera I, Janody F, Leeds N, Duveau F & Treisman JE (2008) Pygopus activates Wingless target gene transcription through the mediator complex subunits Med12

and Med13. *Proc. Natl. Acad. Sci. U. S. A.* **105:** 6644–9

Cedar H & Bergman Y (2009) modification : patterns and paradigms. **10:** 295–304

Chen J, Luo Q, Yuan Y, Huang X, Cai W, Li C, Wei T, Zhang L, Yang M, Liu Q, Ye G, Dai X & Li B (2010) Pygo2 associates with MLL2 histone methyltransferase and GCN5 histone acetyltransferase complexes to augment Wnt target gene expression and breast cancer stem-like cell expansion. *Mol. Cell. Biol.* **30:** 5621–35

Chen LF, Mu Y & Greene WC (2002) Acetylation of RelA at discrete sites regulates distinct nuclear functions of NF-kB. *EMBO J.* **21:** 6539–6548

Chen YY, Li BA, Wang HD, Liu XY, Tan GW, Ma YH, Shen SH, Zhu HW & Wang ZX (2011) The role of Pygopus 2 in rat glioma cell growth. *Med. Oncol.* **28:** 631–640

Choi EJ, Seo EJ, Kim DK, Lee SI & Kwon YW (2015) FOXP1 functions as an oncogene in promoting cancer stem cell-like characteristics in ovarian cancer cells. *Oncotarget* **7:** 3506-19

Choudhary C, Weinert BT, Nishida Y, Verdin E & Mann M (2014) The growing landscape of lysine acetylation links metabolism and cell signalling. *Nat. Rev. Mol. Cell Biol.* **15:** 536–550

Clapier CR & Cairns BR (2009) The biology of chromatin remodeling complexes. *Annu. Rev. Biochem.* **78:** 273–304

Clevers H, Loh KM & Nusse R (2014) Stem cell signaling. An integral program for tissue renewal and regeneration: Wnt signaling and stem cell control. *Science* **346:** 1248012

Clevers H & Nusse R (2012) Wnt/β-catenin signaling and disease. *Cell* **149:** 1192–1205

Close P, Creppe C, Gillard M, Ladang A, Chapelle J-P, Nguyen L & Chariot A (2010)

The emerging role of lysine acetylation of non-nuclear proteins. *Cell. Mol. Life Sci.* **67:** 1255–64

Côté J, Quinn J, Workman JL & Peterson CL (1994) Stimulation of GAL4 derivative binding to nucleosomal DNA by the yeast SWI/SNF complex. *Science* **265:** 53–60

Dang C V. (2012) MYC on the path to cancer. *Cell* **149:** 22–35

Dawson M a & Kouzarides T (2012) Cancer epigenetics: from mechanism to therapy. *Cell* **150:** 12–27

Degenhardt Y & Lampkin T (2010) Targeting polo-like kinase in cancer therapy. *Clin. Cancer Res.* **16:** 384–389

Denissov S, Lessard F, Mayer C, Stefanovsky V, van Driel M, Grummt I, Moss T & Stunnenberg HG (2011) A model for the topology of active ribosomal RNA genes. *EMBO Rep.* **12:** 231–237

Dhalluin C, Carlson JE, Zeng L, He C, Aggarwal a K & Zhou MM (1999) Structure and ligand of a histone acetyltransferase bromodomain. *Nature* **399:** 491–496

Dick F a & Rubin SM (2013) Molecular mechanisms underlying RB protein function. *Nat. Rev. Mol. Cell Biol.* **14:** 297–306

Dimitrova E, Turberfield AH & Klose RJ (2015) Histone demethylases in chromatin biology and beyond. *EMBO Rep.* **16:** 1620–39

Dixon J, Edwards SJ, Anderson I, Brass A, Scambler PJ & Dixon MJ (1997) Identification of the complete coding sequence and genomic organization of the Treacher Collins syndrome gene. *Genome Res.* **7:** 223–234

Dynlacht BD, Hoey T & Tjian R (1991) Isolation of coactivators associated with the TATA-binding protein that mediate transcriptional activation. *Cell* **66:** 563–576

Dyson NJ (2016) RB1: A prototype tumor suppressor and an enigma. *Genes Dev.* **30:** 1492–1502

Falkenberg KJ & Johnstone RW (2014) Histone deacetylases and their inhibitors in cancer , neurological diseases and immune disorders. *Nat. Publ. Gr.* **13:** 673–691

Felsenfeld G & Groudine M (2003) Controlling the double helix. *Nature* **421:** 444–448

Fiedler M, Sánchez-Barrena MJ, Nekrasov M, Mieszczanek J, Rybin V, Müller J, Evans P & Bienz M (2008) Decoding of Methylated Histone H3 Tail by the Pygo-BCL9 Wnt Signaling Complex. *Mol. Cell* **30:** 507–518

Filippakopoulos P & Knapp S (2012) The bromodomain interaction module. *FEBS Lett.* **586:** 2692–2704

Filippakopoulos P, Qi J, Picaud S, Shen Y, Smith WB, Fedorov O, Morse EM, Keates T, Hickman TT, Felletar I, Philpott M, Munro S, McKeown MR, Wang Y, Christie AL, West N, Cameron MJ, Schwartz B, Heightman TD, La Thangue N, et al (2010) Selective inhibition of BET bromodomains. *Nature* **468:** 1067–1073

Foley E a & Kapoor TM (2013) Microtubule attachment and spindle assembly checkpoint signalling at the kinetochore. *Nat. Rev. Mol. Cell Biol.* **14:** 25–37

Fox SB, Brown P, Han C, Ashe S, Leek RD, Harris AL & Banham AH (2004) Expression of the forkhead transcription factor FOXP1 Is associated with estrogen receptor α and improved survival in primary human breast carcinomas expression of the forkhead transcription factor FOXP1 is associated with estrogen receptor alpha and impr. *Clin. Cancer Res.* **10:** 3521–3527

Gayatri S & Bedford MT (2014) Readers of histone methylarginine marks. *Biochim. Biophys. Acta - Gene Regul. Mech.* **1839:** 702–710

Ge X, Jin Q, Zhang F, Yan T & Zhai Q (2009) PCAF acetylates b-catenin and improves its stability. *Mol. Biol. Cell* **20:** 419–427

Ghoshal K, Majumder S, Datta J, Motiwala T, Bai S, Sharma SM, Frankel W & Jacob ST (2004) Role of Human Ribosomal RNA (rRNA) Promoter Methylation and of Methyl-CpG-binding Protein MBD2 in the Suppression of rRNA Gene Expression. *J. Biol. Chem.* **279:** 6783–6793

Goldenson B & Crispino JD (2014) The aurora kinases in cell cycle and leukemia. *Oncogene* **34:** 1–9

Goll MG & Bestor TH (2005) Ukaryotic ytosine ethyltransferases. **:** 481–514

Gorski JJ, Pathak S, Panov KI, Kasciukovic T, Panova T, Russell J & Zomerdijk JCBM (2007) A novel TBP-associated factor of SL1 functions in RNA polymerase I transcription. *EMBO J.* **26:** 1560–8

Grandori C, Gomez-Roman N, Felton-Edkins Z a, Ngouenet C, Galloway D a, Eisenman RN & White RJ (2005) c-Myc binds to human ribosomal DNA and stimulates transcription of rRNA genes by RNA polymerase I. *Nat. Cell Biol.* **7:** 311–318

Greenman C, Stephens P, Smith R, Dalgliesh GL, Hunter C, Bignell G, Davies H, Teague J, Butler a, Stevens C, Edkins S, O'Meara S, Vastrik I, Schmidt EE, Avis T, Barthorpe S, Bhamra G, Buck G, Choudhury B, Clements J, et al (2007) Patterns of somatic mutation in human cancer genomes. *Nature* **446:** 153–158

Greer EL & Shi Y (2012) Histone methylation: a dynamic mark in health, disease and inheritance. *Nat. Rev. Genet.* **13:** 343–57

Grigoryev S a & Woodcock CL (2012) Chromatin organization - the 30 nm fiber. *Exp. Cell Res.* **318:** 1448–55

Grunstein M (1997) Histone acetylation in chromatin structure and transcription. *Nature* **389:** 349–352

Gu B, Sun P, Yuan Y, Moraes RC, Li A, Teng A, Agrawal A, Rhéaume C, Bilanchone V, Veltmaat JM, Takemaru KI, Millar S, Lee EYHP, Lewis MT, Li B & Dai X (2009) Pygo2 expands mammary progenitor cells by facilitating histone H3 K4 methylation. *J. Cell Biol.* **185:** 811–826

Gu B, Watanabe K & Dai X (2012b) Pygo2 regulates histone gene expression and H3 K56 acetylation in human mammary epithelial cells. *Cell Cycle* **11:** 79–87

Guérillon C, Larrieu D & Pedeux R (2013) ING1 and ING2: multifaceted tumor suppressor genes. *Cell. Mol. Life Sci.* **70:** 3753–72

Haberland M, Montgomery RL & Olson EN (2009) The many roles of histone deacetylases in development and physiology: implications for disease and therapy. *Nat. Rev. Genet.* **10:** 32–42

Hamamoto R, Saloura V & Nakamura Y (2015) Critical roles of non-histone protein lysine methylation in human tumorigenesis. *Nat. Publ. Gr.* **15:** 110–124

Hanahan D & Weinberg RA (2011) Hallmarks of cancer: The next generation. *Cell* **144:** 646–674

Hanahan D & Weinburg R (2000) The Hallmarks of cancer. *Cell* **100:** 57–70

Hargreaves DC & Crabtree GR (2011) ATP-dependent chromatin remodeling: genetics, genomics and mechanisms. *Cell Res.* **21:** 396–420

Haynes SR, Dollard C, Winston F, Beck S, Trowsdale J & Dawid IB (1992) The bromodomain : a conserved sequence found in human , Drosophila and yeast proteins. *Nuc Acid Res.* **20:** 2603

He TC, Sparks AB, Rago C, Hermeking H, Zawel L, da Costa LT, Morin PJ, Vogelstein B, Kinzler KW, Groden J, Rubinfeld B, Albert I, Souza B, Rubinfeld B, Polakis P, Rubinfeld B, Molenaar M, Behrens J, Korinek V, Morin PJ, et al (1998) Identification of c-MYC as a target of the APC pathway. *Science* **281:** 1509–12

Heix J, Vente A, Voit R, Budde A, Michaelidis TM & Grummt I (1998) Mitotic silencing of human rRNA synthesis: Inactivation of the promoter selectivity factor SL1 by cdc2/cyclin B-mediated phosphorylation. *EMBO J.* **17:** 7373–7381

Hirning U, Schmid P, Schulz W, Rettenberger G & Hameister H (1991) A comparative analysis of N-myc and c-myc expression and cellular proliferation in mouse organogenesis. *Mech. Dev.* **33:** 119–125

Den Hollander J, Rimpi S, Doherty JR, Rudelius M, Buck A, Hoellein A, Kremer M, Graf N, Scheerer M, Hall MA, Goga A, Von Bubnoff N, Duyster J, Peschel C, Cleveland JL, Nilsson JA & Keller U (2010) Aurora kinases A and B are up-regulated by Myc and are essential for maintenance of the malignant state. *Blood* **116:** 1498–1505

Huang DW, Sherman BT & Lempicki R a. (2009) Bioinformatics enrichment tools: Paths toward the comprehensive functional analysis of large gene lists. *Nucleic Acids Res.* **37:** 1–13

Jin Q, Yu L-R, Wang L, Zhang Z, Kasper LH, Lee J-E, Wang C, Brindle PK, Dent SYR & Ge K (2011) Distinct roles of GCN5/PCAF-mediated H3K9ac and CBP/p300-mediated H3K18/27ac in nuclear receptor transactivation. *EMBO J.* **30:** 249–62

Jonckheere N, Mayes E, Shih HP, Li B, Lioubinski O, Dai X & Sander M (2008) Analysis of mPygo2 mutant mice suggests a requirement for mesenchymal Wnt

signaling in pancreatic growth and differentiation. *Dev. Biol.* **318:** 224–235

Jones NC, Lynn ML, Gaudenz K, Sakai D, Aoto K, Rey J-P, Glynn EF, Ellington L, Du C, Dixon J, Dixon MJ & Trainor PA (2008) Prevention of the neurocristopathy {Treacher} {Collins} syndrome through inhibition of p53 function. *Nat. Med.* **14:** 125–133

Kalab P & Heald R (2008) The RanGTP gradient - a GPS for the mitotic spindle. *J. Cell Sci.* **121:** 1577–1586

Katayama H, Sasai K, Kloc M, Brinkley BR & Sen S (2008) Aurora kinase-A regulates kinetochore/chromatin associated microtubule assembly in human cells. *Cell Cycle* **7:** 2691–2704

Kennedy MW, Cha SW, Tadjuidje E, Andrews PG, Heasman J & Kao KR (2010) A co-dependent requirement of xBcl9 and Pygopus for embryonic body axis development in Xenopus. *Dev. Dyn.* **239:** 271–283

Klose RJ & Bird AP (2006) Genomic DNA methylation : the mark and its mediators. **31:**

Kollman JM, Merdes A, Mourey L & Agard D a. (2011) Microtubule nucleation by γ-tubulin complexes. *Nat. Rev. Mol. Cell Biol.* **12:** 709–721

Kouzarides T (2007) Chromatin Modifications and Their Function. *Cell* **128:** 693–705

Kramps T, Peter O, Brunner E, Nellen D, Froesch B, Chatterjee S, Murone M, Züllig S & Basler K (2002) Wnt/wingless signaling requires BCL9/legless-mediated recruitment of pygopus to the nuclear beta-catenin-TCF complex. *Cell* **109:** 47–60

Kreso A & Dick JE (2014) Evolution of the cancer stem cell model. *Cell Stem Cell* **14:** 275–291

Kress TR, Sabò A & Amati B (2015) MYC: connecting selective transcriptional control

to global RNA production. *Nat. Rev. Cancer* **15:** 593–607

Krivega I & Dean A (2012) Enhancer and promoter interactions-long distance calls. *Curr. Opin. Genet. Dev.* **22:** 79–85

Lake BB & Kao KR (2003) Pygopus is required for embryonic brain patterning in Xenopus. *Dev. Biol.* **261:** 132–148

Lessard F, Morin F, Ivanchuk S, Langlois F, Stefanovsky V, Rutka J & Moss T (2010) Article The ARF Tumor Suppressor Controls Ribosome Biogenesis by Regulating the RNA Polymerase I Transcription Factor TTF-I. *Mol. Cell***:** 539–550

Leung JY, Kolligs FT, Wu R, Zhai Y, Kuick R, Hanash S, Cho KR & Fearon ER (2002) Activation of AXIN2 Expression by beta-Catenin-T Cell Factor. **277:** 21657–21665

Lévy L, Wei Y, Labalette C, Wu Y, Renard C, Buendia MA, Le L & Neuveut C (2004) Acetylation of β -Catenin by p300 Regulates β -Catenin-Tcf4 Interaction. *Mol. Cell. Biol.* **24:** 3404–14

Li B, Mackay DR, Ma J & Dai X (2004) Cloning and developmental expression of mouse pygopus 2, a putative Wnt signaling component. *Genomics* **84:** 398–405

Li B, Rhéaume C, Teng A, Bilanchone V, Munguia J, Hu M, Jessen S, Piccolo S, Waterman M & Dai X (2007a) Developmental phenotypes and reduced Wnt signaling in mice deficient for pygopus 2. *Genesis* **45:** 318–425

Li J, Sutter C, Parker DS, Blauwkamp T, Fang M & Cadigan KM (2007b) CBP/p300 are bimodal regulators of Wnt signaling. *EMBO J.* **26:** 2284–94

Li J & Wang C-Y (2008) TBL1-TBLR1 and beta-catenin recruit each other to Wnt target-gene promoter for transcription activation and oncogenesis. *Nat. Cell Biol.* **10:** 160–169

Li M, Chao L, Wu J, Xu H, Shen S, Chen S, Gao X, Yu N & Wang Z (2015) Pygo2 siRNA Inhibit the Growth and Increase Apoptosis of U251 Cell by Suppressing Histone H3K4 Trimethylation. *J. Mol. Neurosci.* **56:** 949–955

Lin CY, Lovén J, Rahl PB, Paranal RM, Burge CB, Bradner JE, Lee TI & Young RA (2012) Transcriptional amplification in tumor cells with elevated c-Myc. *Cell* **151:** 56–67

Liu Y, Dong Q-Z, Wang S, Fang C-Q, Miao Y, Wang L, Li M-Z & Wang E-H (2013) Abnormal expression of Pygopus 2 correlates with a malignant phenotype in human lung cancer. *BMC Cancer* **13:** 346

Lohrum MAE, Ludwig RL, Kubbutat MHG, Hanlon M & Vousden KH (2003) Regulation of HDM2 activity by the ribosomal protein L11. *Cancer Cell* **3:** 577–587

Lombardi PM, Cole KE, Dowling DP & Christianson DW (2011) Structure, mechanism, and inhibition of histone deacetylases and related metalloenzymes. *Curr. Opin. Struct. Biol.* **21:** 735–743

Luger K, Mäder a W, Richmond RK, Sargent DF & Richmond TJ (1997) Crystal structure of the nucleosome core particle at 2.8 A resolution. *Nature* **389:** 251–260

Ma H, Nguyen C, Lee K-S & Kahn M (2005) Differential roles for the coactivators CBP and p300 on TCF/beta-catenin-mediated survivin gene expression. *Oncogene* **24:** 3619–31

Malynn BA, Alboran IM De, Hagan CO, Bronson R, Davidson L, Depinho RA & Alt FW (2000) N- myc can functionally replace c- myc in murine development , cellular growth , and differentiation. *Genes Dev.* **14:** 1390–1399

Martínez-Balbás M a, Bauer UM, Nielsen SJ, Brehm a & Kouzarides T (2000)

Regulation of E2F1 activity by acetylation. *EMBO J.* **19:** 662–671

McGranahan N & Swanton C (2015) Biological and therapeutic impact of intratumor heterogeneity in cancer evolution. *Cancer Cell* **27:** 15–26

McStay B & Grummt I (2008) The epigenetics of rRNA genes: from molecular to chromosome biology. *Annu. Rev. Cell Dev. Biol.* **24:** 131–157

Miller TCR, Rutherford TJ, Birchall K, Chugh J, Fiedler M & Bienz M (2014) Competitive Binding of a Benzimidazole to the Histone-Binding Pocket of the Pygo PHD Finger. *ACS Chem Biol*. **9:** 2864-74

Monda JK & Cheeseman IM (2015) Chromosome Segregation: A Spatial Code to Correct Kinetochore–Microtubule Attachments. *Curr. Biol.* **25:** R601–R603

Moore W, Zhang C & Clarke P (2002) Targeting of RCC1 to chromosomes is required for proper mitotic spindle assembly in human cells. **12:** 1442–1447

Mosimann C, Hausmann G & Basler K (2009) β-catenin hits chromatin: regulation of Wnt target gene activation. *Nat Rev Mol Cell Biol* **10:** 276–86

Moss T (2004) At the crossroads of growth control; making ribosomal RNA. *Curr. Opin. Genet. Dev.* **14:** 210–217

Moss T, Langlois F, Gagnon-Kugler T & Stefanovsky V (2007) A housekeeper with power of attorney: The rRNA genes in ribosome biogenesis. *Cell. Mol. Life Sci.* **64:** 29–49

Musselman CA & Kutateladze TG (2011) Handpicking epigenetic marks with PHD fingers. *Nucleic Acids Res.* **39:** 9061–9071

Musselman CA, Lalonde M-E, Côté J & Kutateladze TG (2012) Perceiving the epigenetic landscape through histone readers. *Nat. Struct. Mol. Biol.* **19:** 1218–27

Nagy Z & Tora L (2007) Distinct GCN5/PCAF-containing complexes function as co-activators and are involved in transcription factor and global histone acetylation. *Oncogene* **26:** 5341–57

Narlikar GJ, Sundaramoorthy R & Owen-Hughes T (2013) Mechanisms and functions of ATP-dependent chromatin-remodeling enzymes. *Cell* **154:** 490–503

Nie Z, Hu G, Wei G, Cui K, Yamane A, Resch W, Wang R, Green DR, Tessarollo L, Casellas R, Zhao K & Levens D (2012) c-Myc Is a Universal Amplifier of Expressed Genes in Lymphocytes and Embryonic Stem Cells. *Cell* **151:** 68–79

Nikonova AS, Astsaturov I, Serebriiskii IG, Dunbrack RL & Golemis E a. (2013) Aurora A kinase (AURKA) in normal and pathological cell division. *Cell. Mol. Life Sci.* **70:** 661–687

O'Sullivan AC, Sullivan GJ & McStay B (2002) UBF binding in vivo is not restricted to regulatory sequences within the vertebrate ribosomal DNA repeat. *Mol. Cell. Biol.* **22:** 657–668

Ohzeki J, Bergmann JH, Kouprina N, Noskov VN, Nakano M, Kimura H, Earnshaw WC, Larionov V & Masumoto H (2012) Breaking the HAC Barrier : Histone H3K9 acetyl / methyl balance regulates CENP-A assembly. *EMBO J.* **31:** 2391–2402

Ohzeki J & Larionov V (2015) Genetic and epigenetic regulation of centromeres : a look at HAC formation. *Chromosome Res.* **23:** 87–103

Parker DS, Jemison J & Cadigan KM (2002) Pygopus, a nuclear PHD-finger protein required for Wingless signaling in Drosophila. *Development* **129:** 2565–76

Parker DS, Ni YY, Chang JL, Li J & Cadigan KM (2008) Wingless signaling induces widespread chromatin remodeling of target loci. *Mol. Cell. Biol.* **28:** 1815–28

Patel JH, Du Y, Ard PG, Carella B, Chen C, Rakowski C, Chatterjee C, Lieberman PM, Lane WS, Blobel G a, Mcmahon SB & Phillips C (2004) The c-MYC Oncoprotein Is a Substrate of the Acetyltransferases hGCN5 / PCAF and TIP60. *Mol Cell Biol.* **24:** 10826–10834

Pestov DG, Lapik YR & Lau LF (2008) Assays for ribosomal RNA processing and ribosome assembly. *Curr. Protoc. Cell Biol.* **22:** 22.11

Popadiuk CM, Xiong J, Wells MG, Andrews PG, Dankwa K, Hirasawa K, Lake BB & Kao KR (2006) Antisense suppression of pygopus2 results in growth arrest of epithelial ovarian cancer. *Clin. Cancer Res.* **12:** 2216–23

Porter IM, McClelland SE, Khoudoli G a., Hunter CJ, Andersen JS, McAinsh AD, Blow JJ & Swedlow JR (2007) Bod1, a novel kinetochore protein required for chromosome biorientation. *J. Cell Biol.* **179:** 187–197

Price BD & D'Andrea AD (2013) Chromatin remodeling at DNA double-strand breaks. *Cell* **152:** 1344–54

Prieto JL & McStay B (2007) Recruitment of factors linking transcription and processing of pre-rRNA to NOR chromatin is UBF-dependent and occurs independent of transcription in human cells. *Genes Dev.* **21:** 2041–2054

Prieve MG & Waterman ML (1999) Nuclear Localization and Formation of $^{N}_{L}$ -Catenin – Lymphoid Enhancer Factor 1 Complexes Are Not Sufficient for Activation of Gene Expression. *Mol. Cell. Biol.* **19:** 4503–4515

Proudfoot N (2016) Transcriptional termination in mammals: Stopping the RNA polymerase II juggernaut. *Science* **352:** aad9926

Reichow SL, Hamma T, Ferré-D'Amaré AR & Varani G (2007) The structure and

function of small nucleolar ribonucleoproteins. *Nucleic Acids Res.* **35:** 1452–1464

Ren B, Cam H, Takahashi Y, Volkert T, Terragni J, Young R a & Dynlacht BD (2002) E2F integrates cell cycle progression with DNA repair , replication , and E2F integrates cell cycle progression with DNA repair , replication , and G 2 / M checkpoints. **2:** 245–256

Roth M & Chen WY (2014) Sorting out functions of sirtuins in cancer. *Oncogene* **33:** 1609–20

Roth SY & Iol MOLCELLB (1998) Mammalian GCN5 and P / CAF Acetyltransferases Have Homologous Amino-Terminal Domains Important for Recognition of Nucleosomal Substrates. *Mol Cell Biol.* **18:** 5659–5669

Roussel P, André C, Comai L & Hernandez-Verdun D (1996) The rDNA transcription machinery is assembled during mitosis in active NORs and absent in inactive NORs. *J. Cell Biol.* **133:** 235–246

Russell J & Zomerdijk JCBM (2005) RNA-polymerase-I-directed rDNA transcription, life and works. *Trends Biochem. Sci.* **30:** 87–96

Saha A, Wittmeyer J & Cairns BR (2002) Chromatin remodeling by RSC involves ATP-dependent DNA translocation. *Genes Dev.* **16:** 2120–2134

Sainsbury S, Bernecky C & Cramer P (2015) Structural basis of transcription initiation by RNA polymerase II. *Nat. Rev. Mol. Cell Biol.* **16:** 129–143

Sakai D & Trainor PA (2009) Treacher Collins syndrome: Unmasking the role of Tcof1/treacle. *Int. J. Biochem. Cell Biol.* **41:** 1229–1232

Sanij E & Hannan RD (2009) The role of UBF in regulating the structure and dynamics of transcriptionally active rDNA chromatin. *Epigenetics* **4:** 374–382

Santos-Rosa H, Schneider R, Bannister AJ, Sherriff J, Bernstein BE, Emre NCT, Schreiber SL, Mellor J & Kouzarides T (2002) Active genes are tri-methylated at K4 of histone H3. *Nature* **419:** 407–411

Scholz C, Weinert BT, Wagner SA, Beli P, Miyake Y, Qi J, Jensen LJ, Streicher W, McCarthy AR, Westwood NJ, Lain S, Cox J, Matthias P, Mann M, Bradner JE & Choudhary C (2015) Acetylation site specificities of lysine deacetylase inhibitors in human cells. *Nat Biotech* **33:** 415–423

Schwab KR, Patterson LT, Hartman HA, Song N, Lang RA, Lin X & Potter SS (2007) Pygo1 and Pygo2 roles in Wnt signaling in mammalian kidney development. *BMC Biol.* **5:** 15

Shav-Tal Y, Blechman J, Darzacq X, Montagna C, Dye B, Patton J, Singer R & Zipori D (2005) Dynamic sorting of nuclear components into distinct nucleolar caps during transcriptional inhibition. *Mol. Biol. Cell* **16:** 2395–2413

Shi Y, Lan F, Matson C, Mulligan P, Whetstine JR, Cole PA, Casero RA & Shi Y (2004) Histone demethylation mediated by the nuclear amine oxidase homolog LSD1. *Cell* **119:** 941–953

Shih I, Yu J, He T, Vogelstein B & Kinzler KW (2000) The beta-Catenin Binding Domain of Adenomatous Polyposis Coli Is Sufficient for tumor suppression. **21231:** 1671–1676

Shtutman M, Zhurinsky J, Simcha I, Albanese C, D'Amico M, Pestell R & Ben-Ze'ev A (1999) The cyclin D1 gene is a target of the beta-catenin/LEF-1 pathway. *Proc. Natl. Acad. Sci. U. S. A.* **96:** 5522–7

Sierra J, Yoshida T, Joazeiro C a & Jones K a (2006) The APC tumor suppressor

counteracts beta-catenin activation and H 3 K 4 methylation at Wnt target genes. *Genes Dev.* **20:** 586

Sikorski TW & Buratowski S (2009) The basal initiation machinery: beyond the general transcription factors. *Curr. Opin. Cell Biol.* **21:** 344–351

Sirri V, Roussel P & Hernandez-Verdun D (1999) The mitotically phosphorylated form of the transcription termination factor TTF-1 is associated with the repressed rDNA transcription machinery. *J. Cell Sci.* **112:** 3259–68

Song N, Schwab KR, Patterson LT, Yamaguchi T, Lin X, Potter SS & Lang R a (2007) pygopus 2 has a crucial, Wnt pathway-independent function in lens induction. *Development* **134:** 1873–85

Städeli R & Basler K (2005) Dissecting nuclear Wingless signalling: Recruitment of the transcriptional co-activator Pygopus by a chain of adaptor proteins. *Mech. Dev.* **122:** 1171–1182

Sun P, Watanabe K, Fallahi M, Lee B, Afetian ME, Rheaume C, Wu D, Horsley V & Dai X (2014) Pygo2 regulates β-catenin-induced activation of hair follicle stem/progenitor cells and skin hyperplasia. *Proc. Natl. Acad. Sci. U. S. A.* **111:** 10125-20

Sun Y, Kolligs FT, Hottiger MO, Mosavin R, Fearon ER & Nabel GJ (2000) Regulation of beta -catenin transformation by the p300 transcriptional coactivator. *Proc. Natl. Acad. Sci. U. S. A.* **97:** 12613–12618

Sweet T, Yen W, Khalili K & Amini S (2008) Evidence for involvement of NFBP in processing of ribosomal RNA. *J. Cell. Physiol.* **214:** 381–388

Tanaka K (2013) Regulatory mechanisms of kinetochore-microtubule interaction in

mitosis. *Cell. Mol. Life Sci.* **70:** 559–579

Tanaka TU (2010) Kinetochore-microtubule interactions: steps towards bi-orientation. *EMBO J.* **29:** 4070–4082

Tanenbaum ME & Medema RH (2010) Mechanisms of Centrosome Separation and Bipolar Spindle Assembly. *Dev. Cell* **19:** 797–806

Teo J-L & Kahn M (2010) The Wnt signaling pathway in cellular proliferation and differentiation: A tale of two coactivators. *Adv. Drug Deliv. Rev.* **62:** 1149–55

Tessarz P & Kouzarides T (2014) Histone core modifications regulating nucleosome structure and dynamics. *Nat. Rev. Mol. Cell Biol.* **15:** 703–708

Tetsu O & McCormick F (1999) Beta-catenin regulates expression of cyclin D1 in colon carcinoma cells. *Nature* **398:** 422–426

Thompson B, Townsley F, Rosin-Arbesfeld R, Musisi H & Bienz M (2002) A new nuclear component of the Wnt signalling pathway. *Nat. Cell Biol.* **4:** 367–73

Tie F, Banerjee R, Stratton C a, Prasad-Sinha J, Stepanik V, Zlobin A, Diaz MO, Scacheri PC & Harte PJ (2009) CBP-mediated acetylation of histone H3 lysine 27 antagonizes Drosophila Polycomb silencing. *Development* **136:** 3131–3141

Townsley FM, Cliffe A & Bienz M (2004) Pygopus and Legless target Armadillo / β - catenin to the nucleus to enable its transcriptional co-activator function. **6:** 626–633

Tsukada Y, Fang J, Erdjument-Bromage H, Warren ME, Borchers CH, Tempst P & Zhang Y (2006) Histone demethylation by a family of JmjC domain-containing proteins. *Nature* **439:** 811–816

Tsuneoka M, Nakano F, Ohgusu H & Mekada E (1997) c-myc activates RCC1 gene expression through E-box elements. *Oncogene* **14:** 2301–2311

Tzenov YR, Andrews P, Voisey K, Gai L, Carter B, Whelan K, Popadiuk C & Kao KR (2015) Selective estrogen receptor modulators and betulinic acid act synergistically to target ER α and SP1 transcription factor dependent Pygopus expression in breast cancer. *J Clin Path.* **69:** 518-26

Tzenov YR, Andrews PG, Voisey K, Popadiuk P, Xiong J, Popadiuk C & Kao KR (2013) Human papilloma virus (HPV) E7-mediated attenuation of retinoblastoma (Rb) induces hPygopus2 expression via Elf-1 in cervical cancer. *Mol. Cancer Res.* **11:** 19–30

Valdez BC, Henning D, So RB, Dixon J & Dixon MJ (2004) The Treacher Collins syndrome (TCOF1) gene product is involved in ribosomal DNA gene transcription by interacting with upstream binding factor. *Proc. Natl. Acad. Sci. U. S. A.* **101:** 10709–14

Valenta T, Hausmann G & Basler K (2012) The many faces and functions of β-catenin. *EMBO J.* **31:** 2714–2736

Verdin E & Ott M (2014) 50 Years of Protein Acetylation: From Gene Regulation To Epigenetics, Metabolism and Beyond. *Nat. Rev. Mol. Cell Biol.* **16:** 258–264

Vernimmen D & Bickmore WA (2015) The Hierarchy of Transcriptional Activation: From Enhancer to Promoter. *Trends Genet.* **31:** 696–708

Visa N & Percipalle P (2010) Nuclear functions of actin. *Cold Spring Harb. Perspect. Biol.* **2:**

Vogelstein B & Kinzler KW (1993) The multistep nature of cancer. *Trends Genet.* **9:** 138–41

Vogelstein B, Papadopoulos N, Velculescu VE, Zhou S, Diaz L a & Kinzler KW (2013)

Cancer genome landscapes. *Science* **339:** 1546–58

Wang CY, Petryniak B, Thompson CB, Kaelin WG & Leiden JM (1993) Regulation of the Ets-related transcription factor Elf-1 by binding to the retinoblastoma protein. *Science* **260:** 1330–1335

Wang H, Fu J, Xu D, Xu W, Wang S, Zhang L & Xiang Y (2016) Downregulation of Pygopus 2 inhibits vascular mimicry in glioma U251 cells by suppressing the canonical Wnt signaling pathway. *Oncol. Lett.* **11:** 678–684

Wang Z, Zang C, Rosenfeld JA, Schones DE, Barski A, Cuddapah S, Cui K, Roh T-Y, Peng W, Zhang MQ & Zhao K (2008) Combinatorial patterns of histone acetylations and methylations in the human genome. *Nat. Genet.* **40:** 897–903

Wang ZX, Chen YY, Li BA, Tan GW, Liu XY, Shen SH, Zhu HW & Wang HD (2010) Decreased pygopus 2 expression suppresses glioblastoma U251 cell growth. *J. Neurooncol.* **100:** 31–41

Watanabe K, Fallahi M & Dai X (2013) Chromatin effector Pygo2 regulates mammary tumor initiation and heterogeneity in MMTV-Wnt1 mice. **33:** 632–642

Weisbrod S (1982) Active chromatin. *Nature* **297:** 289–295

Westermark UK, Wilhelm M, Frenzel A & Henriksson MA (2011) Seminars in Cancer Biology The MYCN oncogene and differentiation in neuroblastoma. *Semin. Cancer Biol.* **21:** 256–266

Wolf D, Rodova M, Miska EA, Calvet JP & Kouzarides T (2002) Acetylation of ??-catenin by CREB-binding protein (CBP). *J. Biol. Chem.* **277:** 25562–25567

Wright KJ & Tjian R (2009) Wnt signaling targets ETO coactivation domain of TAF4/TFIID in vivo. *Proc. Natl. Acad. Sci. U. S. A.* **106:** 55–60

Yang, Xiang-Jiao; Ogryzko, Vasily; Nishikawa, Jun-ichi; Howard, Bruce; Nakatani Y (1996) Yang-Nature-1996. *Nature* **382:** 319–24

Yang L, Lin C, Jin C, Yang JC, Tanasa B, Li W, Merkurjev D, Ohgi K a, Meng D, Zhang J, Evans CP & Rosenfeld MG (2013) lncRNA-dependent mechanisms of androgen-receptor-regulated gene activation programs. *Nature* **500:** 598–602

Yang XJ, Ogryzko V V, Nishikawa J, Howard BH & Nakatani Y (1996) A p300/CBP-associated factor that competes with the adenoviral oncoprotein E1A. *Nature* **382:** 319–324

Yao Z, Duan S, Hou D, Wang W, Wang G, Liu Y, Wen L & Wu M (2010) B23 acts as a nucleolar stress sensor and promotes cell survival through its dynamic interaction with hnRNPU and hnRNPA1. *Oncogene* **29:** 1821–34

Zaret KS & Carroll JS (2011) Pioneer transcription factors: Establishing competence for gene expression. *Genes Dev.* **25:** 2227–2241

Zhang S, Li J, He F & Wang X-M (2015a) Abnormal nuclear expression of Pygopus-2 in human primary hepatocellular carcinoma correlates with a poor prognosis. *Histopathology* **67:** 176–184

Zhang S, Li J, Liu P, Xu J & Zhao W (2015b) Pygopus-2 promotes invasion and metastasis of hepatic carcinoma cell by decreasing E-cadherin expression. Oncotarget **6:** 11074-86

Zhang Y & Lu H (2009) Signaling to p53: Ribosomal Proteins Find Their Way. *Cancer Cell* **16:** 369–377

Zhou Q, Li T & Price DH (2012) RNA polymerase II elongation control. *Cold Spring Harb. Symp. Quant. Biol.* **81:** 119–43

Zhou SY, Xu ML, Wang SQ, Zhang F, Wang L & Wang HQ (2014) Overexpression of Pygopus-2 is required for canonical Wnt activation in human lung cancer. *Oncol. Lett.* **7:** 233–238

Zindy F, Eischen CM, Randle DH, Kamijo T, Cleveland JL, Sherr CJ & Roussel MF (1998) Myc signaling via the ARF tumor suppressor regulates p53-dependent apoptosis and immortalization. *Genes Dev.* **12:** 2424–2433